Master's Thesis

Czech Technical University in Prague

F3

Faculty of Electrical Engineering
Department of Microelectronics

Design of an E-compressor Motor Control solution for use in the Automotive Application.

Bc. Michal Kopiar

Supervisor: Ing. Vít Záhlava, CSc.
Field of study: Electronics and Communication
May 2023

MASTER'S THESIS ASSIGNMENT

I. Personal and study details

Student's name: **Kopiar Michal** Personal ID number: **483680**

Faculty / Institute: **Faculty of Electrical Engineering**

Department / Institute: **Department of Microelectronics**

Study program: **Electronics and Communications**

Specialisation: **Electronics**

II. Master's thesis details

Master's thesis title in English:

Design of an E-compressor Motor Control Solution for Use in the Automotive Application.

Master's thesis title in Czech:

Návrh řízení motoru e-kompresoru pro použití v automobilovém průmyslu.

Guidelines:

1) Investigate general motor control solutions and point out main challenges of high voltage motor controller design.
2) Propose a prototype design of the motor controller for e-compressor.
3) Verify the functionality of individual function blocks of the design.
4) Specify the commercial aspect of the assignment.

Bibliography / sources:

1) Design of Rotating Electrical Machines, Juha Pyrhonen; Tapani Jokinen; Valeria Hrabovcova, ISBN: 978-0-470-69516-6
2) LEONHARD, Werner. Control of electrical drives. 3rd ed. Berlin: Springer, 2001.
3) B. Jayant Baliga: 'Fundamentals of Power Semiconductor Devices', Springer, 2008

Name and workplace of master's thesis supervisor:

Ing. Vít Záhlava, CSc. Department of Microelectronics FEE

Name and workplace of second master's thesis supervisor or consultant:

Date of master's thesis assignment: **31.01.2023** Deadline for master's thesis submission: __________

Assignment valid until: **22.09.2024**

Ing. Vít Záhlava, CSc. Supervisor's signature	prof. Ing. Pavel Hazdra, CSc. Head of department's signature	prof. Mgr. Petr Páta, Ph.D. Dean's signature

III. Assignment receipt

The student acknowledges that the master's thesis is an individual work. The student must produce his thesis without the assistance of others, with the exception of provided consultations. Within the master's thesis, the author must state the names of consultants and include a list of references.

16.5.2023

Date of assignment receipt Student's signature

Acknowledgements

This thesis could not originate without the help of my colleagues, friends and family.

I would like to thank my supervisor Ing. Vít Záhlava, CSc. for sharing his valuable expertise in this field and providing me with consultations and irreplaceable feedback.

Great thanks also goes to Daniel Kohout and Jiří Ryba for supervising, consulting and enabling this thesis from the side of STMicroelectronics.

Special thanks goes to Ing. Stanislav Tomášek for consulting the thesis and his patience as well as all members of eForce FEE Prague formula for providing external support for this thesis.

My thanks also goes to all past and current colleagues in STMicroelectronics, without whom this project as well as my thesis would not be possible.

And most importantly, I would like to thank my family, girlfriend and friends for all the support I have gotten during my studies.

Declaration

I hereby declare that the presented Master's thesis is my own work and that I have cited all sources of information in accordance with the ethical principles when elaborating an academic final thesis.

....

Michal Kopiar
In Prague, 26. May 2023

Abstract

This thesis presents a study on the design and implementation of a high voltage motor controller prototype for electric vehicle (EV) e-compressors, with an emphasis on advanced power electronics, control algorithms, and robust hardware design.

The motor controller features SiC transistors in a B6 configuration, onboard microcontroller, resolver interface circuitry, and insulated USB communication, among other components, all meticulously arranged on a high voltage PCB. The design adheres to automotive standards for high voltage applications and integrates robust protection mechanisms, such as Over Current Protection (OCP).

The viability of the controller is demonstrated through laboratory testing and is further discussed in the context of commercial production, highlighting its potential for cost reduction and scalability. The study also elaborates on the significant role of the e-compressor and its associated controller in enhancing the thermal management of EV batteries, thereby contributing to the performance and reliability of EVs.

Keywords: electric motor, motor controller, powertrain, IGBT, SiC, CAN Bus, vehicle dynamics, PMSM , rotational sensor, resolver, hardware development

Supervisor: Ing. Vít Záhlava, CSc.
Katedra mikroelektroniky,
Technická 1902/2, Praha 6

Abstrakt

Tato práce představuje studii o návrhu a implementaci prototypu vysokonapěťového měniče pro e-kompresory elektrických vozidel (EV), s důrazem na pokročilou výkonovou elektroniku, řídící algoritmy a robustní hardwarový design.

Měnič obsahuje tranzistory SiC v konfiguraci B6, vestavěný mikrokontrolér, obvodové rozhraní resolveru a izolovanou komunikaci USB, mezi dalšími komponentami, vše pečlivě uspořádané na vysokonapěťové DPS. Design dodržuje automobilové standardy pro vysokonapěťové aplikace a integruje robustní ochranné mechanismy, jako je ochrana proti přetížení (OCP).

Proveditelnost měniče je demonstrována prostřednictvím laboratorních testů a je dále diskutována v kontextu komerční výroby, což zdůrazňuje její potenciál pro snížení nákladů a škálovatelnost. Studie také objasňuje významnou roli e-kompresoru a s ním spojeného měniče při zlepšení termálního managementu baterií EV, čímž přispívá k výkonnosti a spolehlivosti EV.

Klíčová slova: elektrický motor, motor controller, hnací ústrojí, IGBT, SiC, CAN zběrnice, dynamika vozidla, PMSM, rotačný senzor, resolver, hardwarový vývoj

Překlad názvu: Návrh řízení motoru e-kompresoru pro použití v automobilovém průmyslu.

Contents

Figures

Chapter 1

Used symbols and units

Unless stated otherwise, all units used in this thesis in accordance to International System of Units (SI) and following is the list of symbols used.

Symbol	Unit	Explanation
C	Farad[F]	Capacitance
E_c	Joule[J]	Energy stored in capacitor
$E_c final$	Joule[J]	Energy stored in capacitor after the pulse
$E_c initial$	Joule[J]	Energy stored in capacitor initially
E_{ripple}	Joule[J]	energy of the ripple
f_0	Hertz[Hz]	resonant frequency
f_{sw}	Hertz[Hz]	Switching frequency
HV+, HV-	Volt[V]	High Voltage
I_x	Ampere[A]	Current x
K	[-]	coupling factor
Q	Coulomb[C]	Charge
L	Henry[H]	Inductance
P_1	Pascal[Pa]	Pressure
P_{peak}	Watt[W]	Peak power
T_1	Kelvin[$^\circ K$]	Temperature
t	second[s]	Time
U_{gs}	Volt[V]	Transistors Gate-Source Voltage
U_r	Volt[V]	ripple voltage
V-iso, V+iso, GNDiso	Volt[V]	Insulated power source output voltages
V_1	[m^3]	Volume
V_x	Volt[V]	Voltage x
ω_0	[$rad \cdot s^{-1}$]	resonant angular velocity
α	[$kg \cdot s^{-1}$]	damping
ζ	[$N \cdot s \cdot m^{-1}$]	damping factor

Chapter 2

Foreword

With the electrification of the transport industry, particularly in personal vehicles, the need for an efficient and powerful auxiliary temperature control unit has arisen. Air conditioning or heating of the driver's compartment is a common and indispensable feature in all modern electric and internal combustion vehicles. In the case of the latter, heating is typically achieved by transferring heat from the internal combustion engine to the driver's compartment. For air conditioning, a specialized unit powered by the car's drive belt system and low-voltage electrical system is employed.

There are generally no other requirements for temperature control within internal combustion vehicles, as the combustion engine thermally regulates itself through the exhaust system and turbocharged forced induction, using hot exhaust gases to force air back into the combustion engine. Thermal efficiency of commonly used internal combustion engines ranges between 20% to 30% due to the inefficient process of converting the chemical energy of gasoline to heat and then to torque and mechanical energy. This low thermal efficiency allows car manufacturers to have an abundance of waste heat for the aforementioned purposes.

In contrast, electric vehicles exhibit significantly higher powertrain efficiency, owing to the overall efficiency of converting the electric potential of the battery to torque. This efficiency is continually improved by manufacturers in response to the high demand for increased range in electric vehicles. As compared to internal combustion vehicles, electric vehicles generate significantly less waste heat that could be used for heating. Moreover, there is no straightforward way to utilize this additional thermal energy in electric vehicles, as they lack the direct exhaust system that is essential for internal combustion engines. This problem is further exacerbated by the need for longevity in electric vehicle batteries. Longevity is desirable due to the high cost of electric vehicle batteries and the difficulty of replacement. Additionally, the degradation of EV batteries is significantly influenced by the temperature during their use and storage.

To address the thermal regulation challenges for the driver's compartment and battery in electric vehicles, car manufacturers have implemented e-compressors. These units possess the ability for multi-directional heat transfer based on the actual state that the vehicle is in, as well as adding or removing thermal energy from the entire thermal system itself. [1] [2]

2.0.1 Components of a Car's Air Conditioning System

The air conditioning system in a car consists of several key components, including:

1. Compressor
2. Condenser
3. Expansion Valve or Orifice Tube
4. Evaporator
5. Receiver-Drier or Accumulator

2.0.2 The Cooling Process

The cooling process in a car's AC system can be understood by applying the ideal gas law and the second law of thermodynamics. The combined gas law is given by:

$$\frac{P_1 V_1}{T_1} = k \tag{2.1}$$

where P represents pressure, V represents volume, n represents the number of moles of the gas, k represents the constant, and T represents the temperature in Kelvin.

The second law of thermodynamics states that heat will spontaneously flow from a higher temperature region to a lower temperature region. This principle is essential for understanding the heat exchange processes in the AC system.

Compression

The compressor draws in low-pressure refrigerant gas from the evaporator and compresses it, raising its pressure and temperature according to the ideal gas law. The high-pressure, high-temperature gas is then sent to the condenser.

Condensation

As the refrigerant gas passes through the condenser, it loses heat to the ambient air and transforms into a high-pressure liquid. This process releases the heat absorbed from the cabin earlier, in accordance with the second law of thermodynamics.

Expansion

The high-pressure liquid refrigerant flows through the expansion valve or orifice tube, where its pressure and temperature drop significantly. This reduction causes the refrigerant to partially evaporate, forming a cold, low-pressure gas and liquid mixture.

Evaporation

The cold refrigerant mixture enters the evaporator, where it absorbs heat from the cabin's air, cooling it. The refrigerant fully evaporates into a gas, while a blower fan circulates the cooled air through the cabin. The heat absorption process is driven by the second law of thermodynamics.

Recirculation

The low-pressure refrigerant gas returns to the compressor, and the cycle repeats.

Chapter 3

Introduction and design challenges

In electric vehicles (EV), the absence of a drive belt system to power the compressor necessitates the implementation of a dedicated motor and motor controller. According to the specified requirements, provided by STMicroelectronics, this motor should be capable of withstanding a wide range of input voltages from the main vehicle battery, ranging from 400V to 800V, and deliver at least 5kW of power. Emphasis is placed on high efficiency, reliability, and simplicity of the system. The motor should be driven by a motor controller, to which the same requirements apply and also must be viable to be integrated to the vehicle. Prototype board will be developed first, in order to test all the necessary features and design of this prototype will be the main subject of this thesis.

3.1 Electric Motors

An electric motor is a type of electrical machine that converts electrical energy into mechanical energy through the interaction of magnetic fields between a conductor carrying current and another conductor or permanent magnets. This interaction generates torque on the rotor, the rotating part of the motor. The same process can be reversed to create an electrical current in the motor wires and generate electricity, a process known as regenerative braking. An electric motor consists of a rotor and a stator, with the latter being the stationary or non-moving part of the motor.

One type of motor suitable for e-compressor applications is the brushless direct current (BLDC) motor. This motor features permanent magnets on the rotor and windings on the stator, creating a rotating magnetic field by carefully switching the DC input to the motor phases. BLDC motors are typically powered by three trapezoidal wave phases spaced 120 degrees apart. Among the most common methods, these three phases are created by modulating the trapezoidal waveform in each phase.

While there are other types of electric motors, the permanent magnet synchronous motor (PMSM) is considered the best choice for our use case based on weight and efficiency requirements. Although mechanically similar to the BLDC motor, the PMSM motor exhibits differences in the back electromotive force (EMF) induced on the motor phases when rotating, with a sinusoidal waveform instead of a trapezoidal one. Compared to BLDC motors, PMSMs offer greater efficiency and more stable output torque due to the absence of torque ripple, which is common in BLDC motors.

A PMSM motor consists of permanent magnets in the rotor and windings on the stator. These motors are commonly used as servomotors or traction drives. A motor controller is required to drive the motor, with current sensors and an angular position sensor providing feedback to the motor controller. This can be achieved through sensored operation, using resolvers or encoders, or through sensorless operation employing a mathematical model of the motor in the motor controller to provide a good estimate of the exact position. Both open-loop and closed-loop operations are possible. [3]

3.2 Motor controller

Motor controller is used to create 3-phase alternating current from accumulator's DC supply. This can be seen as a capacitor and 6 transistors in B6 configuration or three half-bridges as can be seen in the picture 3.1. Each single phase is therefore controlled by 2 switches where by switching gates with PWM (Pulse Width Modulation) a sine wave can produced as can be seen in 3.3.

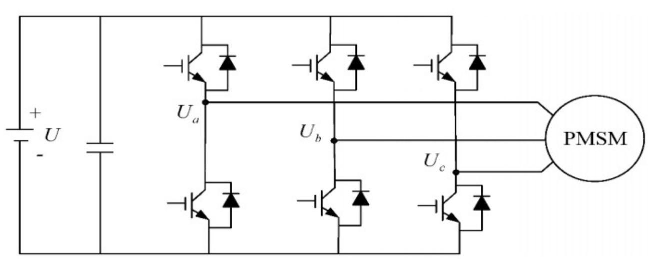

Figure 3.1: Single motor connection schematic

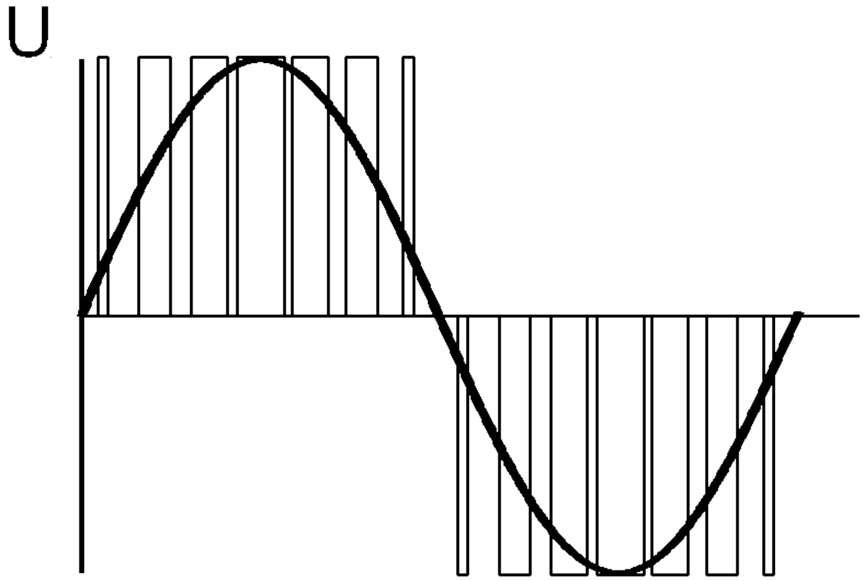

Figure 3.2: PWM single phase modulation of sinusodial wave

There are a few options for high power semiconductors usable for switching, such as Insulated-Gate Bipolar Transistor(IGBT), Metal Oxide Semiconductor Field Effect Transistor(MOSFET) or Silicon Carbide (SiC) Metal Oxide Field Effect Transistor or MOSFET are among the most commonly used for this purpose.

3.2.1 Power electronics

For application purposes, main differences between IGBT and SiC MOSFETs is the characteristic bipolar or unipolar structure. Whereas IGBSs feature Collector-Emitter saturation voltage, SiC transistors do have Drain-Source resistance. This means that the losses in the IGBT are linearly proportional to the current for a given temperature and Gate voltage, in SiC MOSFETs this proportionality is quadratic. SiC MOSFETs also do generally feature faster dynamic characteristics, giving them ability to achieve faster switching frequencies. I will further discuss mainly IGBT and SiC MOSFETs because they are best suited for the high voltage motor control purposes. [4]

3.2.2 BJT and IGBT

A BJT, or Bipolar Junction Transistor, is a type of semiconductor device used primarily for amplification and switching applications in electronic circuits. It belongs to the family of transistors, which are the fundamental building blocks of modern electronic devices.[5]

The BJT consists of three layers of semiconductor material: the emitter, base, and collector, with two junctions formed between them. It comes in two types: NPN (which has an n-type emitter, p-type base, and n-type collector) and PNP (which has a p-type emitter, n-type base, and p-type collector). The operation of a BJT depends on the movement of charge carriers (electrons and holes) across the junctions between the layers.

In a BJT, a small current flowing through the base-emitter junction controls a larger current flowing between the collector and emitter, effectively allowing the BJT to amplify a signal or act as a switch. The properties of a BJT, such as its current gain, make it suitable for various applications, including audio amplifiers, oscillators, and digital logic circuits.

An Insulated-Gate Bipolar Transistor (IGBT) is a type of semiconductor device primarily used in power electronics for switching and controlling electric power. It combines the features of both Metal-Oxide-Semiconductor Field-Effect Transistors (MOSFETs) and Bipolar Junction Transistors (BJTs), resulting in a device that exhibits high input impedance, fast switching speeds, and the ability to handle high voltages and currents.

The IGBT structure consists of four alternating layers of P-type and N-type semiconductor material, forming a PNP or NPN transistor pair along with a MOSFET gate structure. The gate terminal of the IGBT is insulated from the rest of the device, which is why it is called an insulated-gate transistor. This insulation enables the IGBT to be controlled by a relatively small voltage, like a MOSFET, while still offering the high current-carrying capacity and low conduction losses of a BJT.

IGBTs are widely used in various applications, such as motor drives, power supplies, inverters, and electric vehicle systems, where efficient and precise control of high voltages and currents is essential. Their ability to switch rapidly and handle high power levels makes them suitable for these demanding applications.

3.2.3 MOSFET

A MOSFET, or Metal-Oxide-Semiconductor Field-Effect Transistor, is a widely-used semiconductor device in electronic circuits for amplification and switching applications. As a voltage-controlled device, the current flowing through it is determined by the voltage applied to the gate terminal.

The MOSFET structure consists of source, drain, and gate terminals, with the gate separated from the semiconductor material by a thin insulating layer, typically made of silicon dioxide. This insulated gate structure leads to the device's high input impedance, enabling the MOSFET to consume minimal power during operation.

There are two main types of MOSFETs: n-channel (nMOS) and p-channel (pMOS). In n-channel MOSFETs, the majority charge carriers are electrons, while in p-channel MOSFETs, the majority charge carriers are holes. MOSFETs can be employed in both analog and digital circuits and are frequently found in power supplies, motor drives, and digital logic circuits.

In recent years, Silicon Carbide (SiC) MOSFETs have emerged as an advanced alternative to traditional silicon-based MOSFETs. SiC is a wide-bandgap semiconductor material that offers several advantages over silicon, including higher thermal conductivity, low-on-state resistance and lower junction capacitance. Consequently, SiC MOSFETs are well-suited for high-power and high-temperature applications, such as electric vehicles, renewable energy systems, and power electronics.

While MOSFETs generally provide faster switching speeds, lower power consumption, and higher input impedance compared to other transistor types like Bipolar Junction Transistors (BJTs), they may exhibit higher conduction losses and lower current handling capabilities in certain situations. However, SiC MOSFETs help to address some of these limitations, making them a compelling choice for various demanding applications.

3.2.4 Input capacitance

Input capacitance has to be incorporated into the design to ensure proper function during the systems transient phenoma and to protect the switching silicon from sudden voltage peaks that may occur. This capacitor has to have proper voltage rating for the accumulator, and sufficient capacity.

3.3 Motor Control Algorithms and Strategies

Motor control algorithms and strategies are techniques employed to govern the operation of electric motors in various applications, ensuring optimal performance, energy efficiency, and precise control. These algorithms and strategies can be broadly divided into two groups: scalar control and vector control. [6]

3.3.1 Scalar control

Scalar control techniques modulate the magnitude of voltage and frequency applied to the motor, without considering the spatial relationship between motor current and magnetic flux [7]. Some common scalar control strategies include:

1. Volts/Hertz (V/Hz) control: This method maintains a constant voltage-to-frequency ratio, providing a simple and cost-effective way to control induction motors. However, it lacks high dynamic performance and precision. It can be also used for PMSM motors, mainly during sensorless start-up, but sufferers from worst efficiency.

2. Slip regulation control: This strategy adjusts motor voltage to control the slip (difference between synchronous and rotor speed) and maintain the desired torque output and is only viable for induction motors.

3.3.2 Vector control

Vector control techniques, also known as field-oriented control (FOC), decouple the torque-producing and magnetizing components of motor current, allowing independent control of torque and magnetic flux. This results in superior dynamic performance, precision, and energy efficiency. Common vector control strategies include:

1. Direct Torque Control (DTC): This method directly calculates and controls the torque and magnetic flux produced by the motor, allowing for rapid torque and flux control responses. DTC does not require pulse-width modulation (PWM) or coordinate transformations, making it more computationally efficient.[8]

2. Indirect Field-Oriented Control (IFOC): This technique employs coordinate transformations to align the rotor flux with a specific axis, enabling separate control of torque and magnetic flux. IFOC requires a pulse-width modulation (PWM) inverter to modulate voltage applied to the motor, and it relies on motor parameter estimation for accurate control.

These motor control algorithms and strategies are implemented using digital signal processors (DSPs), microcontrollers, or field-programmable gate arrays (FPGAs), which enable real-time processing and precise motor control. The choice of algorithm and strategy depends on the specific application requirements, motor type, and desired performance characteristics. [**idkj**]

3.3.3 Vector Control and Field-Oriented Control (FOC)

Vector control, also known as field-oriented control (FOC), is an advanced motor control technique that significantly improves the dynamic performance, precision, and energy efficiency of electric motors, particularly for AC motors such as induction motors (IMs) and permanent magnet synchronous motors (PMSMs). The primary goal of FOC is to decouple the torque-producing (active) and magnetizing (reactive) components of motor current, allowing independent control of torque and magnetic flux. This decoupling is achieved by transforming motor currents and voltages into a rotating reference frame, typically referred to as the dq-frame, which is aligned with the rotor magnetic field. [9]

Coordinate Transformations

FOC relies on coordinate transformations to align the rotor flux with a specific axis, typically the d-axis, in the rotating reference frame. Following transformations do work for arbitrary number of phases, but i will only apply them for the 3-phase system, since that is the most relevant for the purpose of this thesis.[10] Two commonly used transformations are:

Clarke Transformation converts 3-phase currents (I_a, I_b, I_c) or voltages (V_a, V_b, V_c) into a stationary two-phase $\alpha\beta$-frame (I_α, I_β) or (V_α, V_β). This transform also functions for other quantifiable phase characteristic (eg. voltage or flux). Following is the Clarke transform formula for symmetrical current phase input ($I_0 = 0$).

$$\begin{bmatrix} I_\alpha \\ I_\beta \\ I_0 \end{bmatrix} = \begin{bmatrix} 1 & -\frac{1}{2} & -\frac{1}{2} \\ 0 & \frac{\sqrt{3}}{2} & -\frac{\sqrt{3}}{2} \\ \frac{1}{2} & \frac{1}{2} & \frac{1}{2} \end{bmatrix} \cdot \begin{bmatrix} I_a \\ I_b \\ I_c \end{bmatrix} \tag{3.1}$$

Park Transformation further converts the stationary two-phase $\alpha\beta$-frame currents or voltages into the rotating dq-frame, aligned with the rotor magnetic field. The resulting currents are I_d and I_q, and the resulting voltages are V_d and V_q. Park transform for the I_d and I_q reference frame can be written as following:

$$\begin{bmatrix} I_d \\ I_q \\ I_0 \end{bmatrix} = \begin{bmatrix} \cos(\theta) & \sin(\theta) & 0 \\ -\sin(\theta) & \cos(\theta) & 0 \\ 0 & 0 & 1 \end{bmatrix} \cdot \begin{bmatrix} I_\alpha \\ I_\beta \\ a_0 \end{bmatrix} \tag{3.2}$$

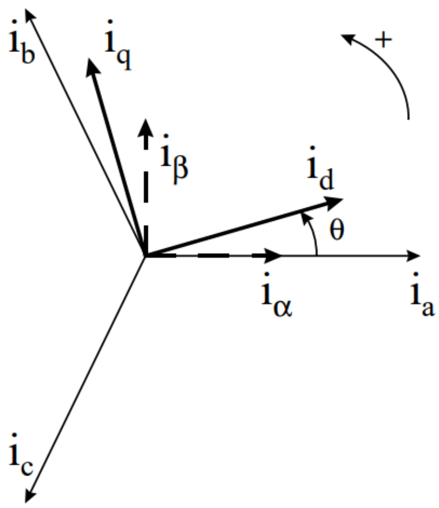

Figure 3.3: Illustration of the stator current transformation from the stationary a, b, c reference frame to the rotating d, q reference frame, highlighting the relationship between the two coordinate systems in electric motor control

The inverse of these transformations can be used to convert the currents or voltages back from the dq-frame to the three-phase system. Park transformation is typically used in combination with the rotor electrical angle or an angle derived from a position sensor or an observer algorithm.

Torque and Flux Control

With the currents and voltages transformed into the dq-frame, the torque-producing component of the current (I_q) can be controlled independently of the magnetizing component (I_d). For example, in a PMSM, by controlling the I_q current, the motor torque can be precisely regulated, while the I_d current is typically set to zero to minimize losses. In an induction motor, the I_d current can be adjusted to control the rotor magnetic flux.

Current Controllers and Pulse-Width Modulation (PWM)

Current controllers, such as Proportional-Integral (PI) controllers, are used to regulate the dq-frame currents (I_d and I_q) based on the desired torque and flux commands. The output of these controllers is a voltage reference in the dq-frame (V_d^* and V_q^*). These voltage references are then transformed back to the three-phase system using the inverse Park and Clarke transformations.

Finally, the three-phase voltage references are used to generate PWM signals for the power electronic converter, typically a three-phase voltage-source inverter (VSI). The VSI modulates the voltages applied to the motor, effectively controlling the motor's torque and flux according to the FOC algorithm.

In summary, vector control and FOC enable independent control of torque and magnetic flux in electric motors, resulting in superior dynamic performance, precision, and energy efficiency. The technique relies on coordinate transformations, current controllers, and PWM, making it a more sophisticated approach than scalar control methods.

3.4 Open and Closed Loop Operation, Sensored and Sensorless Control

Electric motor control techniques can be implemented in either open-loop or closed-loop configurations, and with sensored or sensorless approaches, depending on the desired performance, application requirements, and cost constraints. [11]

Open Loop Operation

Open-loop motor control, also known as scalar control, operates without feedback, relying solely on the predefined relationship between input voltage, frequency, and motor speed. In this method, the motor is controlled by adjusting the input voltage and frequency according to a predetermined profile, such as a constant volts-per-hertz (V/Hz) ratio. Open-loop operation is simple, cost-effective, and suitable for applications with modest performance requirements and no need for precise motor speed or torque control.

Closed Loop Operation

Closed-loop motor control, often used in vector control methods like field-oriented control (FOC), employs feedback to continuously monitor and adjust motor operation based on real-time performance. The feedback can come from sensors measuring motor speed, position, or current, or from sensorless estimation techniques. Closed-loop systems typically use current controllers, such as proportional-integral (PI) controllers, to regulate motor current in the dq-frame, ensuring precise control of torque and magnetic flux. Closed-loop operation provides superior dynamic performance, energy efficiency, and precise control, making it suitable for applications with stringent requirements, such as electric vehicles and industrial automation.

3.4.1 Sensored and Sensorless Control

Sensored Control

Sensored control methods rely on physical sensors, such as encoders, resolvers, or Hall-effect sensors, to provide information about motor speed, position, or current. This feedback allows for precise control of motor operation in closed-loop systems. Sensored control offers high accuracy and fast response times, but it also increases system complexity, cost, and maintenance requirements due to the need for additional hardware.

Sensorless Control

Sensorless control methods estimate motor parameters, such as speed, position, or current, without using physical sensors. Instead, they rely on mathematical models, algorithms, or signal processing techniques to derive the necessary information from the motor's inherent electrical characteristics. Some common sensorless methods include back-EMF estimation, sliding-mode observers, and model reference adaptive control (MRAC). Sensorless control reduces system complexity, cost, and maintenance requirements compared to sensored control, but it often has limitations in terms of accuracy, low-speed operation, and dynamic response.

Other angular position sensors do exist, but I will only elaborate more on resolvers, since this is what will be used for e-compressor board testing, I have the most experience using them and they are planned to be included in the current design.

Information about functionality of motor controllers can be found in Stanislav Tomášek's and Miroslav Ryzek's master's theses [12] [13]

3.5 Resolvers in Motor Control

Resolvers are robust rotary position sensors commonly used in motor control applications to provide accurate and reliable feedback on rotor position and speed. They are particularly suitable for harsh environments due to their durability, high-temperature tolerance, and resistance to vibration, dust, and moisture. [14]

3.5.1 Resolver Operation and Construction

A resolver consists of a stator and a rotor, both containing windings. The stator has two sets of windings, known as the sine and cosine windings, placed orthogonally to each other, while the rotor has a single set of windings. The rotor winding is energized by an alternating current, known as the excitation signal, which generates a magnetic field that couples to the stator windings. As the rotor turns, the magnetic coupling between the rotor and stator windings varies, resulting in two sinusoidal output voltages from the stator windings that have a amplitude difference proportional through arctangent function to the rotor's angular position.[15]

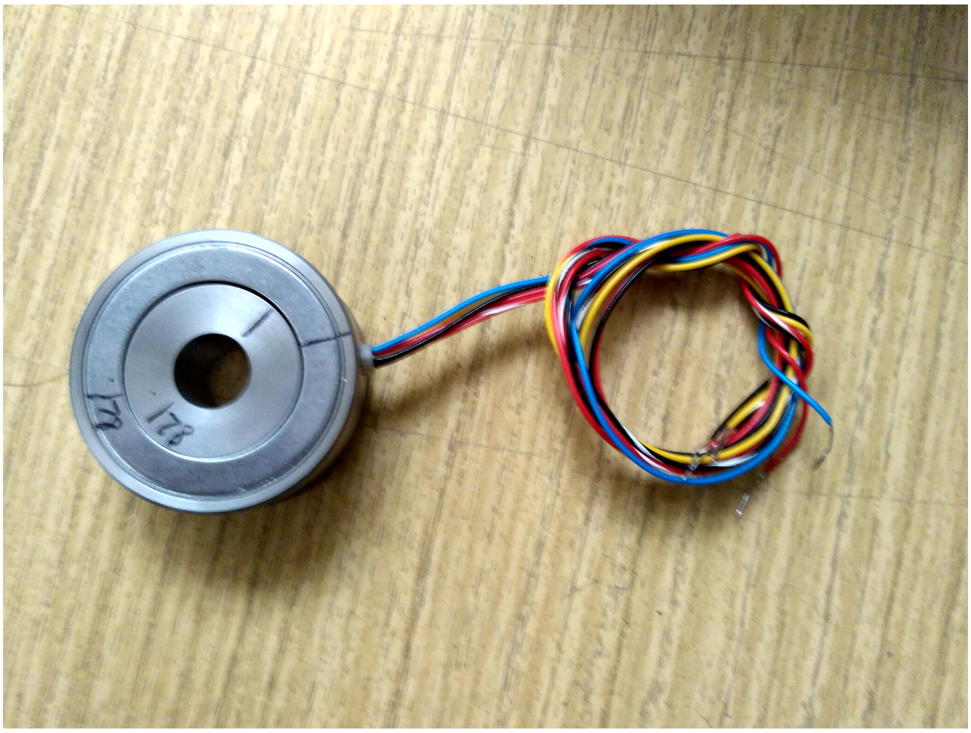

Figure 3.4: RE-15-1-A15 resolver from company ltn-servotechnik

$$V_{\text{sine}} = K \cdot \sin(\theta) \cdot V_{\text{excitation}} \tag{3.3}$$

$$V_{\text{cosine}} = K \cdot \cos(\theta) \cdot V_{\text{excitation}} \tag{3.4}$$

Here, V_{sine} and V_{cosine} are the output voltages from the sine and cosine stator windings, K is the coupling factor, θ is the rotor's angular position, and $V_{\text{excitation}}$ is the excitation signal voltage.

3.5.2 Resolver-to-Digital Conversion

To obtain the rotor's angular position and speed from the resolver's output voltages, a resolver-to-digital converter (RDC) is used. The RDC processes the sine and cosine output voltages and calculates the rotor's angular position using an arctangent function:

$$\theta = \arctan\left(\frac{V_{\text{sine}}}{V_{\text{cosine}}}\right) \tag{3.5}$$

The rotor speed can be determined by differentiating the angular position with respect to time or by using dedicated speed estimation algorithms.

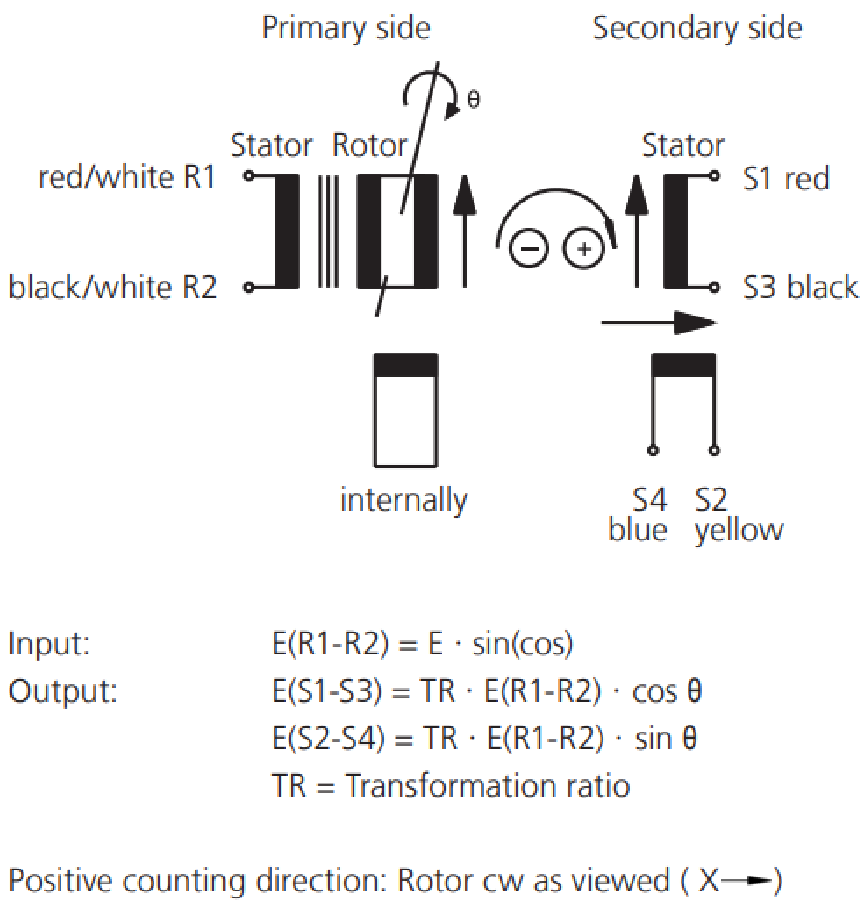

Figure 3.5: RE-15-1-A15 resolver internal schematics [14]

3.5.3 Resolver Applications in Motor Control

In motor control systems, resolvers are particularly beneficial in applications requiring high reliability, precision, and robustness, such as electric vehicle drive systems, aerospace, and industrial automation. Resolvers provide crucial feedback for closed-loop control algorithms, such as field-oriented control (FOC), enabling precise control of torque, speed, and position. They also offer advantages over other types of position sensors, such as optical encoders, in harsh environments due to their ruggedness and lack of sensitivity to contamination. [11]

3.6 Controller Area Network (CAN) Bus in Motor Control Systems

The Controller Area Network (CAN) bus is a robust and widely used communication protocol for interconnecting electronic control units (ECUs) within various applications, including automotive, industrial automation, and motor control systems. The CAN bus offers a simple, cost-effective, and reliable communication solution, enabling real-time data exchange among multiple devices with minimal wiring and overhead. [16]

3.6.1 CAN Bus Protocol and Operation

The CAN protocol, first developed by Bosch in the 1980s, operates at the data link layer of the OSI model and uses a multi-master serial bus architecture. This allows all connected devices, known as nodes, to transmit and receive messages simultaneously without the need for a central bus master or host.

Messages on the CAN bus consist of an identifier, data length code (DLC), and data payload, with a maximum of 8 bytes. CAN uses a non-destructive bitwise arbitration process to prioritize messages on the bus, with lower identifier values having higher priority. In case of a bus contention, the node with the highest priority message wins arbitration and continues transmitting, while other nodes back off and retry later.

3.6.2 CAN Bus Physical Layer and Topology

The CAN bus typically uses a two-wire differential signaling for noise immunity and robustness, with the wires referred to as CAN High (CANH) and CAN Low (CANL). The differential voltage between CANH and CANL represents the logical state of the bus, with a dominant state (logic 0) corresponding to a larger differential voltage and a recessive state (logic 1) corresponding to a smaller differential voltage.

The most common topology for the CAN bus is a linear bus topology, where nodes are connected to a common backbone using short drop lines. Termination resistors are placed at both ends of the bus to minimize signal reflections and ensure proper signal integrity. [17]

3.6.3 CAN Bus in Motor Control Applications

In motor control systems, the CAN bus is used to transmit and receive data among various system components, such as motor controllers, sensors, actuators, and user interfaces. The CAN bus enables real-time communication, fault detection, and system diagnostics, significantly improving system performance, reliability, and maintainability.

Some common uses of the CAN bus in motor control applications include:

- Transmitting control commands, such as speed, torque, or position setpoints, from a supervisory controller to motor drives.
- Exchanging sensor data, such as motor speed, position, current, or temperature, among different system components for monitoring and control.
- Coordinating the operation of multiple motors in multi-axis motion control or multi-motor drive systems.
- Communicating fault and diagnostic information among system components for predictive maintenance and troubleshooting.

3.7 Cooling Techniques for Electric Motors and Motor Controllers

Proper cooling is essential for maintaining the performance, efficiency, and reliability of electric motors and motor controllers. Inadequate cooling can lead to elevated temperatures, which may cause thermal stress, reduced efficiency, and potential damage to components. This section discusses the importance of cooling and common cooling techniques employed in electric motor and motor controller applications.

3.7.1 Thermal Management in Electric Motors

Heat generation in electric motors primarily results from copper losses in the stator windings, iron losses in the magnetic core, and mechanical losses due to friction in bearings and other moving parts. Proper thermal management ensures that the motor operates within safe temperature limits, preventing insulation degradation, demagnetization of permanent magnets, and bearing damage.

Air Cooling

Air cooling is a widely used technique for electric motors, offering a cost-effective and straightforward solution. Depending on the motor size and power rating, air cooling can be achieved through natural convection or forced convection using fans. In natural convection cooling, heat is dissipated passively through the motor housing, while forced convection cooling employs fans to circulate air over the motor surfaces, improving heat transfer and cooling efficiency.

Liquid Cooling

Liquid cooling is an efficient method for high-power or high-performance motor applications, where air cooling may not provide adequate heat dissipation. In liquid-cooled motors, a coolant (typically water or a water-glycol mixture) is circulated through channels in the motor housing or around the stator windings, absorbing heat and transferring it to a heat exchanger or radiator for dissipation. Liquid cooling offers higher heat conductivity and heat transfer capability compared to air cooling, enabling better temperature control and more compact motor designs.

3.7.2 Thermal Management in Motor Controllers

Motor controllers, particularly power electronic devices such as insulated-gate bipolar transistors (IGBTs) and MOSFETs, generate heat due to conduction and switching losses. Effective thermal management is crucial for maintaining the reliability and performance of motor controllers, preventing component failure and ensuring optimal efficiency.

Heat Sinks

Heat sinks are commonly used to dissipate heat in motor controllers. They consist of a thermally conductive material, usually aluminum, with fins or other geometric features designed to maximize the surface area for heat transfer to the surrounding air. Heat sinks can be cooled through natural convection or forced convection using fans. Thermal interface materials (TIMs) are often employed to improve the thermal contact between the power electronic devices and the heat sink, reducing thermal resistance and enhancing heat transfer.

3.7.3 Thermal Properties of SiC MOSFETs and IGBTs

Silicon Carbide (SiC) MOSFETs and Insulated-Gate Bipolar Transistors (IGBTs) are two widely used power semiconductor devices in motor controller applications. Both devices have distinct thermal properties that affect their performance, efficiency, and thermal management requirements.

Silicon Carbide (SiC) MOSFETs compared to IGBT

SiC MOSFETs are known for their superior thermal properties compared to conventional silicon-based devices. Some key advantages of SiC MOSFETs in terms of thermal performance include:

- **Lower Power Losses:** SiC MOSFETs have significantly lower conduction and switching losses compared to silicon based IGBTs, which results in less heat generation during operation. This allows for smaller or less complex cooling systems and can improve overall system efficiency.
- **Higher Thermal Conductivity:** SiC has a higher thermal conductivity than silicon, which allows for better heat spreading within the device and more efficient heat transfer to the cooling system.
- **Higher Temperature Operation:** SiC MOSFETs can operate at higher junction temperatures compared to silicon IGBTs, enabling higher power density and improved reliability in high-temperature environments.

In conclusion, SiC MOSFETs and IGBTs have distinct thermal properties that influence their performance, efficiency, and thermal management requirements in motor controller applications. SiC MOSFETs generally offer superior thermal performance, enabling more compact and efficient cooling solutions, while IGBTs, though more mature and cost-effective, require more robust cooling systems to address their higher power losses and lower thermal conductivity. Engineers must carefully consider these thermal properties when selecting power semiconductor devices and designing cooling systems for motor controllers.

3.8 Automotive Standards for High Voltage Design

In the automotive industry, various standards and guidelines have been established to ensure the safety, reliability, and performance of high voltage systems, such as electric vehicle (EV) powertrains and charging infrastructure. Some of the key standards relevant to high voltage design include:

- **AECQ100** This standard outline the tests and conditions for the automotive grade integrated circuits.
- **AECQ101** Analogically to AECQ100, AECQ101 elaborates on required tests and test conditions for discrete semiconductor devices
- **ISO 26262:** This international standard focuses on the functional safety of electrical and electronic systems in road vehicles, addressing potential hazards caused by system failures and providing a framework for risk assessment, design, and validation.
- **IEC 61851:** This standard covers the conductive charging systems for EVs, specifying requirements for safety, communication, and interoperability between charging equipment and vehicles.
- **UNECE R100:** This regulation, issued by the United Nations Economic Commission for Europe (UNECE), addresses the safety requirements for high voltage components and systems in electrically propelled road vehicles, including protection against electric shock, mechanical stress, and environmental factors.

Compliance with these standards is crucial for ensuring the safety and reliability of high voltage systems in automotive applications, minimizing risks associated with electric shock, electromagnetic compatibility, and system failures, and promoting industry-wide best practices for design, testing, and validation.

3.9 High Voltage PCB Design Challenges

Designing printed circuit boards (PCBs) for high voltage applications presents unique challenges that must be addressed to ensure the safety, reliability, and performance of the system. In this section, we discuss some of the key aspects of high voltage PCB design, including insulation barriers, creepage and clearance, component selection, and trace layout.

3.9.1 Insulation Barriers

Insulation barriers are crucial for isolating high voltage circuits from low voltage circuits or other conductive parts on a PCB. This helps to prevent electrical breakdown, arcing, and unintended current flow between different parts of the circuit. Insulation barriers can be achieved through physical separation, such as air gaps, or by using insulating materials like epoxy or silicone. [18]

3.9.2 Creepage and Clearance

Creepage and clearance are critical parameters in high voltage PCB design, as they determine the minimum distance required between conductive elements to prevent electrical breakdown and arcing. Creepage refers to the distance along the surface of an insulating material between two conductive parts, while clearance is the shortest distance through air between them. Standards such as IEC 60950 and IEC 61010 provide guidelines for minimum creepage and clearance distances based on the working voltage and environmental factors like pollution degree and altitude.

3.9.3 Component Selection

Selecting appropriate components for high voltage applications is essential for ensuring the reliability and safety of the PCB. High voltage components, should be rated for the maximum voltage and temperature conditions they will experience in the application. Additionally, some components may require special insulation or packaging to withstand high voltage stresses and prevent arcing or breakdown. In order to be viable to be used in vehicles, chosen components must adhere to the previously mentioned AECQ100 and AECQ101 standards for integrated circuits and discrete semiconductors respectively.

3.9.4 Trace Layout and Routing

Proper trace layout and routing are critical for managing electric fields and minimizing the risk of arcing or breakdown in high voltage PCBs. Some important considerations for trace layout include:

- **Trace Spacing:** Ensure adequate spacing between high voltage traces to maintain the required creepage and clearance distances.
- **Guard Traces:** Use guard traces or ground planes to shield sensitive low voltage circuits from electric fields generated by high voltage traces.

- **Arc Prevention:** Minimize the risk of arcing by avoiding sharp corners or edges in trace geometry, as these can lead to concentrated electric fields.

- **Thermal Management:** Design traces with sufficient width and thickness to handle the current and heat dissipation requirements of high voltage components, and avoid thermal hotspots.

In summary, high voltage PCB design requires careful attention to insulation barriers, creepage and clearance distances, component selection, and trace layout to ensure the safety, reliability, and performance of the system. By following industry standards and best practices, engineers can effectively address the challenges associated with high voltage PCB design and create robust, reliable solutions for various applications.

Chapter 4

Hardware proposal

In the context of the e-compressor board design, Altium Designer was chosen as the preferred software due to its comprehensive features, powerful capabilities, and ease of use. Altium Designer offers a unified environment for schematic capture, PCB layout, and design documentation, streamlining the design process and enhancing collaboration between team members. Furthermore, its extensive component libraries and advanced design rule checking capabilities facilitate efficient component selection and ensure compliance with industry standards, making it an ideal choice for the development of a high-performance e-compressor board. [13]

4.1 Prototype E-compressor board requirements

Based on the Prototype e-compressor motor controller board should be able to drive 3-phase PMSM motor. This board should accompany all the features necessary for testing and evaluation proposes. Sufficient logic and computing power should be present as well as safety and testing features. Galvanic insulation should be present both, between boards main communication interface and boards micro-controller as well as the high voltage side. Because of this safety feature, board will be split into three galvanicly insulated sections. Redundant features may be added since this board serves mainly as a proof of concept for the e-compressor use case.

USB will be the main communication interface for testing. This USB will be insulated from the rest of the board and should feature USB-UART interface as well as insulated optocuplers or digital insulators. Board will also include CAN interface as the board is aimed at the automotive and CAN bus is widely used in automotive industry as the main communication bus between individual units within the vehicle.

Main computing power will come from micro-controller. Since this definitely is a necessary feature that will be used for the final product, schematic should be minimised and accompany only the base requirements.

For main 3 half bridges used for switching, SiC transistors will be used. Main reason for this choice is the want of cost reduction by increasing the switching frequency and therefore reducing the bulk capacitors on the DC link. These transistors will be accompanied by appropriate insulated gate drivers as well as insulated power supplies.

Current measurement will be done on the output of all three phases. This is necessary for closed loop operation and enables us to implement fast hardware over-current protection for the additional safety.

Resolver excitation and sensing circuitry will be added also as a redundant feature for testing and software implementation.

Low voltage supply schematics will implemented to supply the power for all other functional blocks.

Selection of individual components was mainly done based on the design goals and then based on the availability and cost, since parts of this prototype schematic may be used in future for commercial use. Many parts from ST were easily available and were recommended to me for use as per the intent of the board.

The design process consisted of designing of all the schematics for individual above motioned functional parts.

Specific technical requirements for the board can found in following table.

1. Operating minimal high voltage input 400 V
2. Operating maximal high voltage input 800 V
3. Modulating transistor switching frequency from 15kHz to 70kHz
4. Maximal Power output 5000 W
5. Maximal Current output 12.5 A
6. Low Voltage supply 12 V
7. Safety features in a form of insulated high voltage side and insulated USB
8. redundant features for testing eg. resolver interface, temperature and voltage monitoring and debug LEDs.
9. Replaceable input capacitance for testing.

4.2 Low Voltage Supply

The design of low voltage supply schematics is essential for powering electronic systems and ensuring stable, reliable operation. This section provides an overview of the low voltage supply schematic design process, including key considerations and design steps. For the purpose of this board, input 12 V will be used to power all the electronics. [19]

4.2.1 Power Requirements Analysis

The first step in designing a low voltage supply schematic is to determine the power requirements of the system, including:

- **Voltage Levels:** Identify the voltage levels required by the various components and subsystems in the application.
- **Current Consumption:** Estimate the current consumption of each component or subsystem, considering both steady-state and transient conditions.
- **Power Budget:** Calculate the total power consumption of the system and allocate a power budget for each voltage rail.

4.2.2 Power Supply Selection

Based on the power requirements analysis, select appropriate power supply solutions for each voltage rail. Some common types of low voltage power supplies include:

- **Linear Regulators:** Simple and cost-effective, linear regulators provide a stable output voltage by dissipating excess power as heat. They are suitable for low power applications with minimal noise and efficiency requirements.
- **Switching Regulators:** Switching regulators, such as buck or boost converters, offer higher efficiency and flexibility compared to linear regulators. They are suitable for applications with higher power requirements or strict efficiency constraints.
- **Module-Based Solutions:** Pre-built power supply modules offer a compact, convenient solution for various voltage rails, often with integrated features like filtering, protection, and monitoring.

4.2.3 Schematic Design and Component Selection

With the power supplies selected, proceed to create the schematic, ensuring proper connectivity and component selection:

- **Input and Output Filtering:** Include input and output capacitors to filter voltage ripple and reduce noise in the power supply. Choose capacitors with appropriate voltage and temperature ratings.
- **Protection Circuits:** Implement protection features such as over-voltage, over-current, and short-circuit protection to ensure the safety and reliability of the power supply.
- **Thermal Management:** Consider the power dissipation and thermal performance of components through thermal vias, if necessary.

Following this design process, it was determined that the 12 V supply should be sufficient to power most of the electronics directly, with only auxiliary power supply needed for 5 V required to power microprocessor as well as some logic and gate drivers. Current consumption of the 5 V rail was estimated to be around 450 mA. As a cost reduction and for simplicity of the design, it was desired to use $L4995AJ$ linear regulator from 12 V to 5 V but this regulator is only rated for 500 mA. It was decided then to also include Modul-Based Switched-mode power supply rated for 1 A as a backup.

Auxiliary connector for external 5 V supply was added for testing and evaluation purposes. Built in fuse was not needed, since this prototype will only be powered from laboratory power supply with current limiting capability anyway and for a future, final product board will be fused externally in vehicles fuse-box. Input filter was also added for additional electromagnetic compatibility.

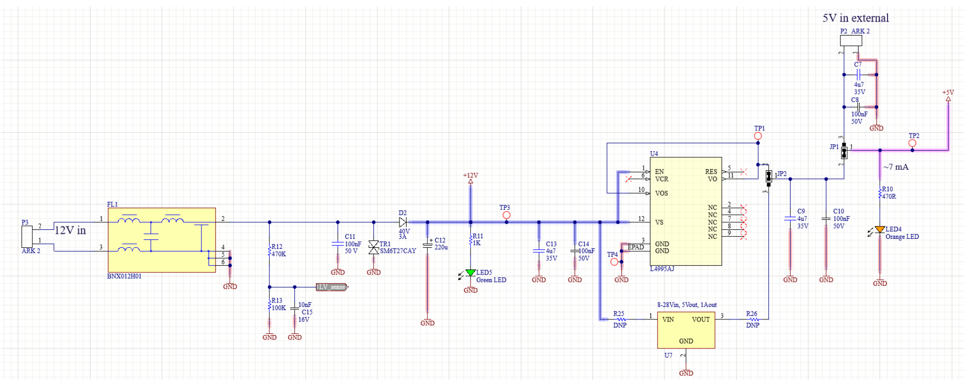

Figure 4.1: Low voltage supply schematic

4.3 High Voltage Side of the E-compressor Board

The high voltage side of an e-compressor board is crucial for effectively controlling and monitoring the electric motor in electrically driven compressors.

4.3.1 B6 SiC Transistor Configuration

The B6 SiC transistor configuration, also known as a six-pack configuration, consists of six Silicon Carbide (SiC) transistors arranged in a three-phase bridge configuration. SiC transistors offer significant advantages over traditional Insulated Gate Bipolar Transistors (IGBTs), such as faster switching speeds, lower switching losses, and improved thermal performance. For low power application such as e-compressor, resistive drain-source characteristic will result in greater efficiency than the constant voltage drop, associated with IGBTs. These characteristics make SiC transistors an excellent choice for high voltage, high power applications like e-compressor motor control. This configuration was chosen as it is a common way of modulating sine wave for each phase. Input common mode choke was also added for additional electromagnetic compatibility. Transistors chosen for this purposes were six, discrete $SCT070HU120G3AG$ MOSFETs. These SiC MOSFETs feature maximal Drain-Source voltage of 1200V, Static drain-source on-resistance of $63m\Omega$ and packaged in HU3PAK. One of the advantages of this packages is dedicated kelvin source pin, which does only carry switching current. [20]

4.3.2 Input Capacitance

The motor controller input capacitance is a critical component for filtering and decoupling the high voltage DC bus. Properly sized input capacitors ensure stable voltage supply to the motor controller, minimize voltage ripple, and reduce the impact of voltage transients caused by switching events. It is essential to choose capacitors with appropriate voltage ratings, capacitance values, and temperature characteristics to ensure reliable operation under various operating conditions.

It is difficult to estimate the input capacitance needed for for this purpose. In practice, there are unknown variables regarding the power source, inductance of the input and output lines and motor parameters. It is possible to to substitute the input schematic including connecting lines and power source with RLC resonant circuit [12] that can be described by following equations:

$$f_0 = 2\pi\omega_0 \tag{4.1}$$

$$\omega_0 = \frac{1}{\sqrt{LC}} \tag{4.2}$$

$$\zeta = \frac{\alpha}{\omega_0} \tag{4.3}$$

$$\alpha = \frac{R}{2L} \tag{4.4}$$

Where R,L,C describe their respective values, f_0 is the resonant frequency of the circuit, ω_0 is the resonant angular velocity, ζ is the damping factor and α is the damping. Critical dampening is the lowest value of ζ where no arbitrary oscillations occur. Solving these equations for C knowing all other variables and having damping factor $\zeta < 1$ (critical dampening), would give us reasonable estimate for input capacitance. This method is not useful for us because of unknown particular use-cases of the e-compressor board.

Therefore i have decided to derive input capacitance from energy needed at a certain voltage and switching frequency to be able to cover energy of the arbitrary switching pulse during peak load scenario with certain ripple. This method disregards power input source and compares only resulted ripple on the capacitor with desired energy and size of the pulse. As input power source is only used here to charge input capacitance and not for directly contributing to negating the resulted ripple, it can be expected to get higher capacitance values than actually needed. Capacitor ESR or equivalent series resistance is though also disregarded, resulting in slightly lower results than expected.

$$E_c = \frac{1}{2}CU^2 \tag{4.5}$$

$$E_{ripple} = \frac{0.5}{f_{sw}} \cdot P_{peak} \tag{4.6}$$

$$E_c initial - E_c final = E_{ripple} \tag{4.7}$$

$$C = \frac{2 \cdot P_{peak}}{f_{sw} \cdot (U^2 - (U - U_r)^2)} \tag{4.8}$$

E_{ripple}... energy of the ripple
f_{sw}... switching frequency
P_{peak}... Peak power
$E_c initial$... Energy stored in capacitor initially
$E_c final$... Energy stored in capacitor after the pulse U... Input DC voltage
U_r... ripple voltage

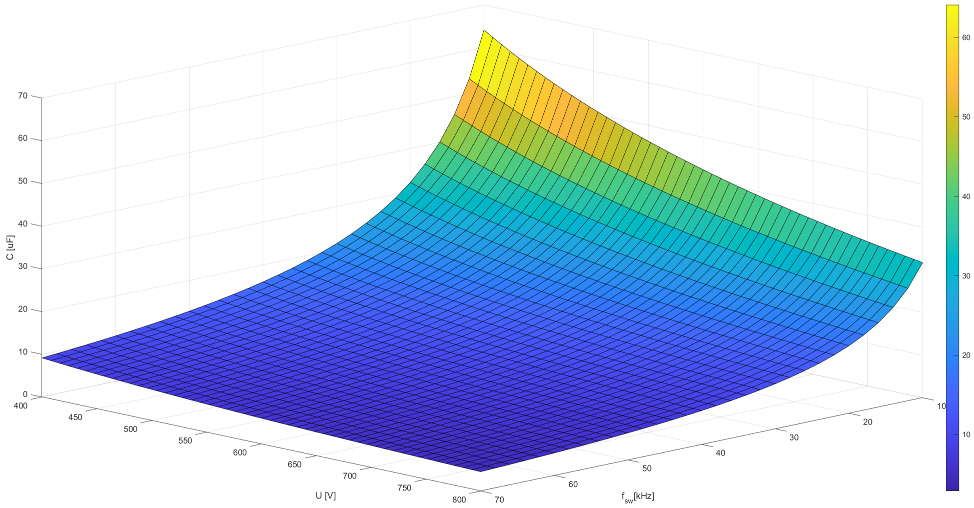

Figure 4.2: 3D graph of minimal input capacitance based on switching frequency and input voltage with fixed ripple

From the equation 4.8, following 3D graph was created. Based on the recommendations from industry experts from STMicroelectronics, voltage ripple of 20V should be acceptable for this application.

Minimal needed capacitance for given voltage ripple varies significantly, based both on the voltage and switching frequency. Minimising the input capacitance in the final design is desirable through space, weight and cost, though for this prototype, it was decided to include variety of footprints capable of housing multiple combinations of capacitors. These capacitors can be added or removed, depending on the exact testing scenario at any given point. Maximal theoretical capacitance needed was around $65\mu F$ but as a safety margin, it was decided to to increase that to $120\mu F$. Even though, through parasitic inductance, it is desirable for the input capacitance to be placed as close to the switching transistors, it is difficult to achieve through proper placement. Any combination of input capacitors will therefore be complimented with smaller decoupling capacitors placed as close as possible to the transistors themselves.

4.3.3 Three-Phase Current Measurement

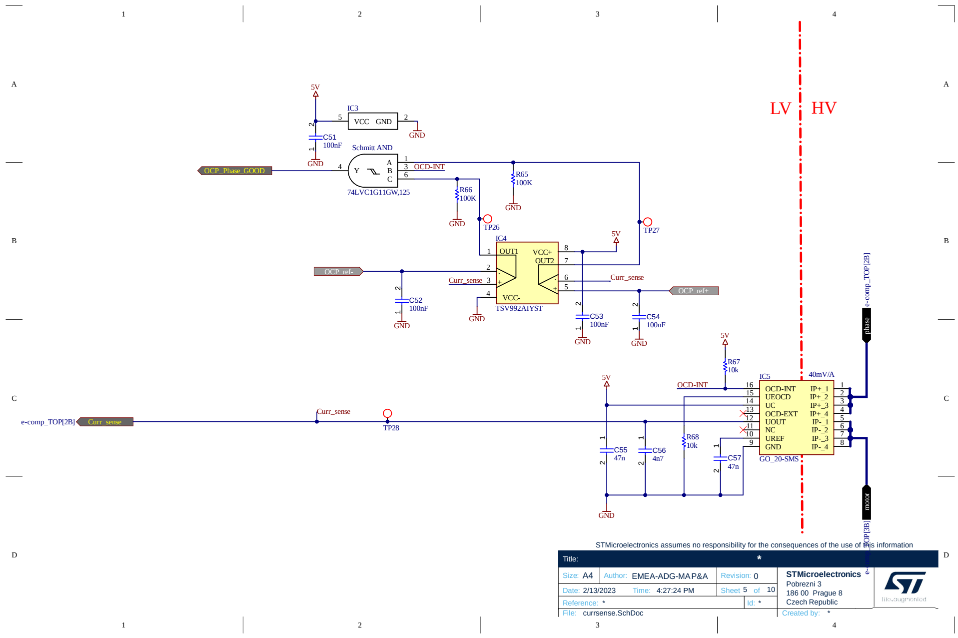

Figure 4.3: Current sensing schematic

Accurate current measurement for all three phases is essential for precise motor control and protection. Current sensors, such as Hall-effect sensors or current transformers, can be used to measure the phase currents in the motor windings. These current measurements are typically fed back to the motor controller, which uses them to implement control algorithms like Field Oriented Control (FOC) or Direct Torque Control (DTC) and to monitor the system for fault conditions like over-current or phase imbalance.

Even though only two current measurements are needed for FOC, for hardware over-current protection it was desirable to measure all three phases. Integrated circuit from LEM GO 20-SMS SP3 was chosen due to its availability and sufficient datasheet ratings.

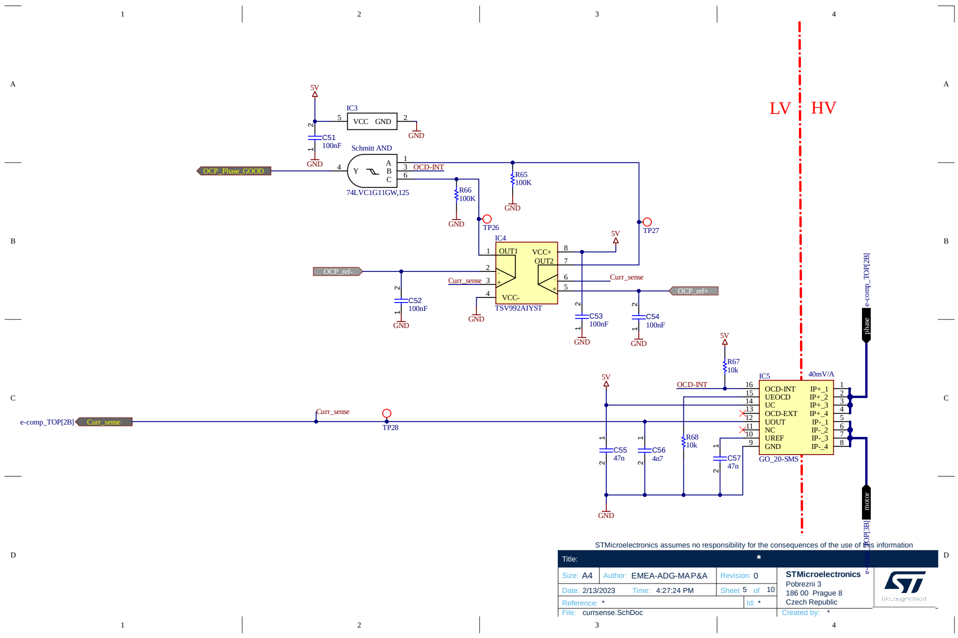

Figure 4.4: Current sensing schematic

4.3.4 Insulated Voltage Measurement

Insulated voltage measurement is vital for monitoring the voltage levels across the motor windings while ensuring electrical isolation between the high voltage side and the low voltage control electronics. Insulated voltage measurements can be achieved using isolated voltage sensors, such as high voltage differential probes or isolated amplifiers. These sensors provide a safe, accurate means of measuring high voltage signals while maintaining the required insulation barriers and meeting creepage and clearance requirements.

Insulated operational amplifier was used with voltage divider across that main DC-link lines that will send analog signal to the microcontrollers analog to digital converters. Additional insulated low voltage source was needed to power high voltage side of this amplifier.

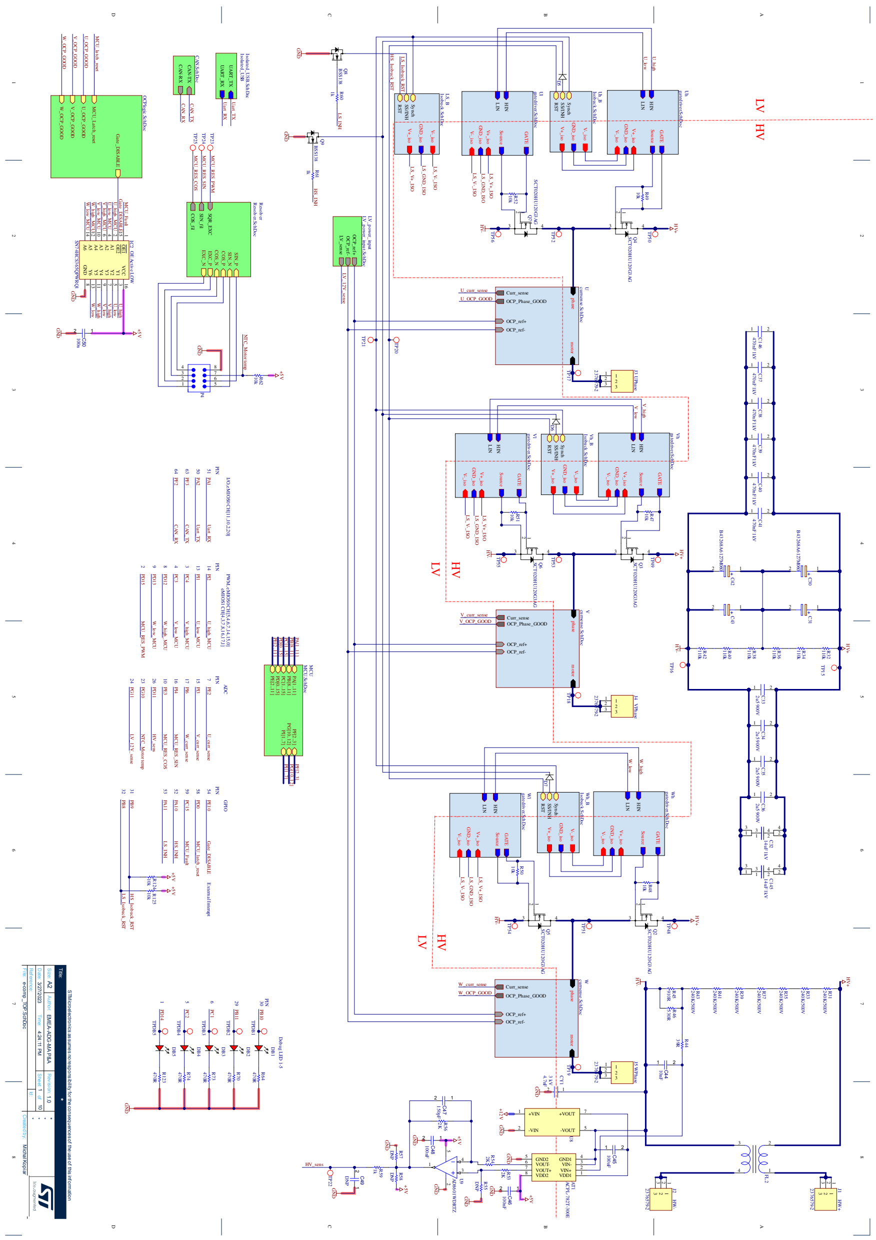

Figure 4.5: Top schematic, including all the functional blocks

4.4 Insulated Gate Drivers and Insulated Power Source Methods for E-compressor Board

For e-compressor boards, ensuring proper isolation between the high voltage side and the low voltage control electronics is crucial for safety and reliability. Insulated gate drivers and insulated power sources play a critical role in maintaining this isolation while providing the necessary drive signals and power supply. This section discusses the use of insulated gate drivers and insulated power source methods applicable for e-compressor boards.

4.4.1 Insulated Gate Drivers

Insulated gate drivers provide electrical isolation between the low voltage control signals and the high voltage power switches, such as SiC transistors or IGBTs, used in the motor control circuit. These gate drivers transfer the control signals across an isolation barrier, allowing for precise and safe control of the power switches.

Since following part of the schematic will be integral to the functionality of the prototype e-compressor board as well as final product, it was advantageous to try minimising the design as much as possible. Chosen were *STGAP2SICSA* for their availability, low cost ant ease of implementation. Gate driver schematic was then implemented as follows:

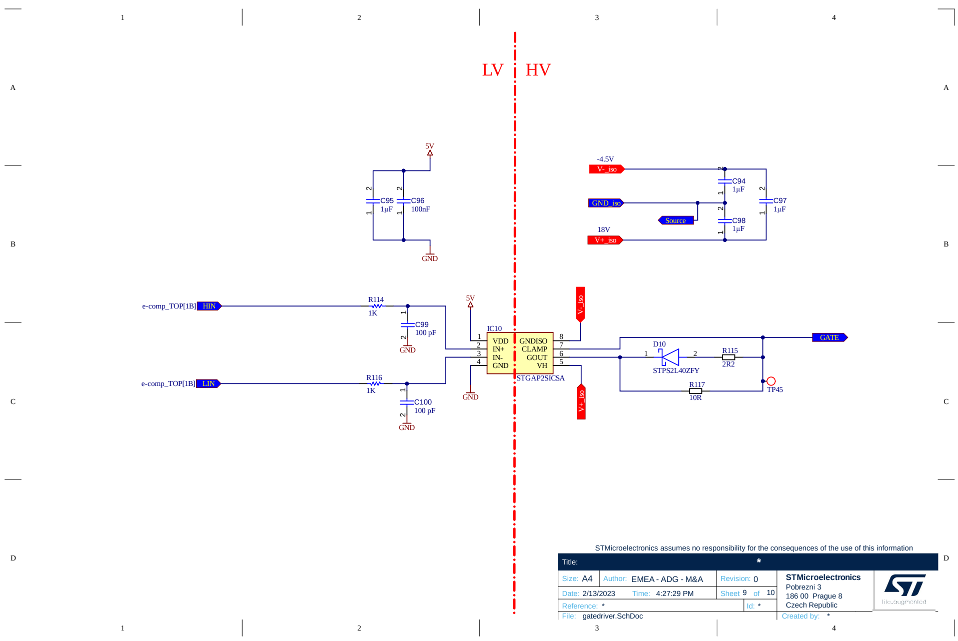

Figure 4.6: Gate driver schematic

It is specifically designed to offer robust protection against detrimental Miller turn-on events. [21]

The Miller effect is an inherent characteristic of these categories of transistors. During periods of rapidly switching voltage or load transient, an undesired increment in the drain-to-source voltage (V_{ds}) can trigger a current via the gate-drain capacitance (C_{gd}), referred to as the Miller capacitance. This inadvertently actuates the transistor, leading to potential short-circuit conditions, which could be damaging.

The Miller clamp counteracts this phenomenon by establishing an additional low-impedance conduit from the gate to the source when the transistor is in the off-state. This configuration ensures that any charge injected into the gate via the Miller capacitance is promptly shunted to the source, thus circumventing an undesired turn-on.

Therefore, the implementation of a Miller clamp significantly enhances the reliability and robustness of power electronic systems employing high-speed or high-power IGBTs and MOSFETs. This is particularly critical in high-voltage or high-switching-frequency applications.

4.4.2 Insulated power source

In addition to insulated gate drivers, e-compressor boards require isolated power sources to supply the necessary voltage rails for the high voltage side components such as gate drivers. Driving the individual transistors properly does require negative voltage U_{gs} of -4.5V for gate closure as well as positive +18V for the gate to fully open. These values were taken directly from the transistors datasheet. Since transistors source of all low side switches will be the same $HV-$, one insulated power source will be enough for driving. Source of high side transistors will be the output phase and the insulated power sources will require properer phase biasing which will be different for each phase.

It leads us to the implementation of four insulated power sources. Power requirement for these sources can be estimated from the parasitic Gate-Source capacitance and switching frequency. It can be assumed as well, that implemented power source will need to power one charging and one discharging of the parasitic Gate-Source capacitance per switching cycle. Full voltage range of the power source will therefore need to be 22.5V and calculating for worst case scenario of $70kHz$ switching frequency. Data-sheet value for Gate-Source charge is $36nC$

$$P = U \cdot I \tag{4.9}$$

$$I = \frac{Q}{t} \tag{4.10}$$

$$t = \frac{1}{f_{sw}} \tag{4.11}$$

$$P = 2 \cdot U \cdot Q \cdot f_{sw} = 0.1134W \tag{4.12}$$

With sufficient safety margin it can assumed that the peak power draw for each transistor to be $0.2W$. This would result in power source leading to the three low side transistors being able to provide at least $0.6W$ of power.

Due to the part availability, robustness and sufficient power requirements to power switching for all low side transistors, it was decided to use $A6986ITR$ controller in the iso-buck topology. Even though not required as per power delivery, for ease of implementation and component ordering, it was decided that the this power source would also be used for high-side transistors. It also features Miller clamp which is an integral feature of Insulated-Gate Bipolar Transistor (IGBT) and Metal-Oxide-Semiconductor Field-Effect Transistor (MOSFET) gate drivers.

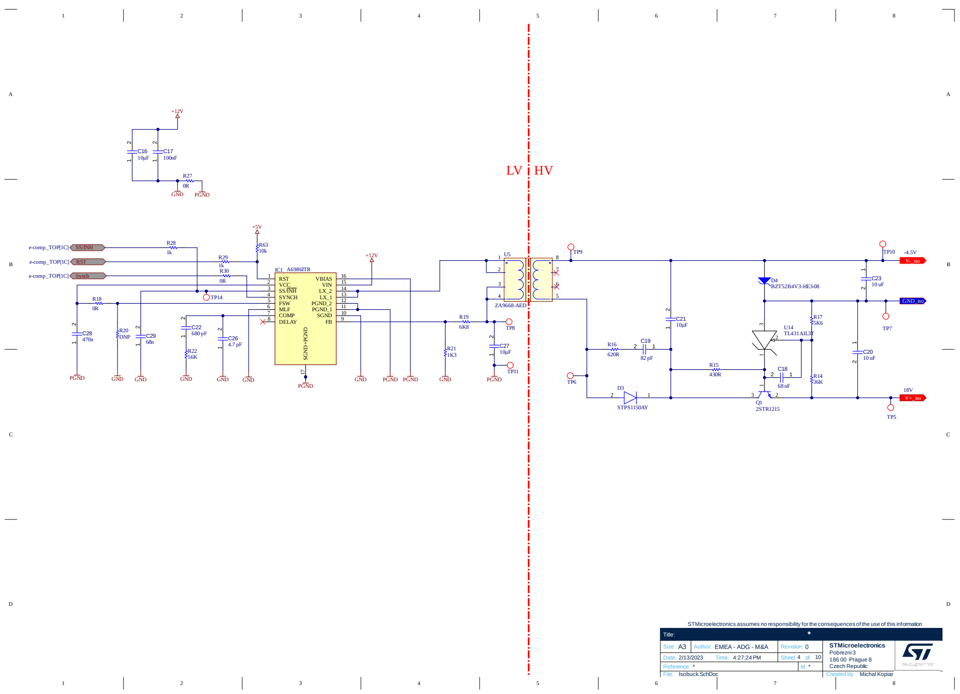

Figure 4.7: Iso-Buck schematic implementation

4.5 Microcontroller, Insulated USB, and CAN Implementation for E-compressor Board

In the design of an e-compressor board, proper implementation of the microcontroller, USB, and CAN interfaces is crucial to ensure efficient communication and data transfer between various components. This section discusses the integration of these elements in the context of an e-compressor board, with a focus on the insulated USB interface.

4.5.1 Microcontroller

The microcontroller serves as the central processing unit for the e-compressor board, orchestrating the control of the motor and coordinating communication with other vehicle systems. The microcontroller firmware includes algorithms for motor control, fault detection, and protection mechanisms. In addition, it is responsible for interfacing with the gate drivers, current and voltage sensors, and communication interfaces such as USB and CAN.

An essential aspect of the microcontroller's functionality is the integration of Analog-to-Digital Converters (ADCs) and precision timers. ADCs are required for accurate measurement and processing analog signals from various sensors, such as current and voltage sensors, which are crucial for motor control and diagnostics. Precision timers, on the other hand, enable precise control of motor commutation and PWM signals for the gate drivers, ensuring efficient and smooth motor operation. Furthermore, timers can be utilized for implementing time-critical tasks, such as fault detection and protection mechanisms, as well as coordinating the execution of multiple tasks within the microcontroller firmware. For this purpose, $SPC584B$ microcontroller was chosen due to its availability, low power consumption and sufficient peripherals for the e-compressor application. I addition, for programming and testing needs, JTAG interface was also implemented.

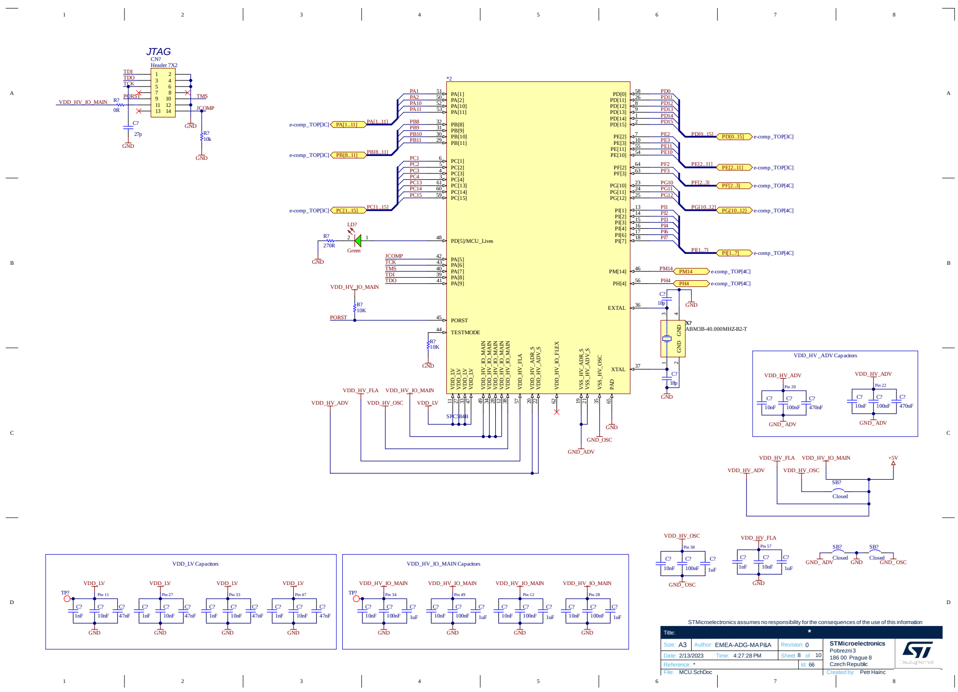

Figure 4.8: Microcontroller schematic implementation

4.5.2 Insulated USB Interface

An insulated USB interface is employed in the e-compressor board to ensure safe and reliable data exchange between the board and external devices such as a PC. Insulation of the USB interface helps in preventing ground loops, reducing noise, and protecting the board from potential damage due to voltage spikes or surges. Optocouplers or digital isolators are typically used to achieve the necessary insulation, ensuring that data can be transmitted while maintaining electrical isolation between the e-compressor board and the connected device.

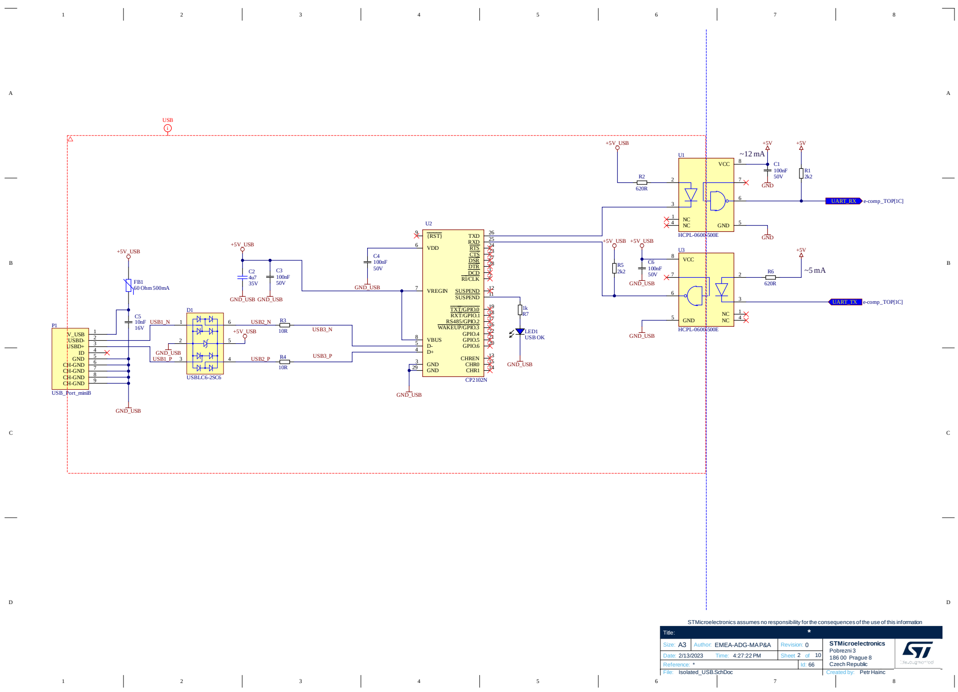

Figure 4.9: Insulated USB interface

4.5.3 CAN Interface

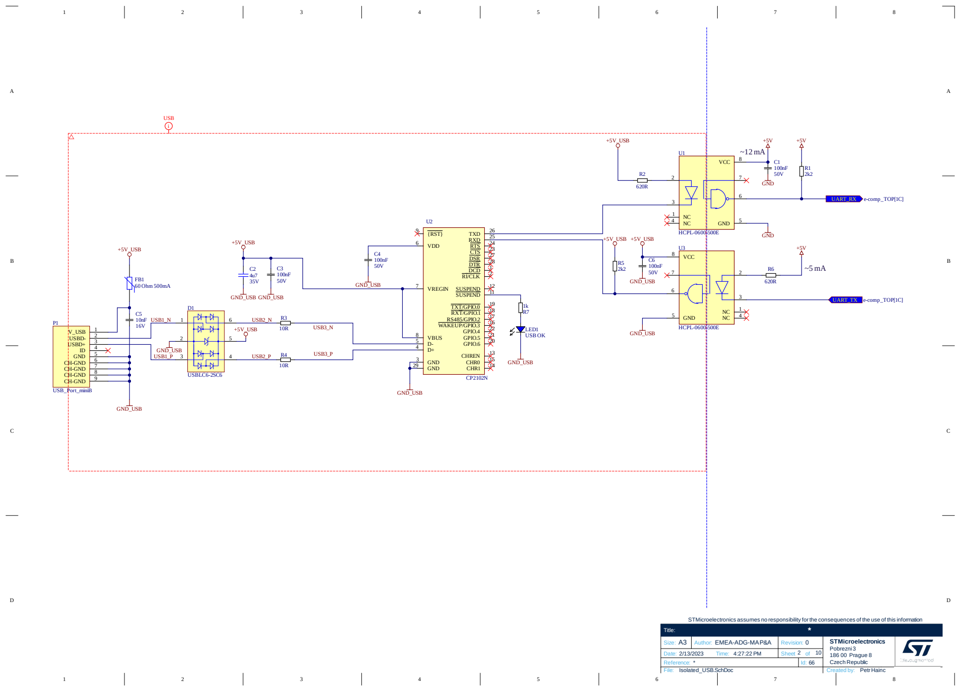

Figure 4.10: CAN interface schematic

The Controller Area Network (CAN) interface is a widely adopted communication protocol in the automotive industry. The integration of a microcontroller, insulated USB interface, and CAN communication in the e-compressor board design is essential for effective motor control, data exchange, and interaction with other vehicle systems. By carefully implementing these elements, engineers can develop a highly efficient and reliable e-compressor board that meets the stringent requirements of modern electric vehicles.

4.6 Over-current protection circuitry

In the context of an prototype e-compressor board, implementing effective over-current protection (OCP) is essential to ensure the safety and reliability of the system. This section discusses the design of hardware-based OCP mechanisms and highlights their importance in preventing potential damage to the motor, power electronics, and other components of the e-compressor board. [22]

Over-current conditions can result from various factors, such as short circuits, excessive motor loads, or control algorithm failures. If left unaddressed, over-current can lead to overheating, component degradation, or catastrophic failure, posing significant risks to the system and its surrounding environment. Therefore, implementing robust OCP mechanisms is crucial to detect and mitigate over-current events promptly, thereby enhancing the safety and longevity of the e-compressor board.

4.6.1 Hardware OCP Mechanisms

Hardware-based OCP mechanisms rely on dedicated components and circuits to monitor current levels and respond to over-current events autonomously, without relying on the microcontroller's intervention. Some common hardware OCP mechanisms include:

- **Current Sensing:** Accurate current sensing is the foundation of effective OCP. Current sensors, are employed to monitor the current flowing through the motor or power electronics. The sensed current is then compared to a predefined threshold to detect over-current events.
- **Comparators and Thresholds:** Comparators are used to compare the sensed current with a predefined threshold. When the current exceeds the threshold, the comparator triggers a response to protect the system from over-current damage.
- **Protection Circuitry:** Upon detection of an over-current event, the protection circuitry acts to mitigate the issue. This may involve disabling the gate drivers or activating fault indicators to alert the microcontroller and other systems.
- **Latch:** Detected over-current must keep mitigating proper functionality until external action takes place.

4.6.2 Benefits of Hardware OCP

Hardware OCP mechanisms offer several benefits, including:

- Fast response times, allowing for prompt detection and mitigation of over-current events
- Autonomous operation, reducing the burden on the microcontroller and ensuring protection even in the event of firmware issues or microcontroller failures
- Enhanced system reliability, by minimizing the risk of damage to critical components and extending their service life

Schematic implementation takes signal from current measurement for all three phases individually 4.4. For fast damage mitigation, positive and negative maximums are compared to the adjustable references 4.1. These three signals then represent, weather the detected current is within set boundaries. This logic signal is then supplied to the positive-edge-triggered D-Type Flip-Flop where positive edge detection enables us to prevent self unlatching due to series of over current failures and provides extremely fast response to the given signal. Flip-Flop can be reset by microcontrollers signal or external button on the PCB.

All gate driving signals are buffered 4.5, with our OCP output enabling this buffer, effectively shutting down all the gate signals and fully switching off all the main switching SiC transistors.

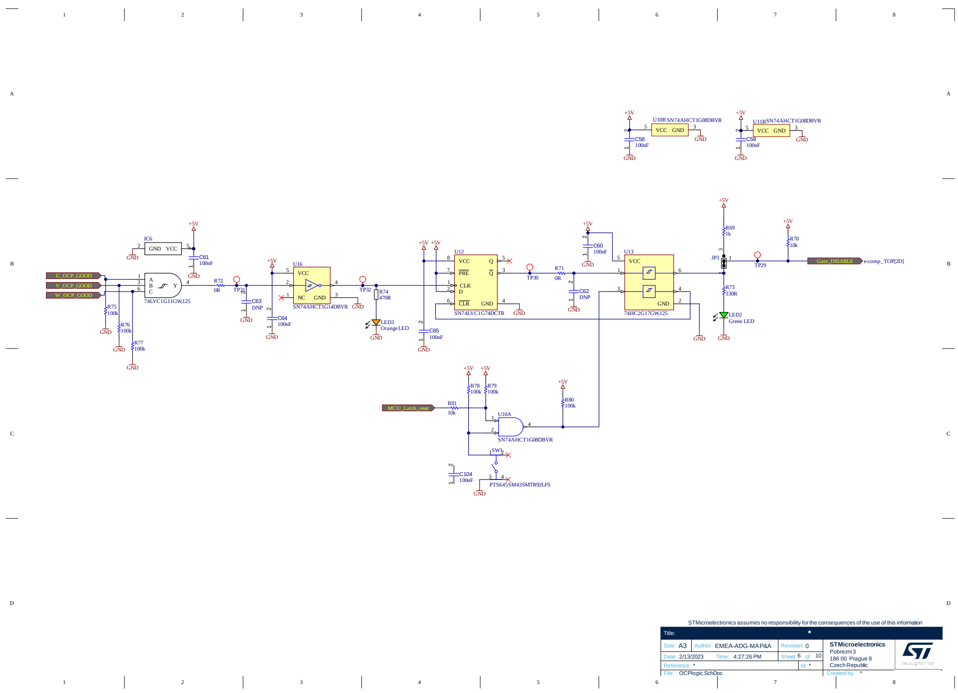

Figure 4.11: Over-current protection logic

4.7 Resolver interface

Resolvers are widely used for precise rotor position sensing, which is essential for effective motor control. This section discusses the design and implementation of resolver excitation circuitry and signal evaluation methods, focusing on their role in obtaining accurate rotor position information.

4.7.1 Resolver Excitation Circuitry

The excitation circuitry plays a critical role in the operation of a resolver, providing a sinusoidal excitation signal to the resolver's primary winding. This signal is typically generated using an oscillator followed by a power amplifier, ensuring a stable and well-defined frequency and amplitude. The excitation signal frequency typically ranges from a few kHz up to tens of kHz, depending on the resolver's specifications and the desired system performance.

In order to maintain signal integrity and minimize the impact of noise or disturbances, it is essential to design the excitation circuitry with proper grounding, shielding, and filtering techniques. Furthermore, the use of high-quality components and robust PCB layout practices can contribute to the overall reliability and accuracy of the resolver system.

4.7.2 Resolver Signal Evaluation

Once the resolver's primary winding is excited, the secondary windings generate sinusoidal signals that are modulated by the rotor's position. The evaluation of these signals is crucial for determining the rotor position accurately. Resolver-to-digital converters (RDCs) or dedicated resolver interface circuits are commonly used for this purpose, performing the following tasks:

- **Signal Conditioning:** Conditioning the resolver's secondary signals, which may involve amplification, filtering, or buffering, to ensure compatibility with the signal evaluation circuitry.
- **Synchronization:** Synchronizing the evaluation process with the excitation signal, typically by using a phase-locked loop (PLL) or similar techniques, to maintain coherence between the excitation and secondary signals.
- **Demodulation and Conversion:** Demodulating the resolver's secondary signals and converting the modulated sinusoids into a digital position value. This process usually involves analog-to-digital conversion, followed by arctangent computation or lookup table-based methods to obtain the rotor position.

4.7.3 Performance Considerations

The accuracy and performance of the resolver system largely depend on the quality of the excitation circuitry and the signal evaluation methods. Some key factors affecting the performance include:

- Excitation signal stability, frequency, and amplitude
- Signal conditioning and filtering techniques
- Synchronization and demodulation algorithms
- Noise immunity and robustness against disturbances

Since the design should account for any potential resolver, excitation as well as input filtering were designed so that with very little changes, it can be made to work with different voltages and frequencies. Extensive simulations were done for this analog part in particular. Simulations shown in figures 4.13 and 4.14 show viability, of designed schematic to filter PWM signal to excitation Sine wave as well as input Sine or Cosine signals filtering to the microcontrollers ADC input.

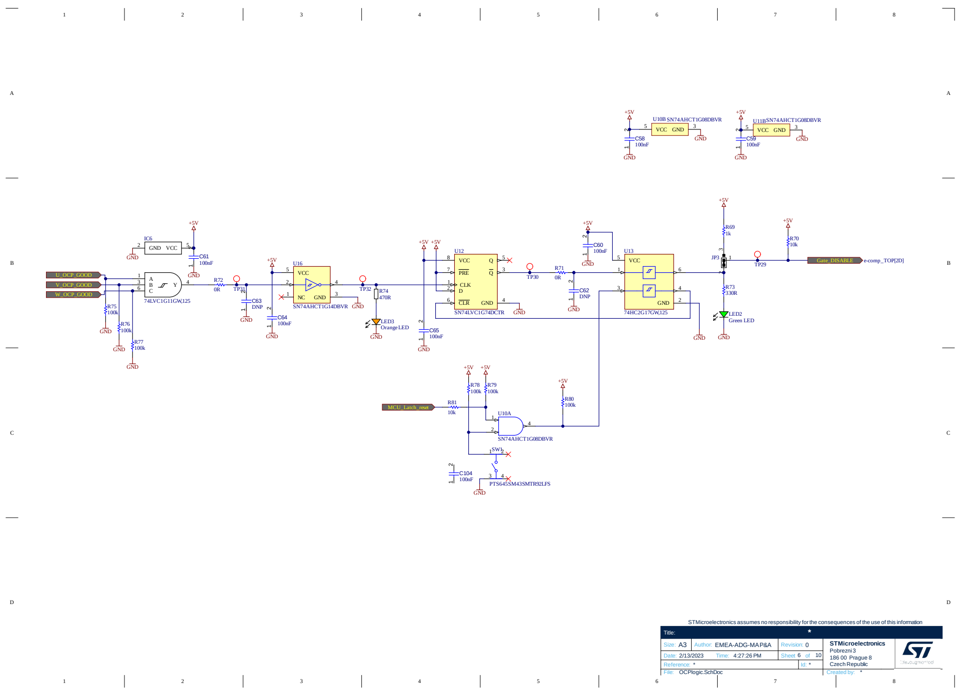

Figure 4.12: Excitation schematic simulation

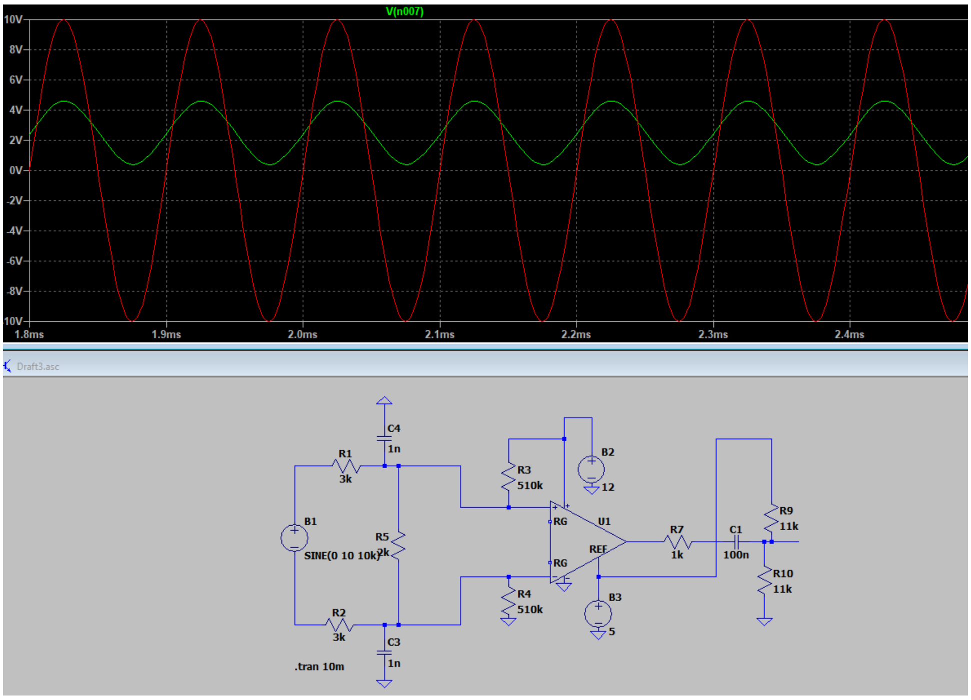

Figure 4.13: Input filtering simulation

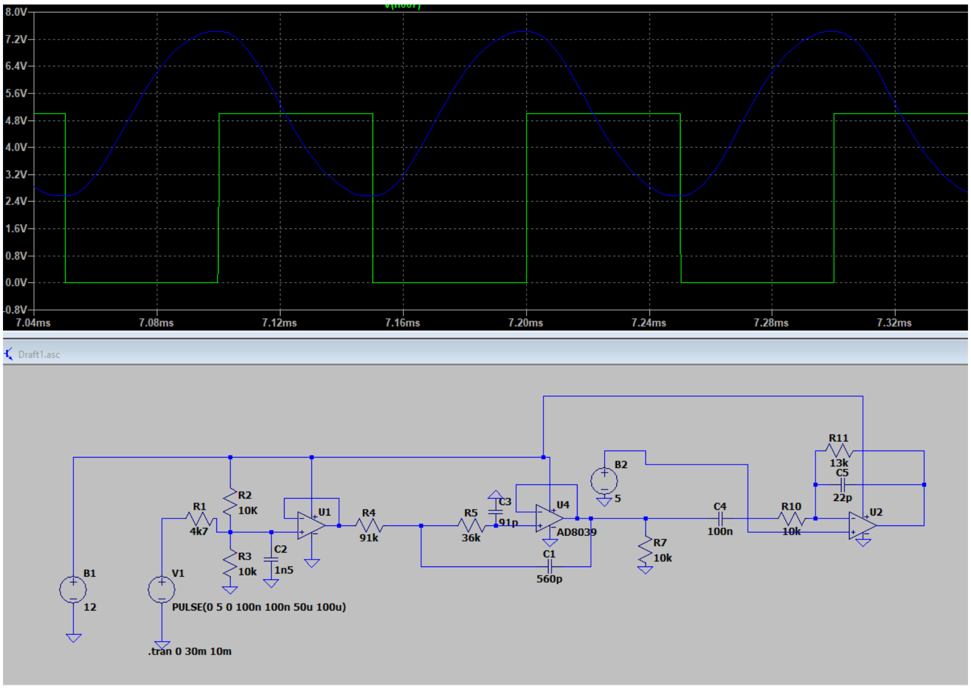

Figure 4.14: Resolver Interface

4.8 Schematic Implementation and Final Board Layout

The transformation of a schematic into a final board layout is a crucial step in the development of an e-compressor board. The process involves translating the abstract representation of the circuit (the schematic) into a physical representation (the PCB layout) that can be manufactured. This section discusses key aspects of this process, including component placement, routing, and design for manufacturability. [23]

4.8.1 Component Placement

The initial step in PCB layout is component placement, which involves arranging the components on the board in a way that optimizes signal integrity, power distribution, thermal management, and board size. For the e-compressor board, high-power components like SiC transistors and capacitors should be placed close to each other to minimize the loop inductance. In contrast, sensitive components, such as the resolver interface circuit, should be placed away from noise sources.

4.8.2 Routing

Once the components are appropriately placed, the next step is routing, which involves connecting the components according to the schematic using PCB traces. Special attention should be given to high-voltage and high-current paths to ensure they can handle the required voltage and current without overheating. Additionally, the routing for sensitive signals, such as resolver signals, should be carefully designed to avoid cross-talk and interference.

4.8.3 Final Layout Verification

Before proceeding to manufacturing, the final layout should be thoroughly verified against the schematic for any errors or discrepancies. This includes checking for missing connections, incorrectly placed components, and potential thermal issues. Tools like Design Rule Check (DRC) and Layout Versus Schematic (LVS) can be employed to automate some parts of this verification process. At the end of this process following design was created and manufactured. Two e-compressor PCBs were populated, one for testing purposes and one for marketing presentation purposes.

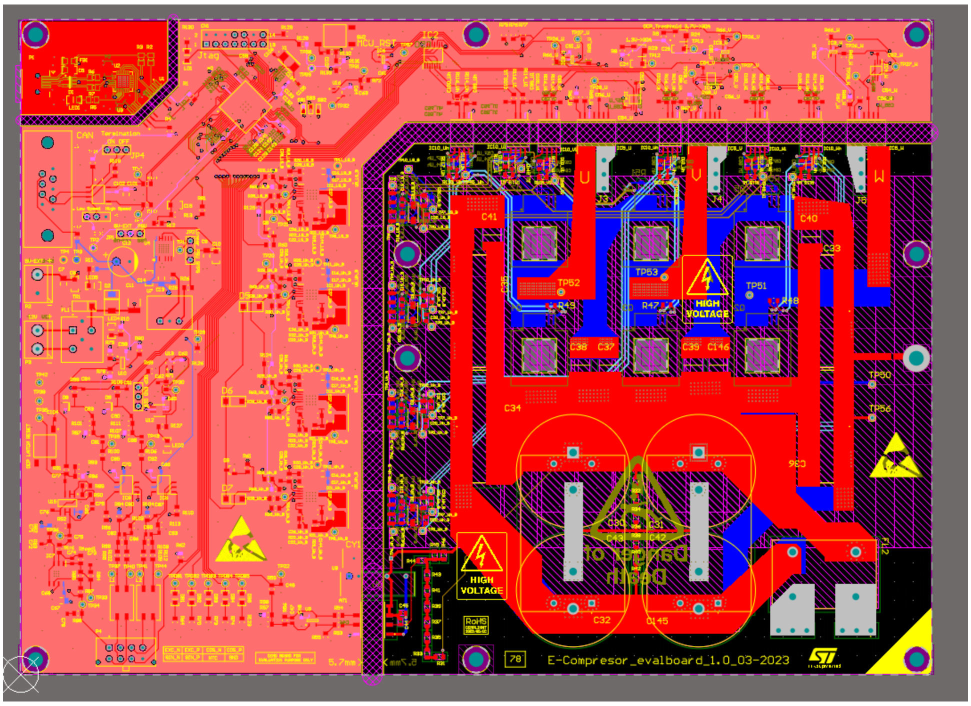

Figure 4.15: Final layout and placement

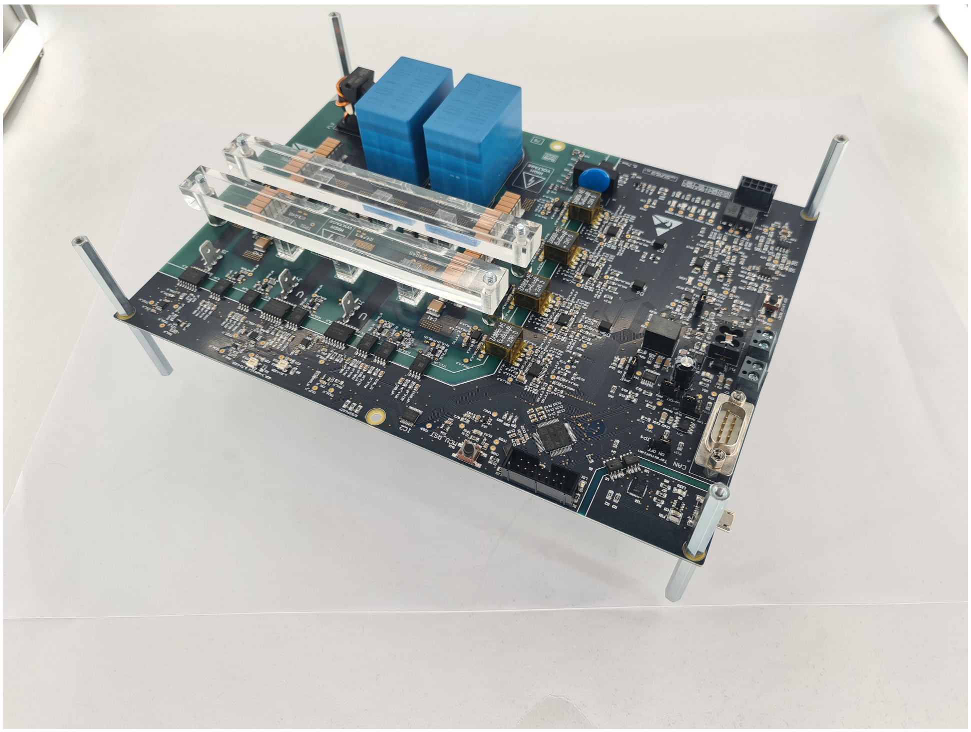

Figure 4.16: Demonstration board with plexiglass cooler

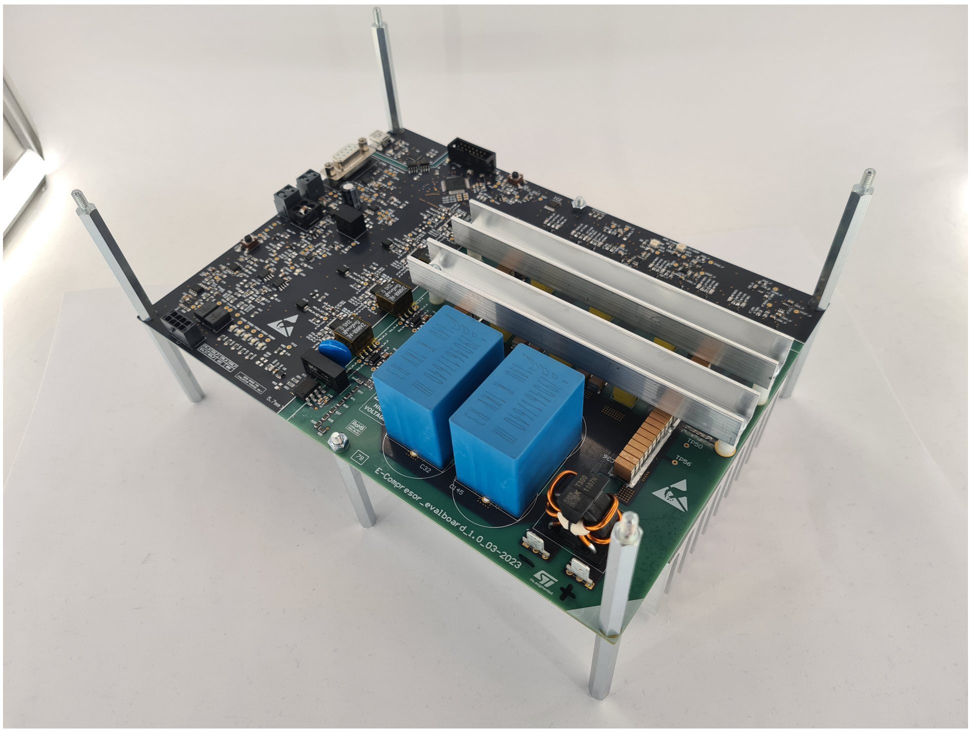

Figure 4.17: Testing board with aluminum cooler

Chapter 5

Testing

E-compressor board testing was subdivided for testing of its individual functional blocks. Power consumption of the 5V system was 430mA and therefore suitable for both options for 5V PSU. All the testing was done in laboratory conditions, with safety limits on all power supplies. Most of the measurements were done using high precision oscilloscope or millimeter, unless specified otherwise.

Figure 5.1: Testing environment and equipment

5.1 Insulated high voltage measurement testing

Testing of the high voltage insulated measurement was extremely important for overall reasons. High linearity was to be expected on the full range of input voltages. Power source available for this testing reached maximum of 750V.

Measurement was done with with oscilloscope, measuring between ground and low voltage side signal output, just before the microcontroller. It can therefore be assumed that microcontrollers ADC will be provided with the same voltages. Reading for the input voltage were taken from the power supply display it self. As there is no switching or current drawn during this testing, it was considered to be the same on the boards measuring points.

Following table represents data measured, as well as comparison to the subsequently calculated linear regression values for the same input voltages.

$$U_{out} = 0.7781 \cdot U_{in} + 2579.2619 \tag{5.1}$$

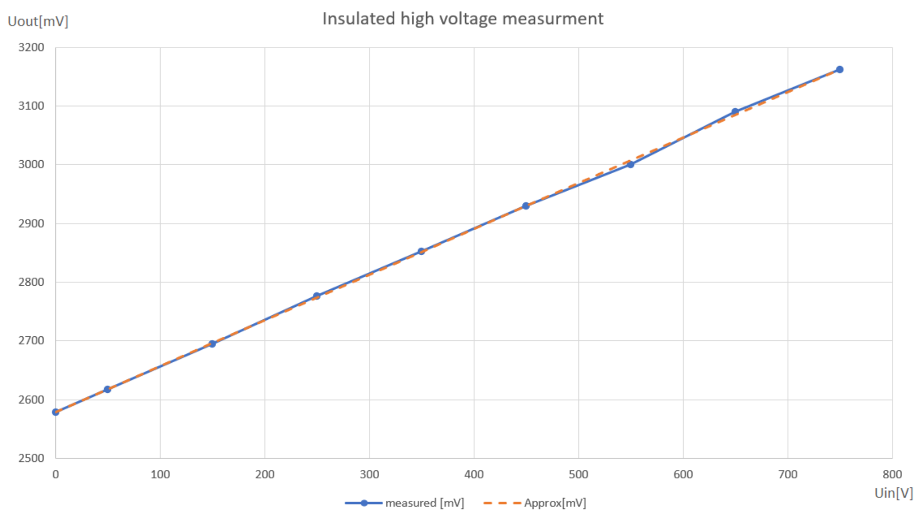

Figure 5.2: Insulated High voltage measurment

With the Linear correlation coefficient being equal to 0.9999 i do presume, that the above mentioned function will be sufficient as an approximation.

Table 5.1: Insulated high voltage measurement data

Uin[V]	measured [mV]	Approx[mV]
0	2579	2579,2619
50	2618	2618,1669
150	2695	2695,9769
250	2776	2773,7869
350	2852	2851,5969
450	2930	2929,4069
550	3001	3007,2169
650	3090	3085,0269
750	3162	3162,8369

5.2 Iso-buck testing

Since the measurement process was already described in previous section, i will further only display measured data and elaborate on the results.

High voltage peak across the diode 5.3 can be attributed to the diodes reverse recovery time in combination with the transformers inherit output inductance. This effect was expected through the prior testing with the iso-buck testing kit as well as datasheet. Output voltages were stable across all four insulated power supplies. All output voltages were between 22.5V and 23V between V-iso and V+iso with GNDiso being 4.5V above the V-iso. Output ripple can be seen in 5.4.

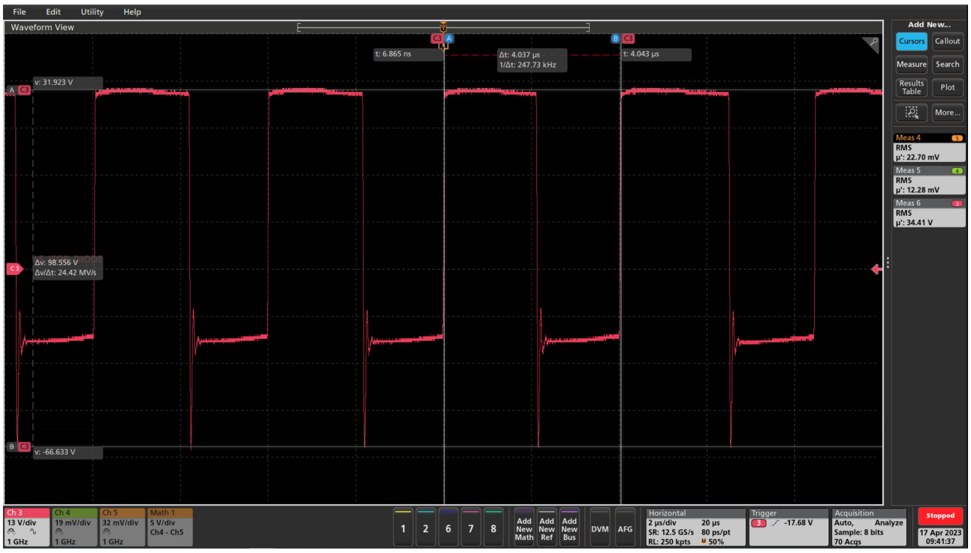

Figure 5.3: Insulated output voltage across D3 diode

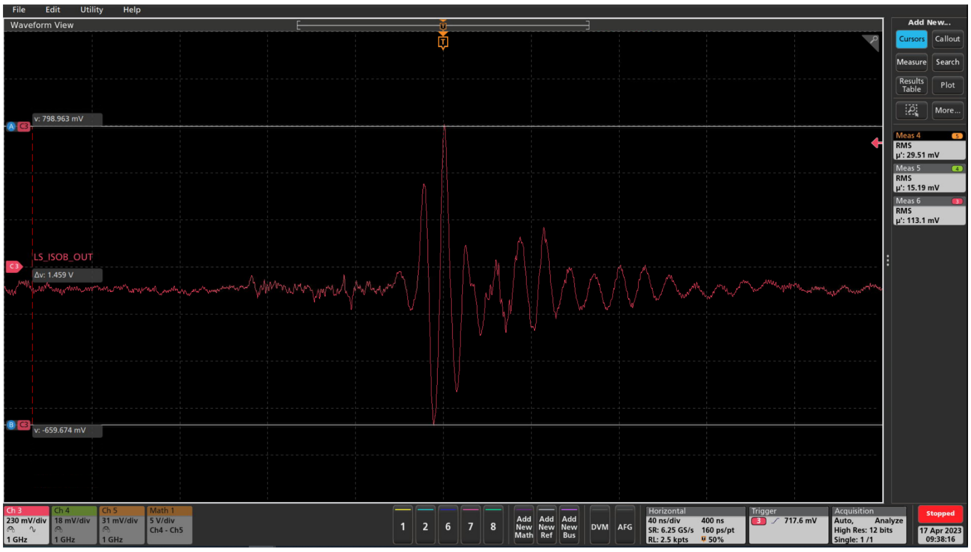

Figure 5.4: Insulated output voltage ripple

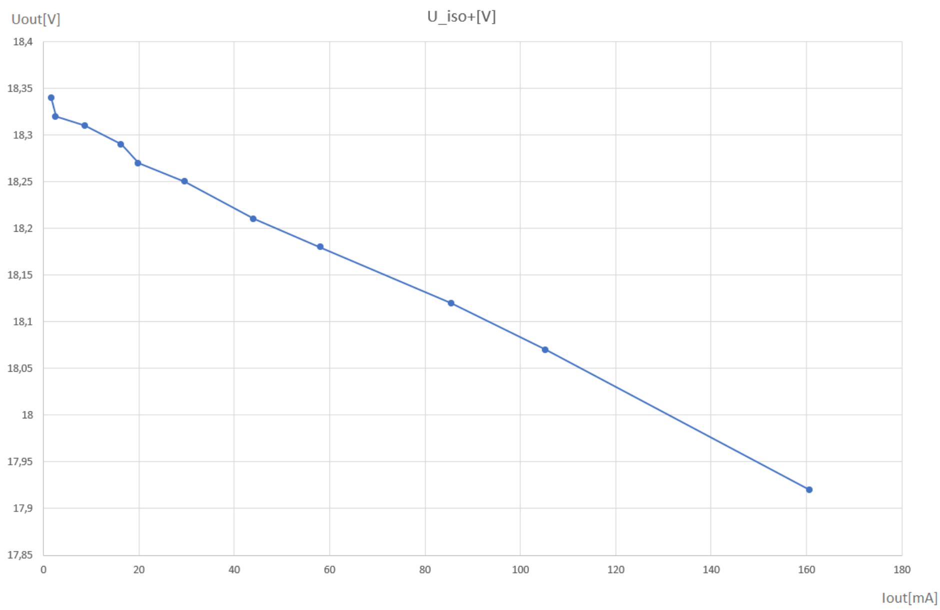

Figure 5.5: Voltage V+iso and GNDiso based on output current

Regulation failed and output voltage dropped to 0 when loaded beyond 160mA. With maximal power drawn of 3.5W, it surpassed the design requirements.

5.3 Hardware over-current protection testing

Evaluating the functionality, and time it takes to trigger the hardware over-current protection was crucial for the further testing of high voltage switching. Primary goal was to determine the speed at which, after an over-current event occurs, the device would disable all further switching and mitigate any potential damage.

For this test, hardware over-current protection was set to $2.5A$ equaling $2.6V$ or $2.4V$ for the current sensor output. Laboratory power supply with current limitation higher than $2.5A$ was connected across the current sensor and manually completing the circuit by touching the open contacts. Current sensor output was monitored, as well as final switching buffer disable signal located after the latch and all the OCP logic. External current measurement was also added observing the current through the wire from power supply generating over current. Significant noise on the can also be observed in the 5.8 figure on current sensor output. This noise appears during active switching and, based on the frequency, is caused by the iso-buck power sources and will have to be addressed in future design. Digital filtration in the microcontroller and proper timing for the ADC should be sufficient for the testing purposes.

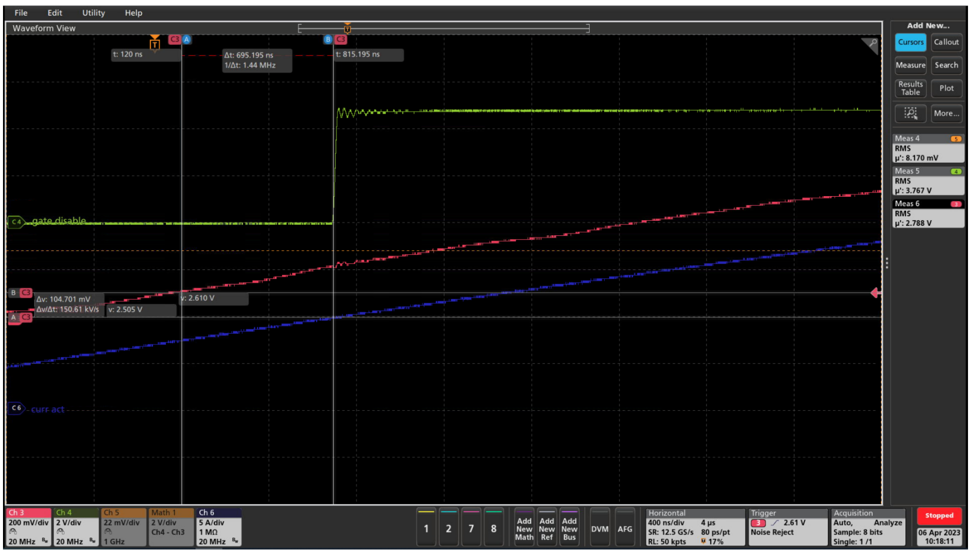

Figure 5.6: Gate disable signal compared to the external current measurement

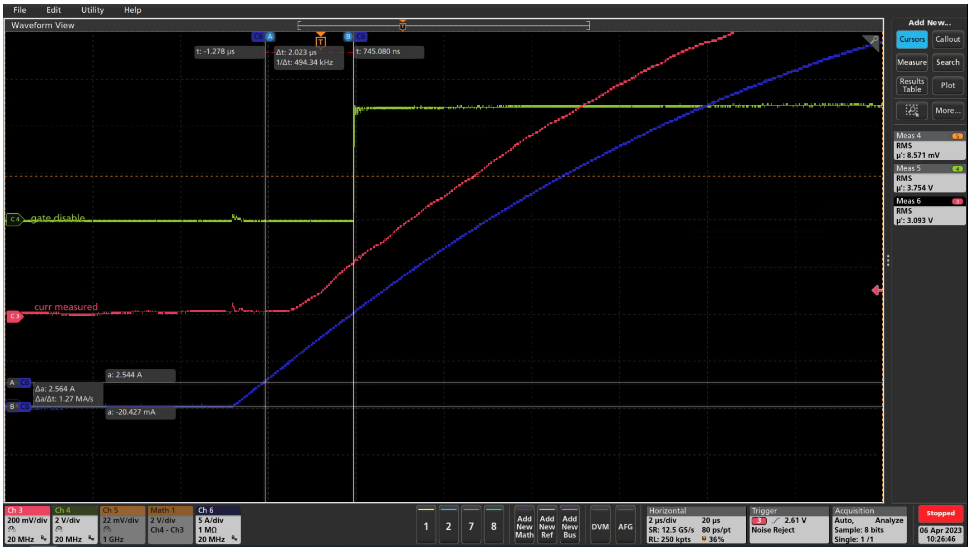

Figure 5.7: Gate disable signal compared to the current sensor output

From the figures 5.7 it can be seen that the over-current logic reacted relatively fast. Only $695nS$ were present between the current sensor output surpassed the preset threshold and gate disable signal reached the final buffer. From the figure 5.6 it can be also seen, that the most delay created, comes from the current sensor itself increasing this overall time to $2\mu S$

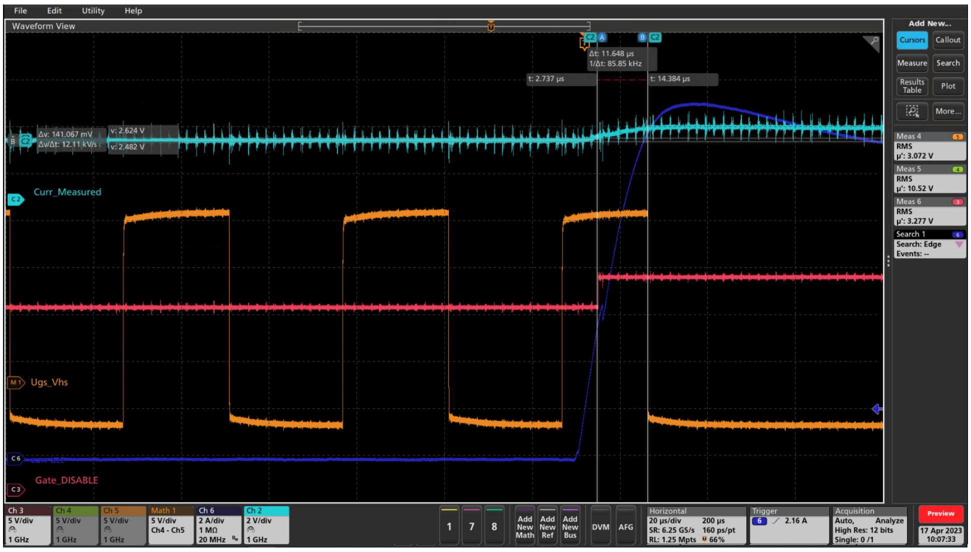

Figure 5.8: U_{gs} signal compared to the gate disable signal

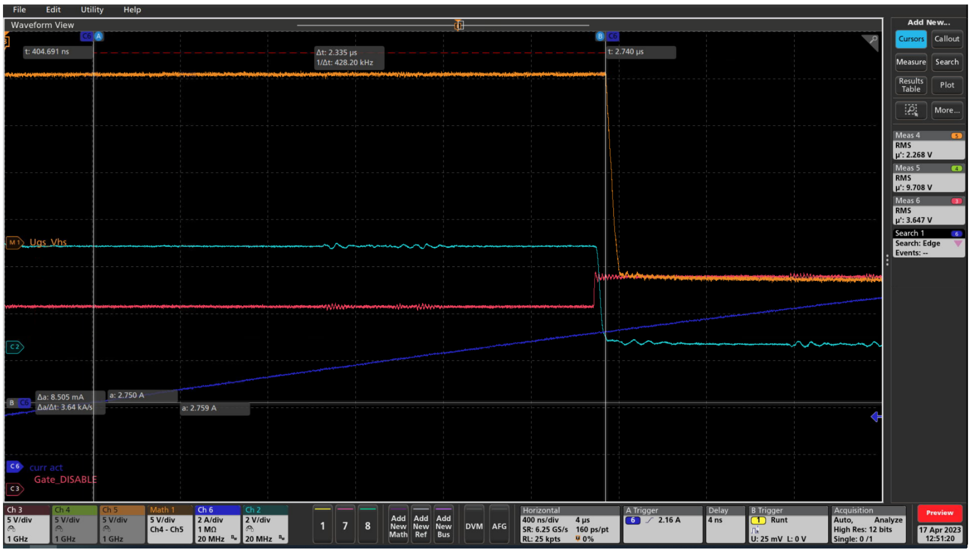

Figure 5.9: U_{gs} signal compared to the external current measurement after modification

Figures 5.8 and 5.9 correspond to the same measurement, but with active gate switching. Potentially fatal flaw was discovered in 5.8 where even though OCP triggers as fast as in previous figures, but disabling the final gate driving buffer does add a significant delay to the actual gate signal. This was found out to be the fault of the final buffer itself, since disabling this buffer does not result in $log(0)$ output, but in high impedance state of the output. Modification in label for the 5.9 figure represents addition of the pull down resistor to the output of the buffer and mitigating this issue, as can be seen in the figure.

5.4 Gate driver testing

Testing of the gate drivers was done through the microcontroller actively switching all the transistors with PWM, not modulating sine wave. No high voltage was present during this testing. Measurement for slew rate for on signal and off signal can be seen in 5.12 and 5.13. Response time to was measured between microcontroller gate control signal and U_{gs} as can be seen in 5.14.

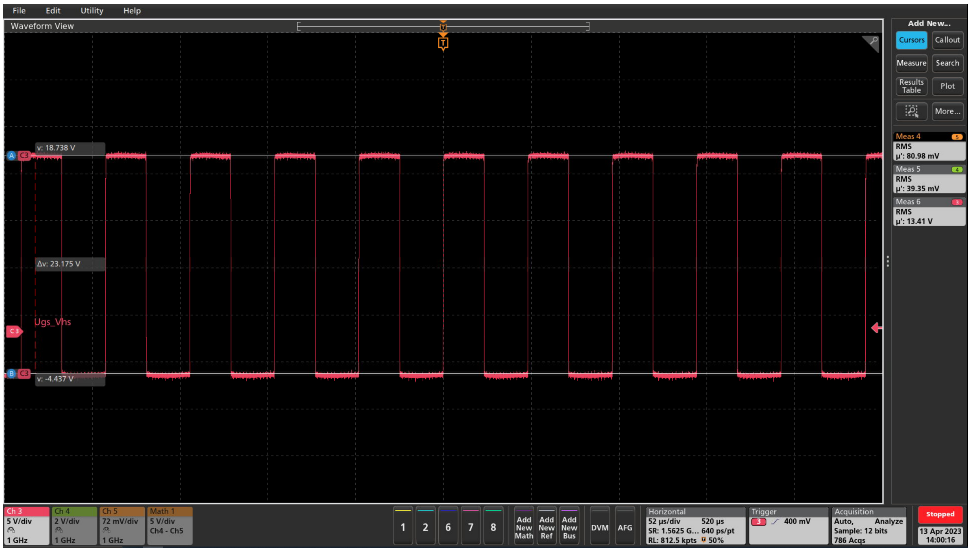

Figure 5.10: U_{gs} switching powerded by iso-buck power source and controlled by MCU

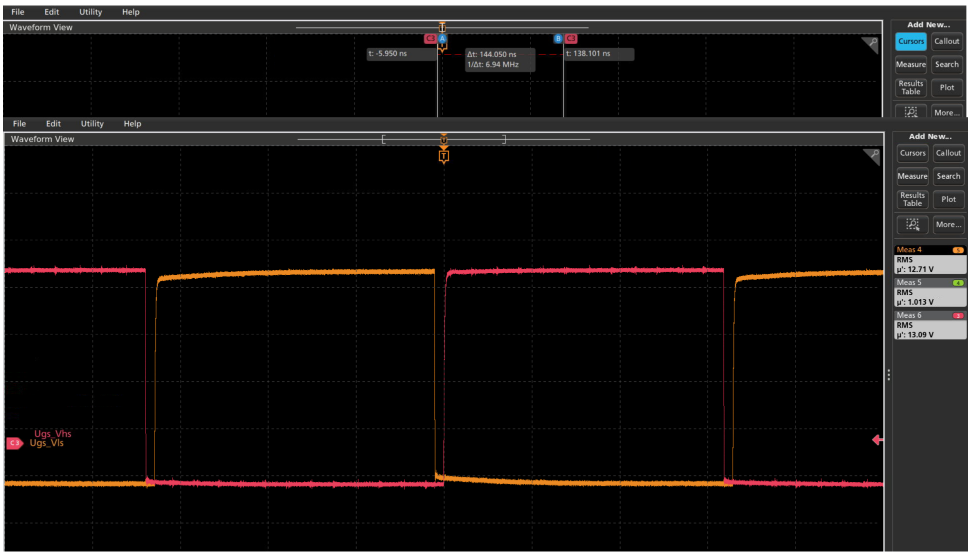

Figure 5.11: U_{gs} of low side compared to the high side showing dead time

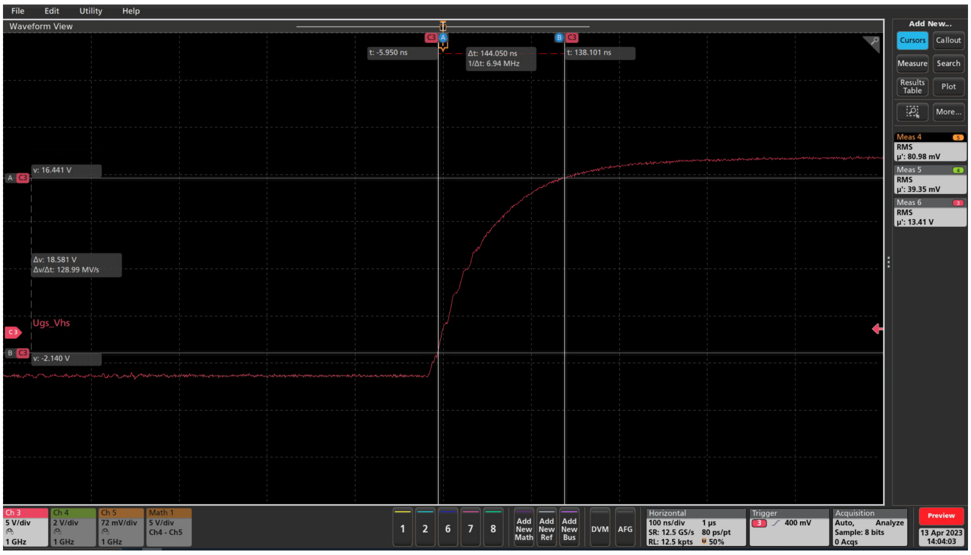

Figure 5.12: U_{gs} ON slew rate

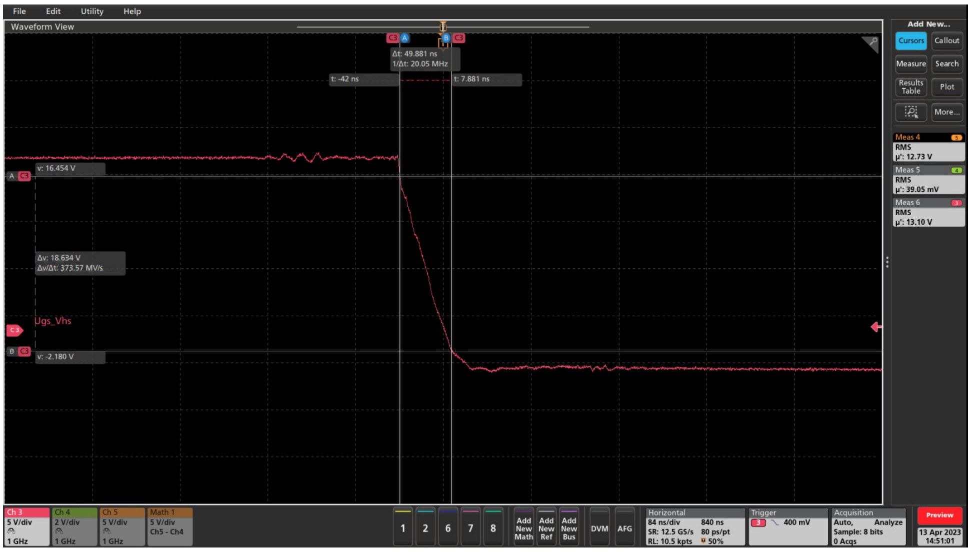

Figure 5.13: U_{gs} OFF slew rate

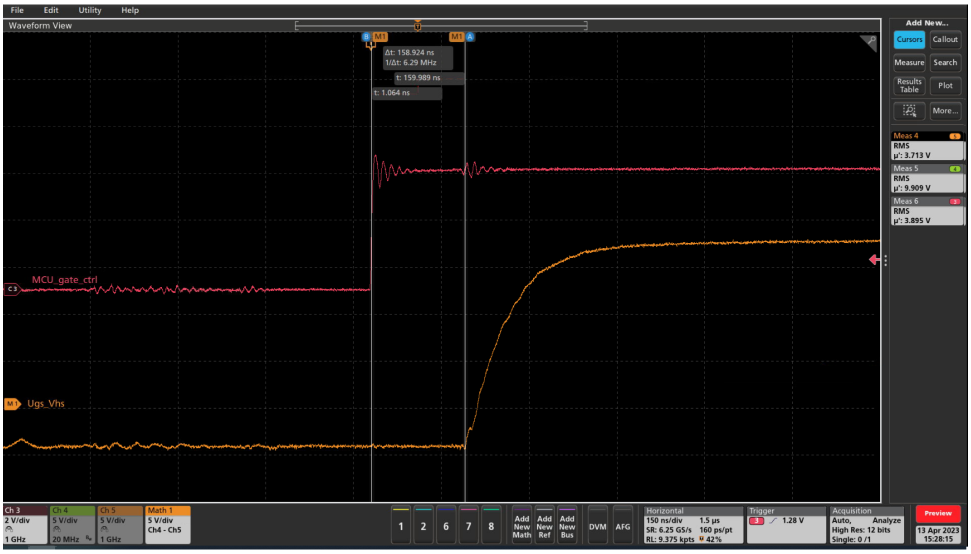

Figure 5.14: U_{gs} signal response time

5.5 Resolver interface testing

For sensing, External signal generator was used as an excitation for resolver. While iso-buck power sources are powered off, negligible phase shift and correct signal attenuation for the microcontrollers ADC can be observed, with the same performance for both sine and cosine signals. 5.15. Noise increases with the simultaneous iso-buck operation as can be seen in 5.16. As in Gate driver testing section, proper decoupling or different method of insulated power sources will have to be implemented.

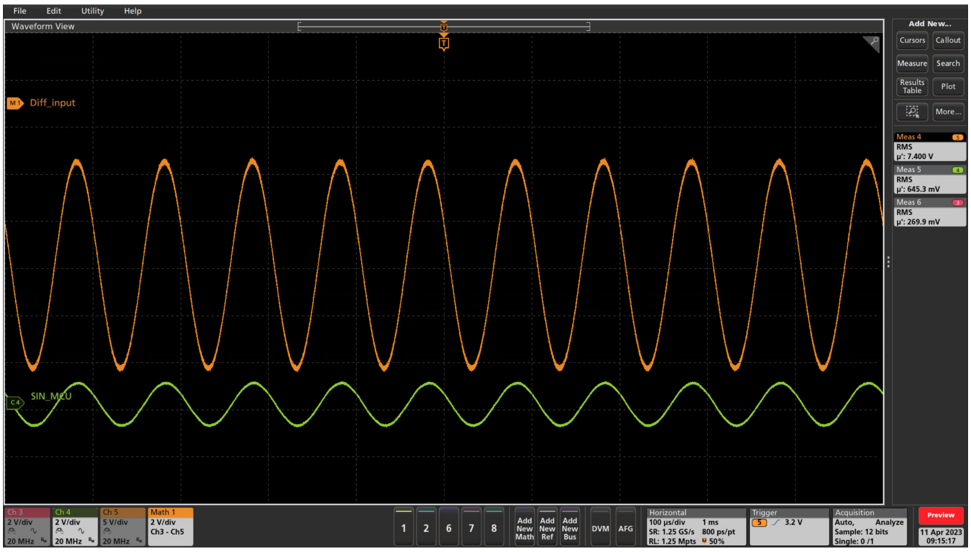

Figure 5.15: External excitation and filtered output

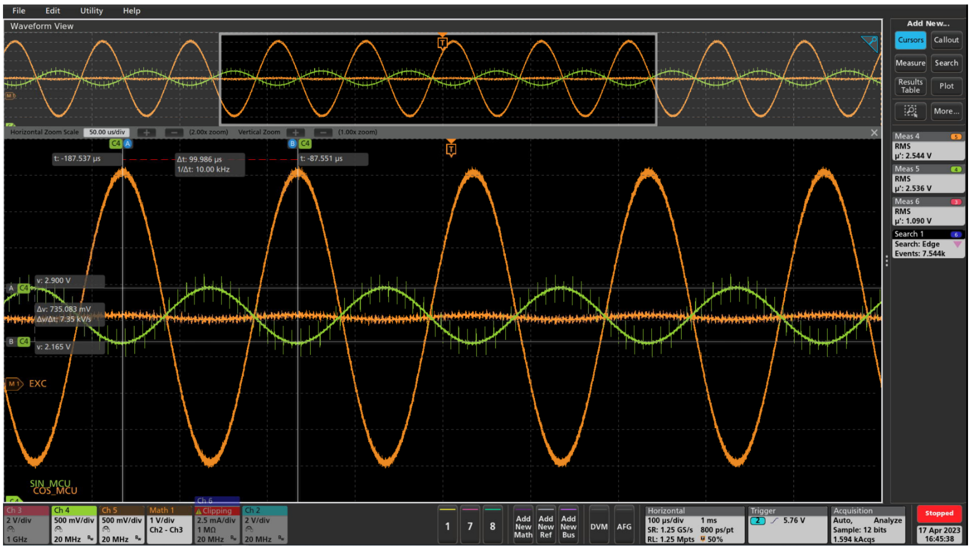

Figure 5.16: External excitation of resolver and filtered outputs

Excitation circuitry failed, due to the insufficient filtering operational amplifier characteristics 5.17. Differential output signal was distorted, and when significantly attenuated when under load from resolver. Since this version of the board is only made for laboratory testing, excitation will be provided by external signal generator.

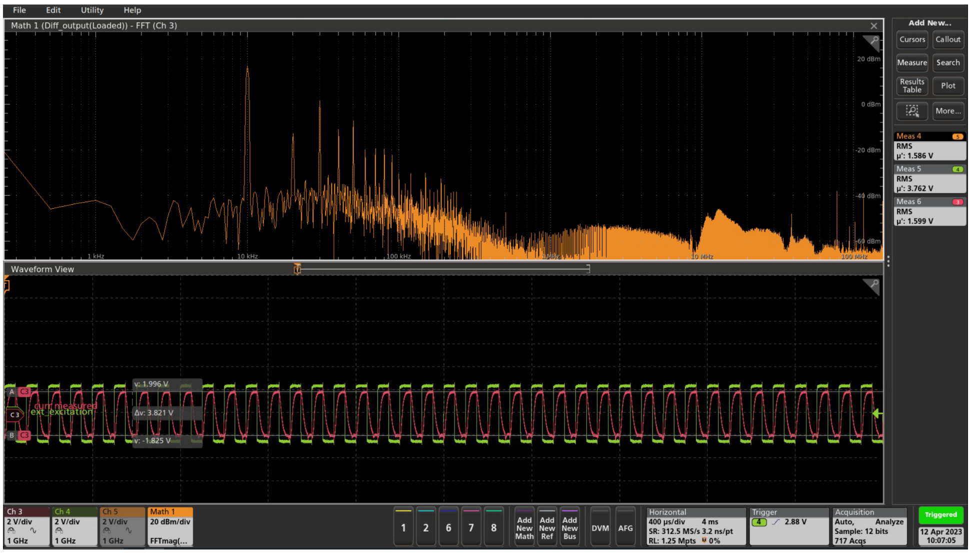

Figure 5.17: PWM filtering for resolver excitation and differential output spectral analysis

Chapter 6

Commercial Viability of e-compressor board

The development of e-compressor boards for electric vehicle and industrial applications is an emerging market with significant growth potential. Component manufacturers have the opportunity to capitalize on this trend by providing cutting-edge technologies and products tailored to the specific requirements of these applications. This chapter examines the commercial viability of developing e-compressor boards from a component manufacturer's viewpoint, focusing on market opportunities, technological advancements, and competitive positioning.

6.1 Market Opportunities

The increasing adoption of electric vehicles and the growing demand for energy-efficient industrial equipment are driving the need for advanced motor control solutions. E-compressor boards represent a vital component in these systems, providing precise control, improved efficiency, and reduced energy consumption. Component manufacturers can benefit from these market trends by offering products that address the unique challenges faced by e-compressor board designers, such as:

- High voltage isolation and safety requirements
- Compact form factors and integration capabilities
- Compliance with automotive and industrial standards
- Enhanced efficiency and thermal performance

6.2 Technological Advancements

To stay competitive and capture market share, component manufacturers must continually invest in research and development to deliver innovative solutions. Key areas of focus for e-compressor board development include:

- Advanced semiconductor materials, such as silicon carbide (SiC) and gallium nitride (GaN), which offer superior performance compared to traditional silicon-based devices
- High-performance insulated gate drivers and power sources with increased reliability and reduced size
- Improved communication interfaces, such as isolated USB and CAN, which enhance data exchange capabilities and facilitate diagnostics
- Innovative cooling and thermal management solutions to optimize performance and prolong component life

6.3 E-compressor and Its Importance in EV Thermal Management

Effective thermal management is crucial for the performance, safety, and longevity of electric vehicle (EV) batteries. E-compressors play a vital role in maintaining optimal operating conditions for EV battery systems by providing precise and efficient cooling. This section discusses the importance of e-compressors in EV thermal management and highlights the challenges and benefits associated with their implementation.

6.3.1 Thermal Management of EV Batteries

Battery temperature significantly impacts the performance and lifespan of an EV. High temperatures can lead to accelerated aging and degradation of battery cells, while low temperatures can negatively affect energy density and charge-discharge rates. Furthermore, excessive temperature gradients within the battery pack may cause uneven aging of cells, leading to reduced performance and increased safety risks. Therefore, proper thermal management is essential to ensure consistent battery performance, extend service life, and enhance the overall safety of EVs.

6.3.2 Role of E-compressor in EV Cooling Systems

E-compressors are a critical component of modern EV cooling systems, which typically employ liquid or refrigerant-based cooling mechanisms to maintain optimal battery temperatures. The e-compressor circulates the refrigerant throughout the cooling system, effectively transferring heat away from the battery cells and other heat-generating components, such as power electronics and electric motors. The advantages of using e-compressors in EV cooling systems include:

- High efficiency and precise temperature control, which contribute to improved battery performance and lifespan
- Compact and lightweight design, allowing for easier integration into the vehicle architecture
- Reduced noise and vibration compared to traditional belt-driven compressors, enhancing the overall driving experience

6.3.3 Challenges and Benefits

Despite their advantages, e-compressors also present some challenges in terms of design, integration, and control. High voltage motor controller design and thermal management of the e-compressor itself are among the key challenges faced by engineers. However, overcoming these challenges can yield significant benefits, including:

- Enhanced overall vehicle efficiency, leading to increased driving range and reduced charging times
- Improved safety and reliability, owing to better temperature control and reduced risk of thermal runaway in battery cells
- Greater flexibility in the design and packaging of EV components, enabling the development of more compact and innovative vehicle architectures

In conclusion, e-compressors play a crucial role in the thermal management of EV batteries, providing efficient and precise cooling solutions that enhance vehicle performance, safety, and longevity. By addressing the challenges associated with e-compressor design and integration, manufacturers can unlock the full potential of this technology and contribute to the continued advancement of the EV industry.

6.4 Competitive Positioning

To establish a strong presence in the e-compressor board market, component manufacturers must differentiate themselves by offering unique value propositions. This can be achieved through various strategies, such as:

- Providing comprehensive system solutions, including hardware, software, and reference designs, to streamline the development process for customers
- Fostering strategic partnerships with leading automotive and industrial OEMs to gain early access to emerging requirements and secure design wins
- Leveraging economies of scale and global supply chain networks to deliver cost-effective and reliable components
- Investing in customer support and engineering services to assist customers in overcoming design challenges and accelerating time-to-market

In conclusion, the development of e-compressor boards presents a promising commercial opportunity for component manufacturers. By focusing on market trends, technological advancements, and competitive positioning, manufacturers can capitalize on the growing demand for advanced motor control solutions and establish a strong foothold in this emerging market.

6.5 Mass Production

Mass production is a crucial factor in the commercial success of e-compressor boards, as it enables manufacturers to meet the increasing demand and reduce production costs. In this section, we discuss the challenges and strategies associated with mass-producing e-compressor boards.

6.5.1 Challenges in Mass Production

Scaling up the production of e-compressor boards presents several challenges:

- Ensuring consistent quality and reliability across large production volumes
- Optimizing production processes to minimize defects and reduce waste
- Sourcing and managing a global supply chain for critical components
- Adapting to evolving market demands and technological advancements

6.5.2 Strategies for Mass Production

To overcome these challenges and achieve successful mass production, manufacturers should consider the following strategies:

- Implementing advanced manufacturing techniques, such as automated assembly lines and testing equipment, to improve production efficiency and reduce human error
- Leveraging economies of scale to negotiate favorable pricing for raw materials and components, thereby reducing overall production costs
- Investing in research and development to continually refine and improve the e-compressor board design, incorporating new technologies and addressing emerging market needs
- Fostering strong relationships with suppliers to ensure timely delivery of components, minimize disruptions, and maintain a flexible supply chain

6.6 General Cost Reduction in Manufacturing

Reducing the manufacturing costs of e-compressor boards is essential for manufacturers to stay competitive and maximize profitability. This section explores strategies for achieving cost reduction in manufacturing.

6.6.1 Design for Manufacturing (DFM)

Implementing Design for Manufacturing (DFM) principles from the early stages of product development can significantly reduce manufacturing costs. DFM considerations include:

- Simplifying the board layout and component placement to streamline assembly processes
- Standardizing components and materials to reduce inventory and sourcing complexity
- Selecting cost-effective manufacturing processes, such as Surface Mount Technology (SMT), to minimize assembly costs

6.6.2 Process Optimization

Optimizing manufacturing processes can lead to increased efficiency and reduced costs:

- Implementing statistical process control (SPC) and other quality management techniques to minimize defects and rework
- Adopting lean manufacturing principles to eliminate waste and improve overall production efficiency
- Regularly reviewing and updating production processes to incorporate new technologies and best practices

6.6.3 Supply Chain Management

Effective supply chain management plays a vital role in reducing manufacturing costs:

- Establishing long-term partnerships with suppliers to negotiate volume discounts and favorable payment terms
- Implementing just-in-time (JIT) inventory management to minimize warehousing costs and reduce obsolescence risk
- Collaborating with suppliers to identify opportunities for cost reduction, such as alternative materials or manufacturing techniques

By adopting these strategies, manufacturers can achieve significant cost reductions in the production of e-compressor boards, thereby enhancing their competitiveness and profitability in the market.

6.7 Conclusion

In this work, we have presented a comprehensive study on the design and implementation of a high voltage motor controller for e-compressors in electric vehicles. The controller leverages advanced power electronics, control algorithms, and robust hardware design principles to deliver high performance and reliability under demanding operating conditions.

We have also discussed the various functional blocks of the motor controller and detailed the challenges and solutions associated with designing and implementing each block. From the SiC transistors in the power stage, the resolver interface circuitry, to the onboard microcontroller, each component plays a critical role in the overall operation of the controller.

The controller's design is further complemented by adherence to automotive standards, ensuring safety and reliability in high voltage applications. A rigorous design process was followed, including meticulous PCB design considerations to meet high voltage insulation requirements, and the implementation of a robust OCP design.

Laboratory testing was performed to validate the design, and the results confirmed the controller's ability to meet its design objectives. In addition, the study also considered the commercial viability of the controller, highlighting potential for cost reduction in mass production and the significant benefits it brings to the EV market, particularly in enhancing thermal management of EV batteries.

In conclusion, the high voltage motor controller designed in this study demonstrates a successful integration of power electronics, control algorithms, and hardware design principles. It not only meets the demanding requirements of e-compressors in EVs but also opens up avenues for future research and development in high-performance motor control solutions for electric vehicles.

6.8 Thesis limitations and following work

This thesis does not include all the work needed to be done as far as evaluation or software implementation. This thesis manly focuses on the hardware aspect and challenges that come with it.

Further testing primarily with motor and dynamometer will be required to fully evaluate all the characteristics of this design. Since the prototype e-compressor board envelops many features implemented primarily for testing, new board will be designed based on the testing results consisting of only the necessary components and function blocks.

This future work will focus on further optimizing the controller's design for potential mass production, cost reduction and improving the efficiency of the power stage, and exploring more advanced control strategies for improved motor performance.

6.9 Table of attachments

1. a6986i.pdf
2. AVA00071509.pdf
3. BNX012H01.pdf
4. cp2102n-datasheet.pdf
5. e-compresorFullSchematic.pdf
6. go-10-20-30-sms-series.pdf
7. l4995.pdf
8. l9616.pdf
9. sct020h120g3ag.pdf
10. sn74hcs365-q1.pdf
11. sn74lvc1g74.pdf
12. spc584b70.pdf
13. stgap2sicsan.pdf
14. za9668.pdf

Appendix A

Acronyms

A

AC

Air conditioning

ADC

Analog-to-Digital Converters

B

BLDC

Brushless Direct Current

BJT

Bipolar Junction Transistor

C

CAN

Controller Area Network

D

DAC

Digital-to-analog converter

DC

Direct current

DLC

Data length code

DRC

Design Rule Check

DSP

Digital signal processors

DTC

Direct Torque Control

DFM

Design for Manufacturing

E

ECU

Electronic control units

EV

Electric vehicle

EMF

Electromotive force

F

FPGA

Field-programmable gate arrays

FOC

Field-oriented control

G

GaN

Gallium nitride

I

IFOC

Indirect Field-Oriented Control

IGBT

Insulated-Gate Bipolar Transistor

J

JIT

Just-in-time

JTAG

Joint Test Action Group

Appendix B

Complete design

Even though parts of this design were already included throughout the thesis, i have decided to include it again in full again here.

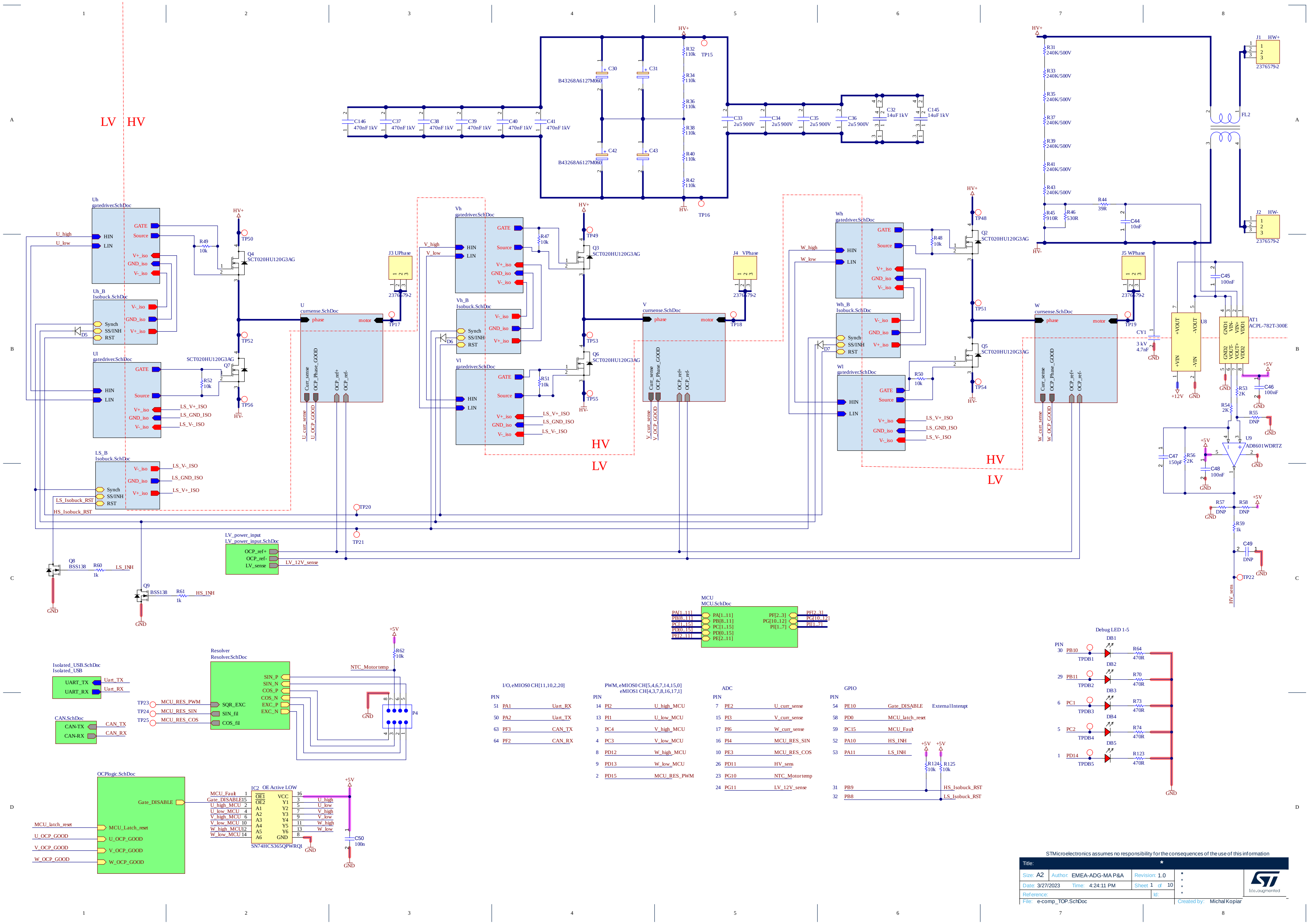

LV
HV
HV+
HV-
B43268A6127M000
C146 470nF 1kV
C37 470nF 1kV
C38 470nF 1kV
C39 470nF 1kV
C40 470nF 1kV
C41 470nF 1kV
C33 2u5 900V
C34 2u5 900V
C35 2u5 900V
C36 2u5 900V
C32 14uF 1kV
C145 14uF 1kV
R31 240K/500V
J1 HW+
J2 HW-
2376579-2
FL2
R44 39R
C44 10nF
R45 910R
R46 530R
Uh gatedriver.SchDoc
Vh gatedriver.SchDoc
Wh gatedriver.SchDoc
Ul gatedriver.SchDoc
Vl gatedriver.SchDoc
Wl gatedriver.SchDoc
Uh_B Isobuck.SchDoc
Vh_B Isobuck.SchDoc
Wh_B Isobuck.SchDoc
LS_B Isobuck.SchDoc
U cursense.SchDoc
V cursense.SchDoc
W cursense.SchDoc
SCT020HU120G3AG
J3 UPhase
J4 VPhase
J5 WPhase
U8
AT1 ACPL-782T-300E
U9 AD8601WDRTZ
LV_power_input LV_power_input.SchDoc
Q8 BSS138
Q9 BSS138
LS_INH
HS_INH
LS_Isobuck_RST
HS_Isobuck_RST
MCU MCU.SchDoc
Isolated_USB.SchDoc Isolated_USB
CAN.SchDoc
Resolver Resolver.SchDoc
NTC_Motor temp
OCPlogic.SchDoc
IC2 OE Active LOW
SN74HCS365QPWRQ1
I/O, eMIOS0 CH[11,10,2,20]
PWM, eMIOS0 CH[5,4,6,7,14,15,0] eMIOS1 CH[4,3,7,8,16,17,1]
ADC
GPIO
Debug LED 1-5
STMicroelectronics assumes no responsibility for the consequences of the use of this information
Size: A2
Author: EMEA-ADG-MA P&A
Revision: 1.0
Date: 3/27/2023
Time: 4:24:11 PM
Sheet 1 of 10
File: e-comp_TOP.SchDoc
Created by: Michal Kopiar

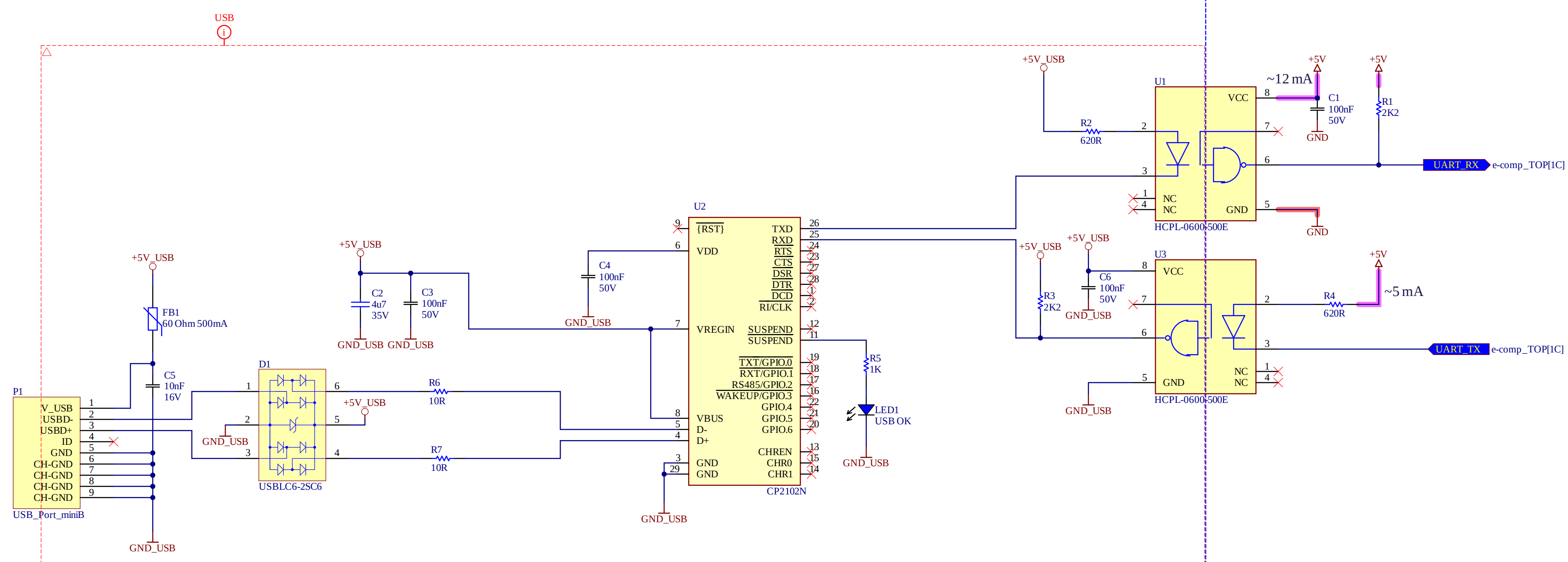

STMicroelectronics assumes no responsibility for the consequences of the use of this information

Title: *			
Size: A3	Author: EMEA-ADG-MAP&A	Revision: 1.0	STMicroelectronics Pobrezni 3 186 00 Prague 8 Czech Republic
Date: 3/27/2023	Time: 4:24:11 PM	Sheet 2 of 10	
Reference: *		Id: 66	
File: Isolated_USB.SchDoc			Created by: Michal Kopiar

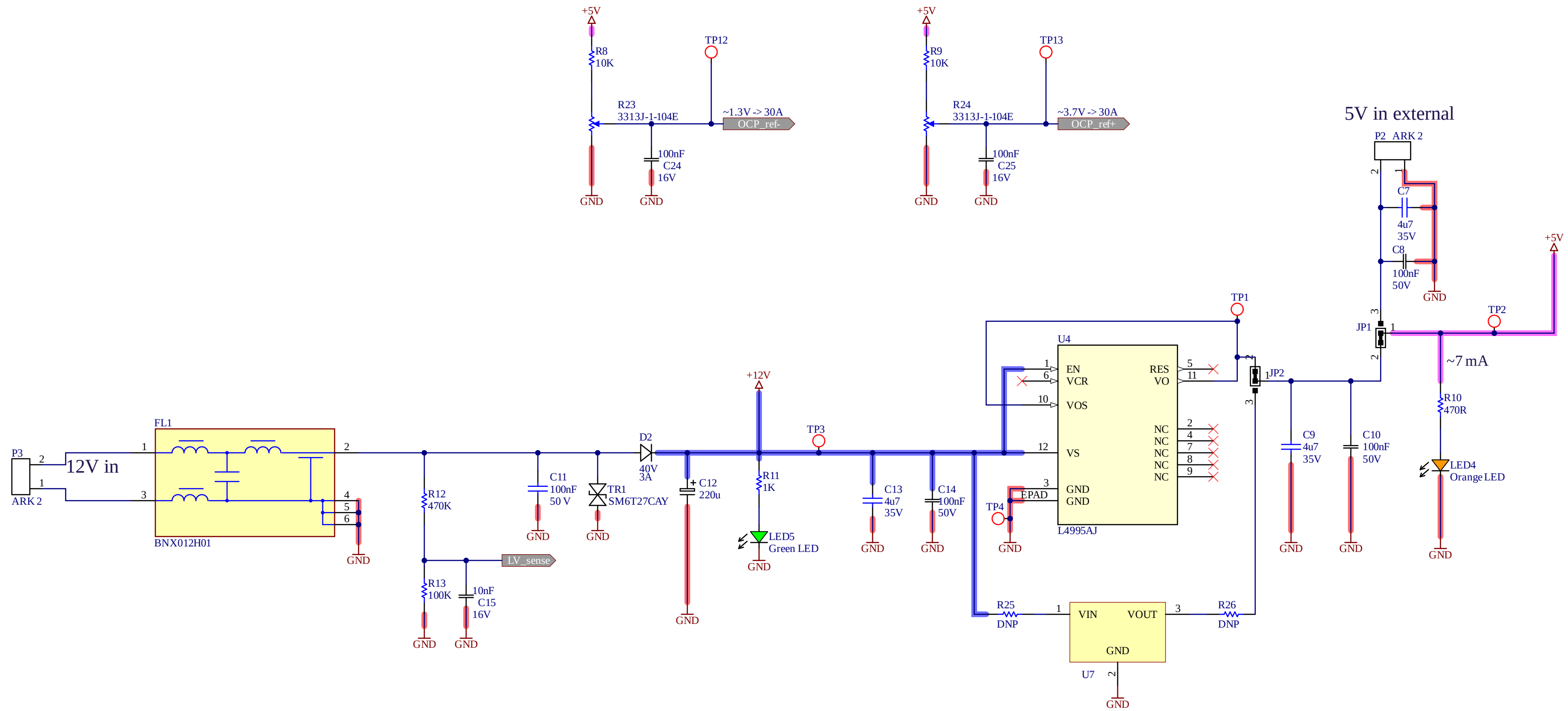

STMicroelectronics assumes no responsibility for the consequences of the use of this information

Title: *			
Size: A3	Author: EMEA-ADG-MAP&A	Revision: 1.0	STMicroelectronics Pobrezni 3 186 00 Prague 8 Czech Republic
Date: 3/27/2023	Time: 4:24:11 PM	Sheet 3 of 10	
Reference: *		Id: 66	
File: LV_power_input.SchDoc			Created by: Michal Kopiar

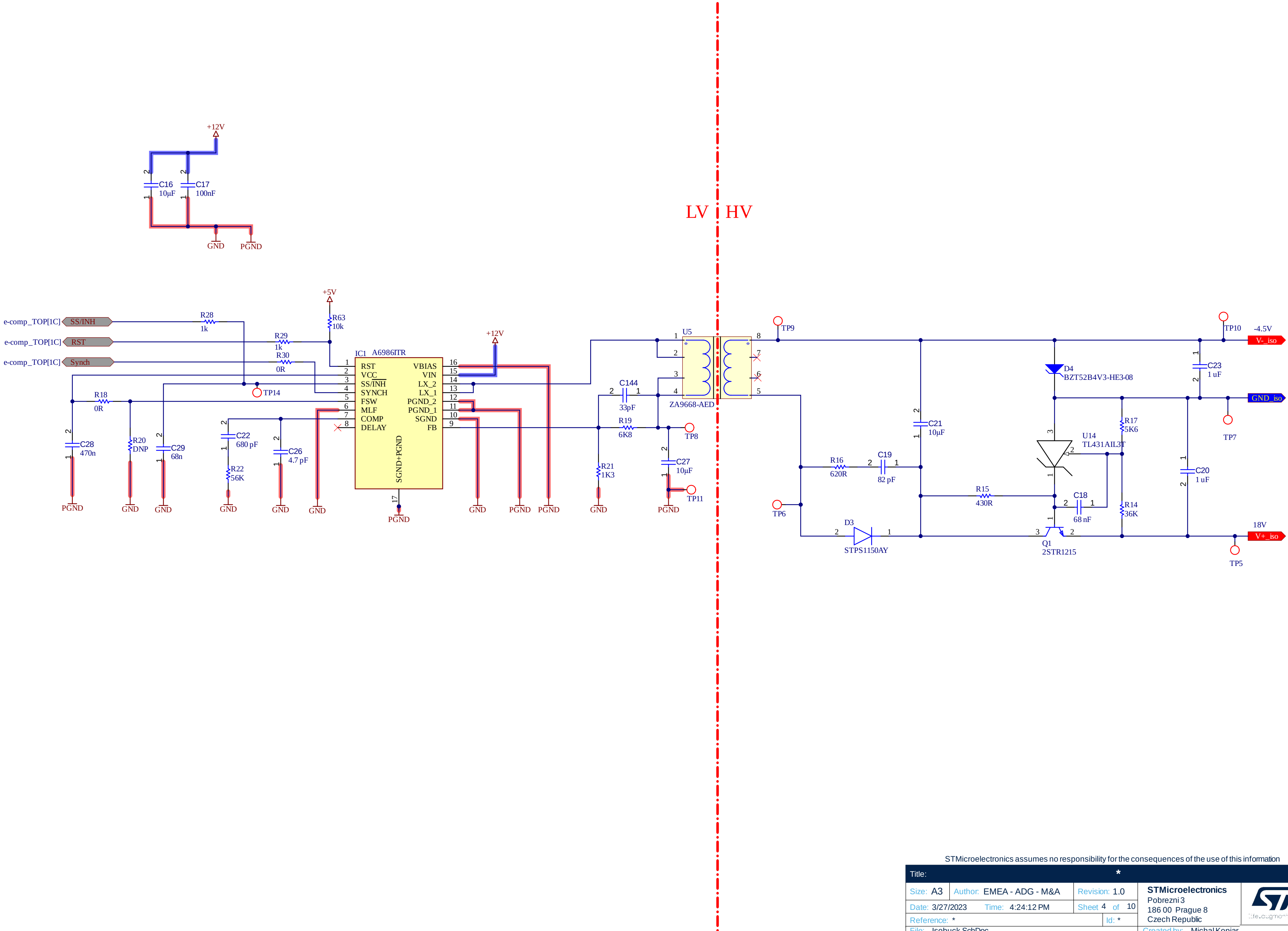

STMicroelectronics assumes no responsibility for the consequences of the use of this information

Title: *			
Size: A3	Author: EMEA - ADG - M&A	Revision: 1.0	STMicroelectronics Pobrezni 3 186 00 Prague 8 Czech Republic
Date: 3/27/2023	Time: 4:24:12 PM	Sheet 4 of 10	
Reference: *		Id: *	
File: Isobuck.SchDoc			Created by: Michal Kopiar

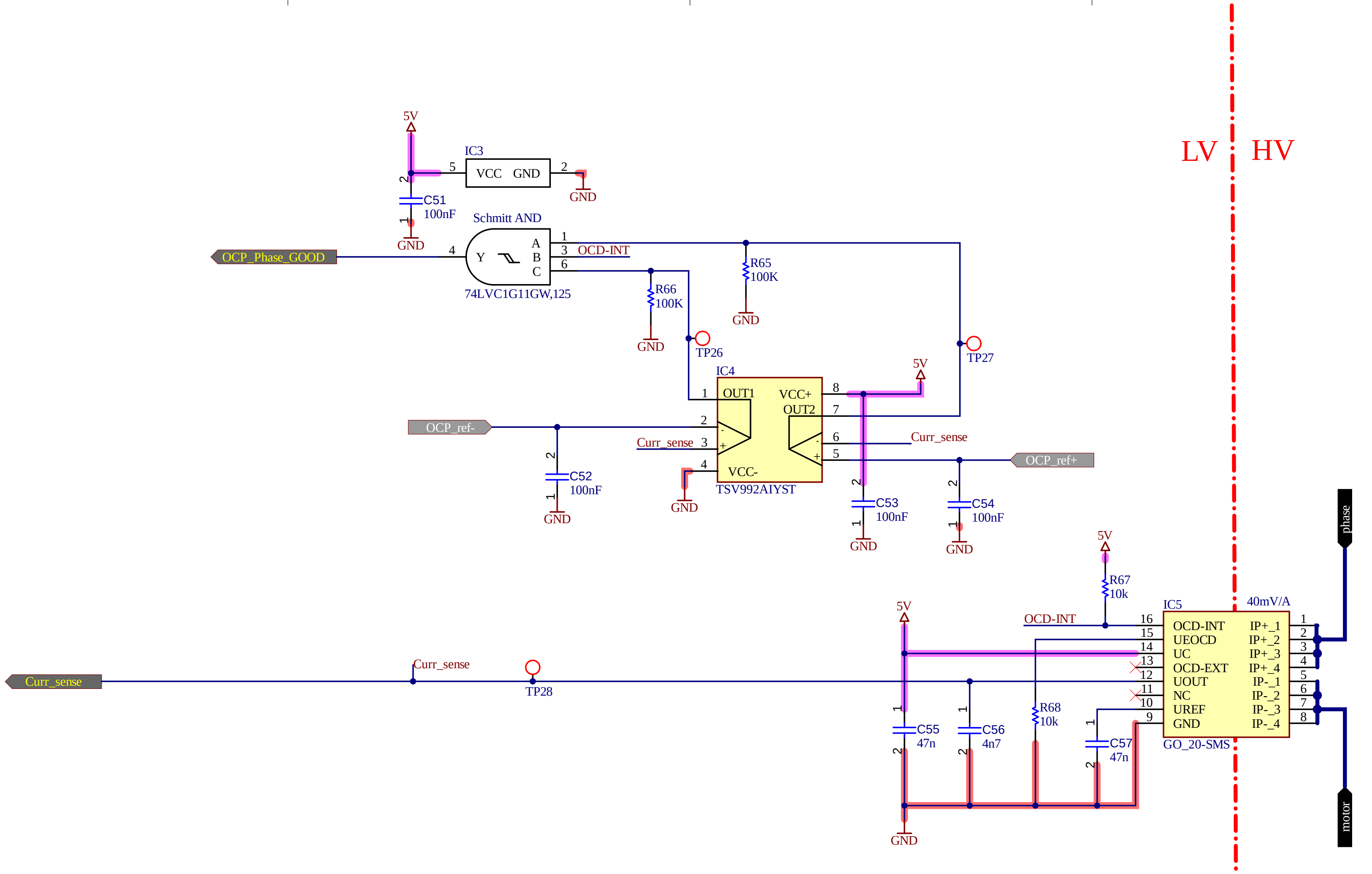

STMicroelectronics assumes no responsibility for the consequences of the use of this information

Title: *			
Size: A4	Author: EMEA-ADG-MA P&A	Revision: 1.0	STMicroelectronics Pobrezni 3 186 00 Prague 8 Czech Republic
Date: 3/27/2023	Time: 4:24:12 PM	Sheet 5 of 10	
Reference: *		Id: *	
File: currsense.SchDoc			Created by: Michal Kopiar

life.augmented

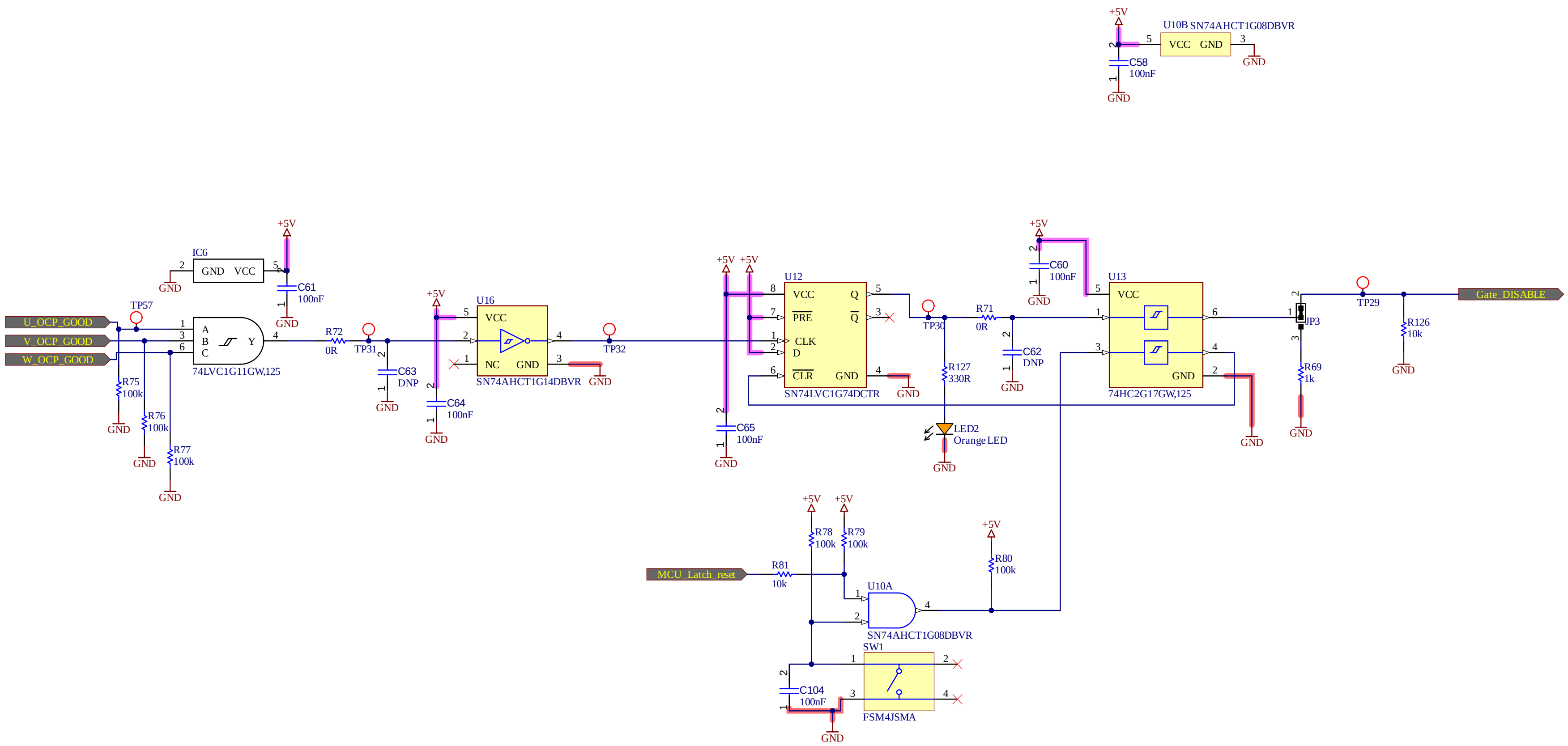

STMicroelectronics assumes no responsibility for the consequences of the use of this information

Title: *			
Size: A3	Author: EMEA-ADG-MAP&A	Revision: 1.0	STMicroelectronics Pobrezni 3 186 00 Prague 8 Czech Republic
Date: 3/27/2023	Time: 4:24:12 PM	Sheet 6 of 10	
Reference: *		Id: *	
File: OCPlogic.SchDoc			Created by: Michal Kopiar

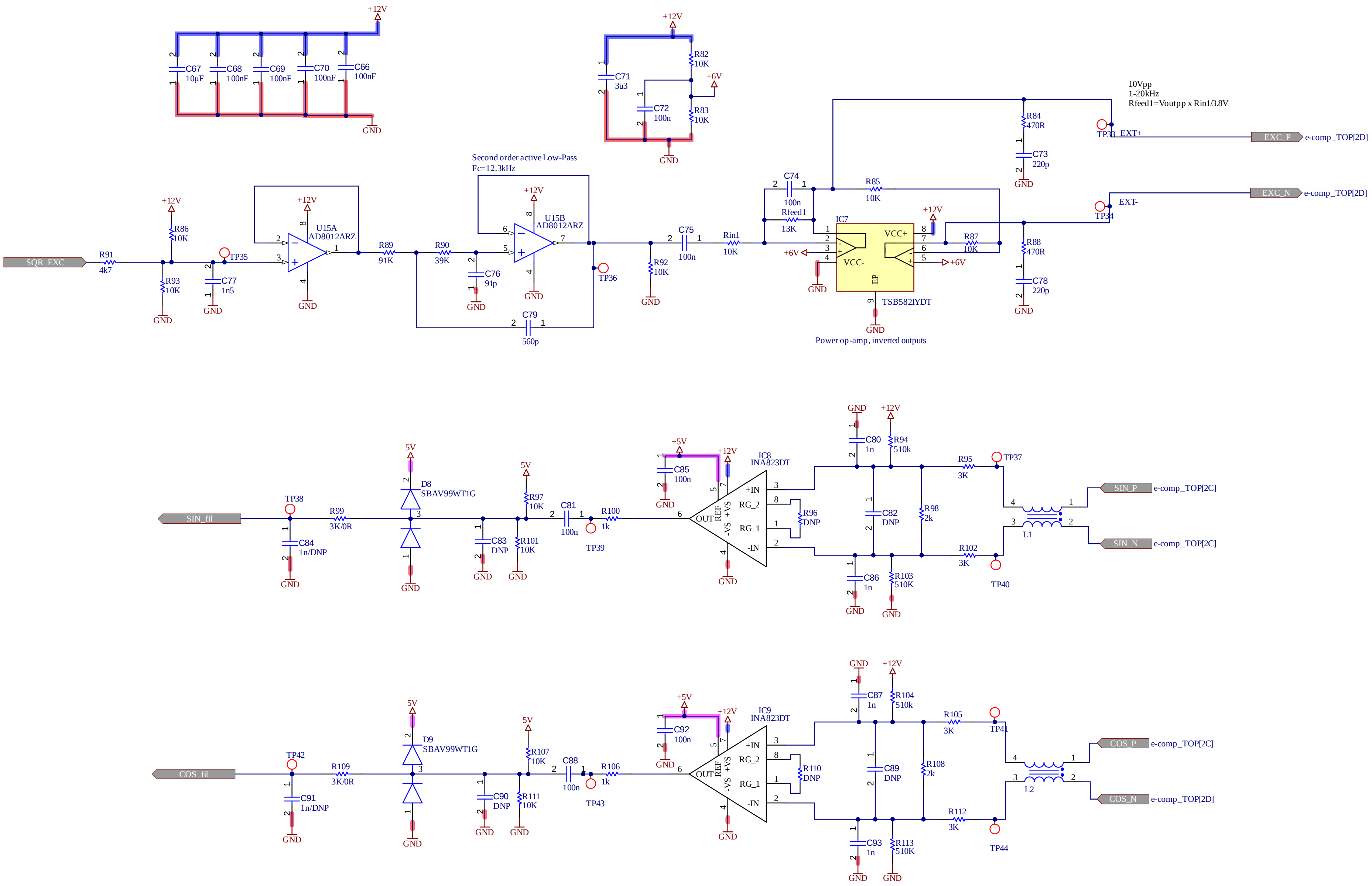

STMicroelectronics assumes no responsibility for the consequences of the use of this information

Title: *			
Size: A3	Author: EMEA-ADG-MAP&A	Revision: 1.0	STMicroelectronics Pobrezni 3 186 00 Prague 8 Czech Republic
Date: 3/27/2023	Time: 4:24:12 PM	Sheet 7 of 10	
Reference: *		Id: *	
File: Resolver.SchDoc			Created by: Michal Kopiar

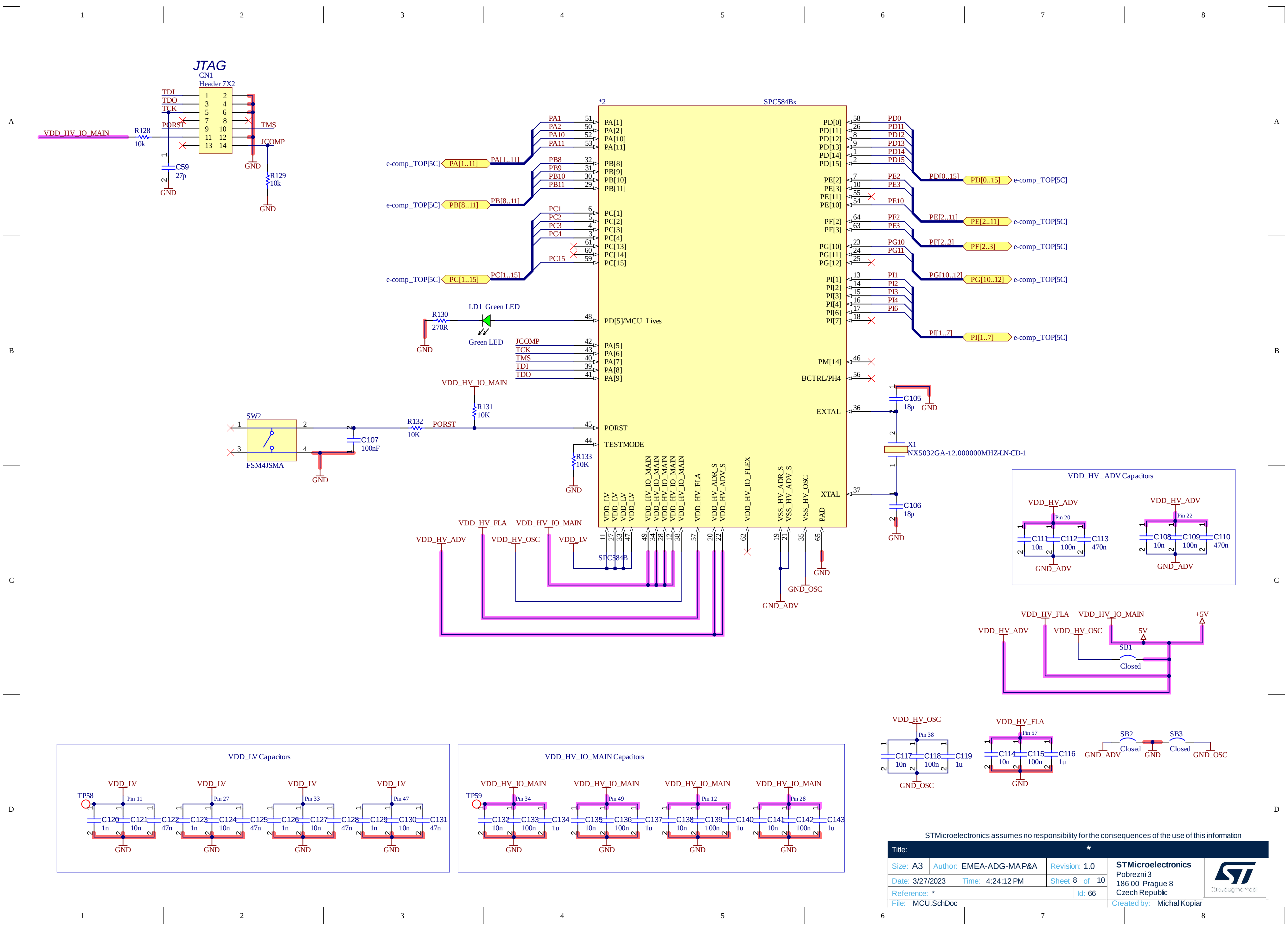
JTAG
CN1
Header 7X2
TDI
TDO
TCK
PORST
TMS
JCOMP
VDD_HV_IO_MAIN
R128
10k
C59
27p
GND
R129
10k
*2
SPC584Bx
PA[1]
PA[2]
PA[10]
PA[11]
PB[8]
PB[9]
PB[10]
PB[11]
PC[1]
PC[2]
PC[3]
PC[4]
PC[13]
PC[14]
PC[15]
PD[5]/MCU_Lives
PA[5]
PA[6]
PA[7]
PA[8]
PA[9]
PORST
TESTMODE
PD[0]
PD[11]
PD[12]
PD[13]
PD[14]
PD[15]
PE[2]
PE[3]
PE[11]
PE[10]
PF[2]
PF[3]
PG[10]
PG[11]
PG[12]
PI[1]
PI[2]
PI[3]
PI[4]
PI[6]
PI[7]
PM[14]
BCTRL/PH4
EXTAL
XTAL
VDD_LV
VDD_HV_IO_MAIN
VDD_HV_FLA
VDD_HV_ADR_S
VDD_HV_ADV_S
VDD_HV_IO_FLEX
VSS_HV_ADR_S
VSS_HV_ADV_S
VSS_HV_OSC
PAD
SPC584B
e-comp_TOP[5C]
PA[1..11]
PB[8..11]
PC[1..15]
PD[0..15]
PE[2..11]
PF[2..3]
PG[10..12]
PI[1..7]
LD1 Green LED
Green LED
R130
270R
SW2
FSM4JSMA
C107
100nF
R132
10K
R131
10K
R133
10K
C105
18p
C106
18p
X1
NX5032GA-12.000000MHZ-LN-CD-1
VDD_HV_ADV
VDD_HV_FLA
VDD_HV_OSC
GND_ADV
GND_OSC
VDD_HV _ADV Capacitors
C111 10n
C112 100n
C113 470n
C108 10n
C109 100n
C110 470n
Pin 20
Pin 22
+5V
5V
SB1
Closed
SB2
SB3
C117 10n
C118 100n
C119 1u
Pin 38
C114 10n
C115 100n
C116 1u
Pin 57
VDD_LV Capacitors
TP58
C120 1n
C121 10n
C122 47n
C123 1n
C124 10n
C125 47n
C126 1n
C127 10n
C128 47n
C129 1n
C130 10n
C131 47n
Pin 11
Pin 27
Pin 33
Pin 47
VDD_HV_IO_MAIN Capacitors
TP59
C132 10n
C133 100n
C134 1u
C135 10n
C136 100n
C137 1u
C138 10n
C139 100n
C140 1u
C141 10n
C142 100n
C143 1u
Pin 34
Pin 49
Pin 12
Pin 28
STMicroelectronics assumes no responsibility for the consequences of the use of this information
Title: *
Size: A3
Author: EMEA-ADG-MAP&A
Revision: 1.0
Date: 3/27/2023
Time: 4:24:12 PM
Sheet 8 of 10
Reference: *
Id: 66
File: MCU.SchDoc
STMicroelectronics
Pobrezni 3
186 00 Prague 8
Czech Republic
Created by: Michal Kopiar

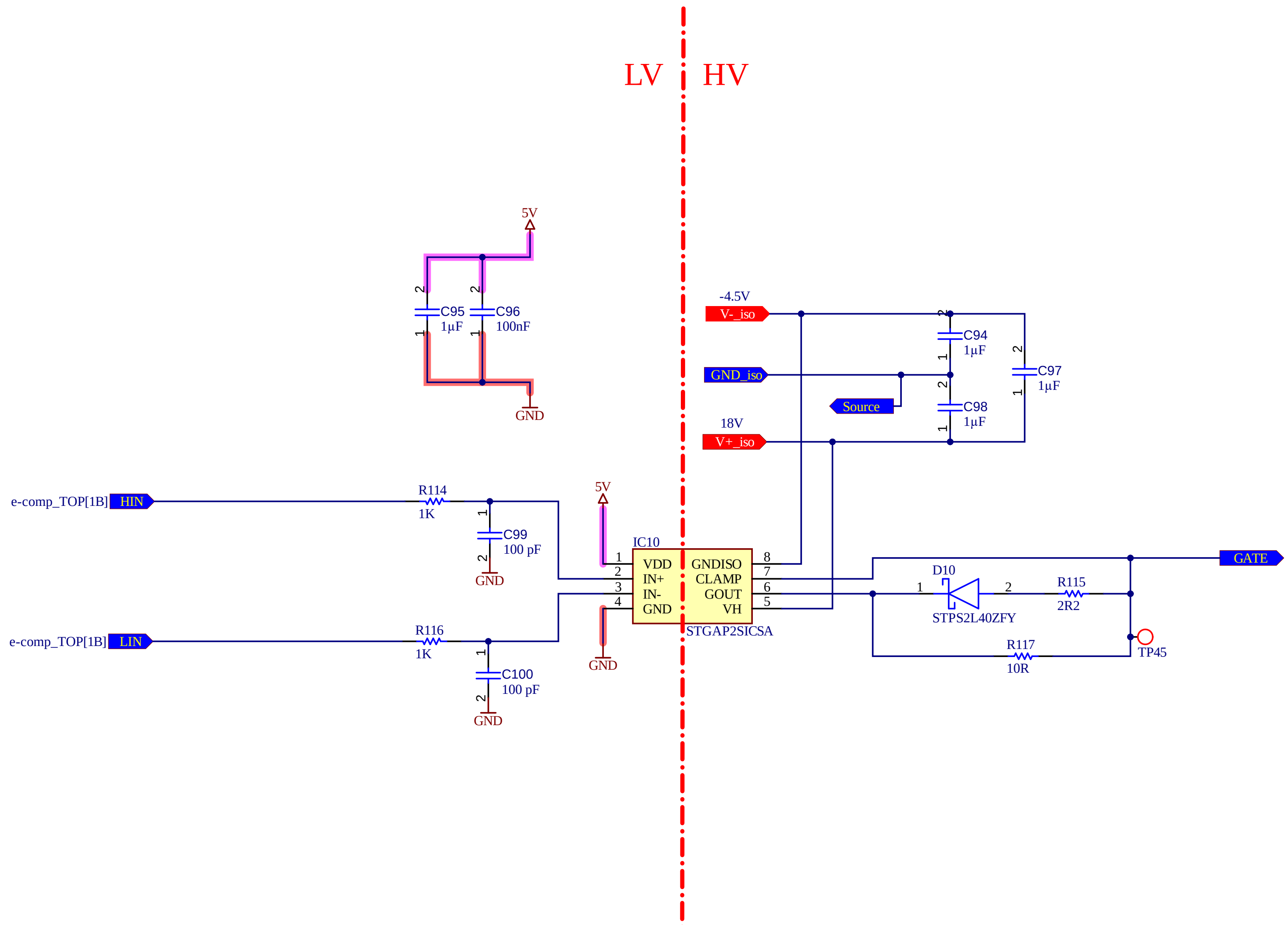

STMicroelectronics assumes no responsibility for the consequences of the use of this information

Title: *			
Size: A4	Author: EMEA - ADG - M&A	Revision: 1.0	STMicroelectronics Pobrezni 3 186 00 Prague 8 Czech Republic
Date: 3/27/2023	Time: 4:24:13 PM	Sheet 9 of 10	
Reference: *		Id: *	
File: gatedriver.SchDoc			Created by: Michal Kopiar

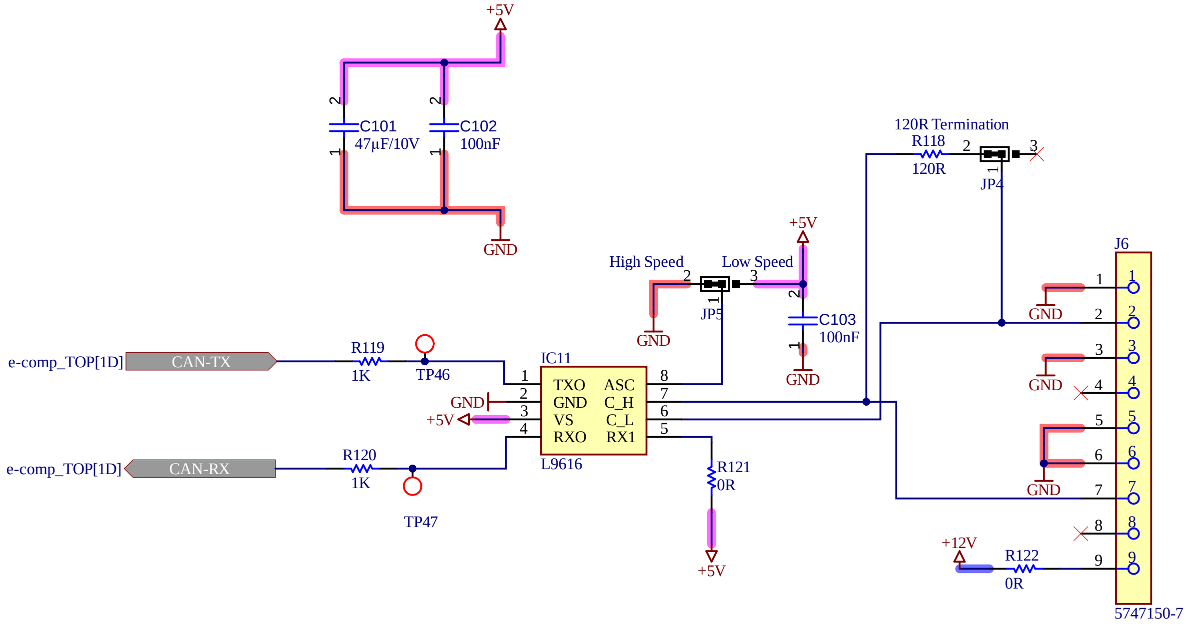

STMicroelectronics assumes no responsibility for the consequences of the use of this information

Title: *			
Size: A4	Author: EMEA-ADG-MA P&A	Revision: 1.0	* * * *
Date: 3/27/2023	Time: 4:24:13 PM	Sheet 10 of 10	
Reference:		Id:	
File: CAN.SchDoc			Created by: Michal Kopiar

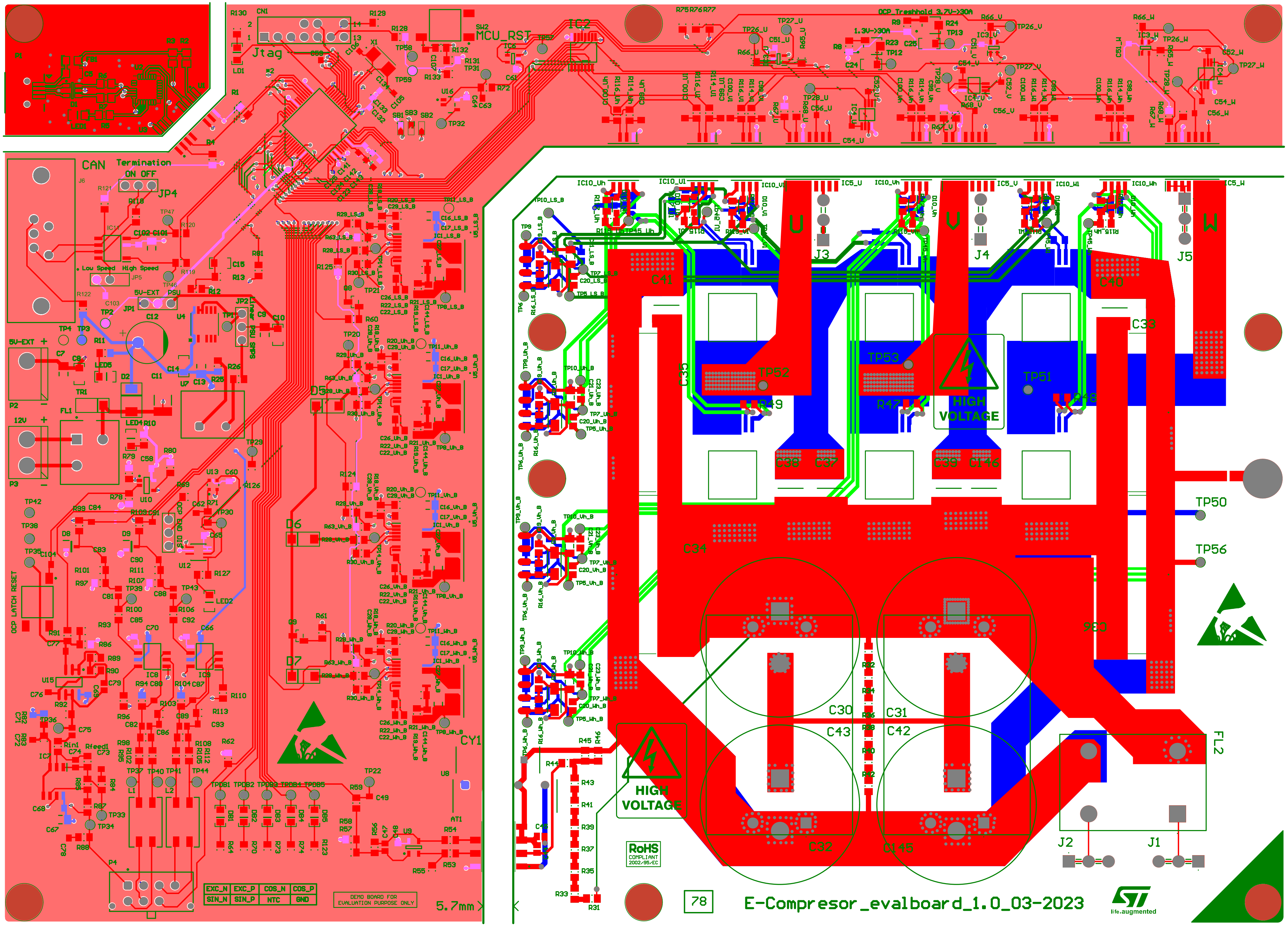

CAN
Termination
ON OFF
JP4
Jtag
MCU_RST
5V-EXT
12V
OCP_Treshhold_3.7V->30A
1.3V->30A
Low Speed
High Speed
OCP LATCH RESET
U
V
W
J1
J2
J3
J4
J5
HIGH VOLTAGE
HIGH VOLTAGE
RoHS
COMPLIANT
2002/95/EC
78
E-Compresor_evalboard_1.0_03-2023
life.augmented
DEMO BOARD FOR
EVALUATION PURPOSE ONLY
EXC_N EXC_P COS_N COS_P
SIN_N SIN_P NTC GND
5.7mm
TP50
TP56

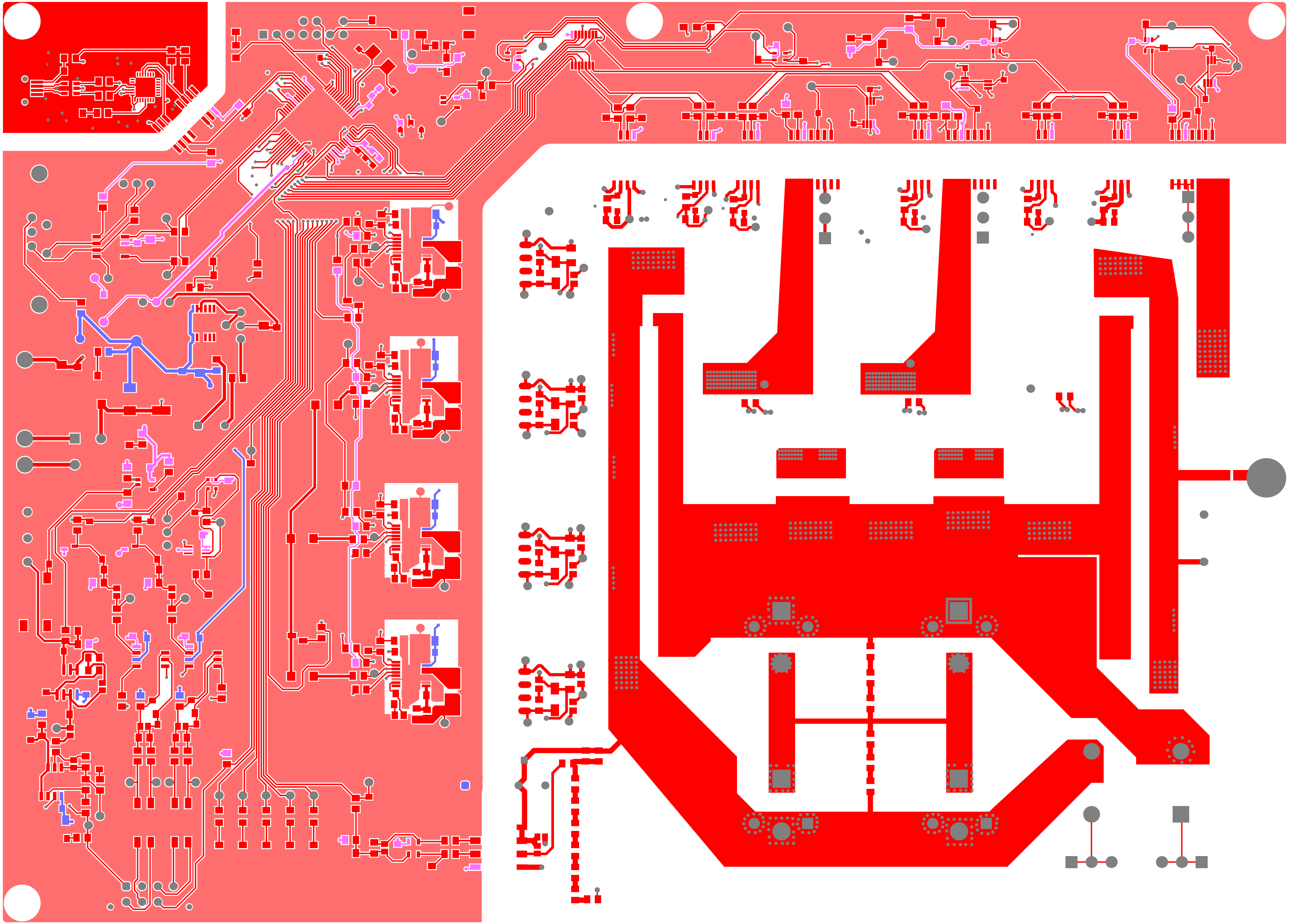

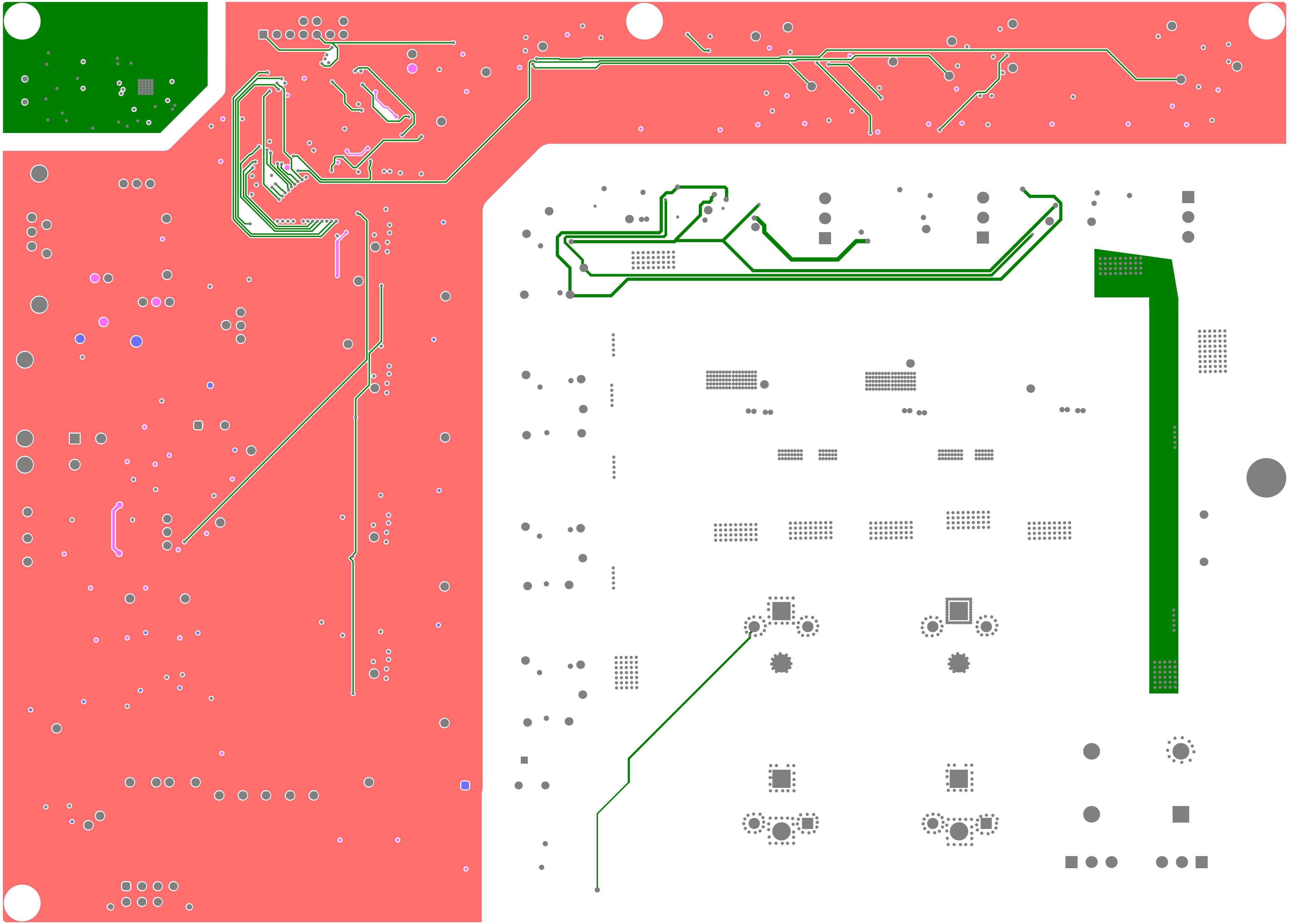

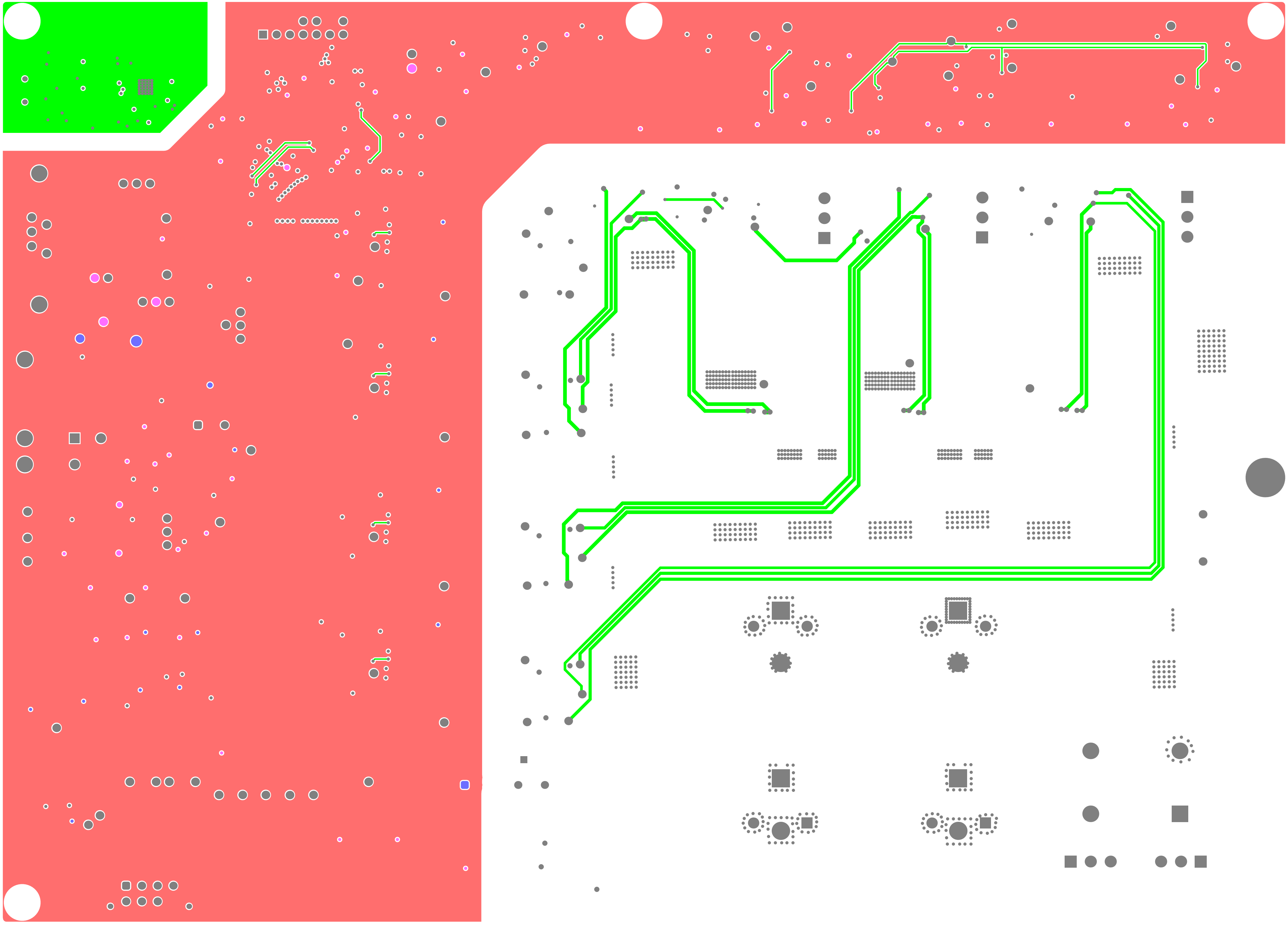

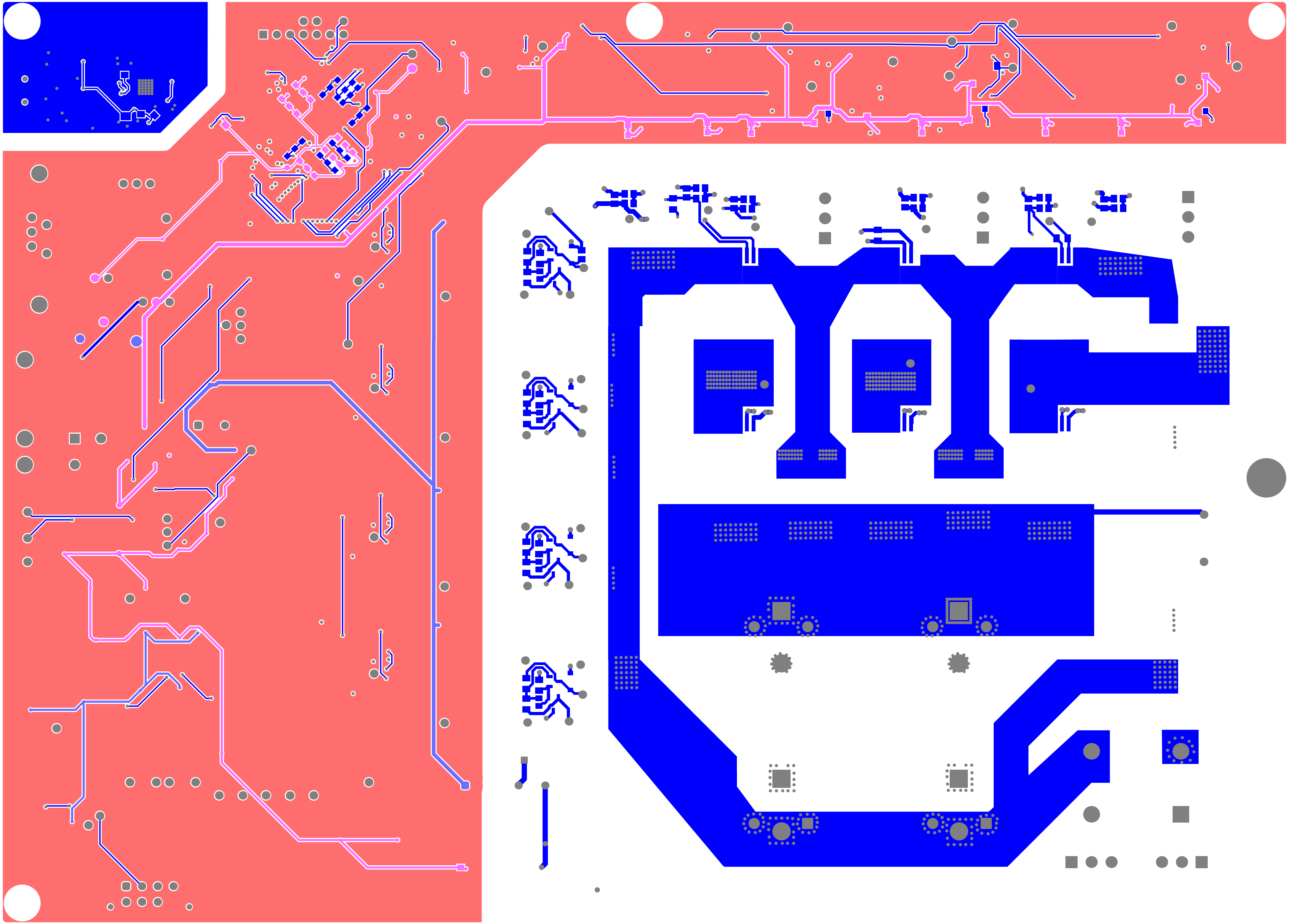

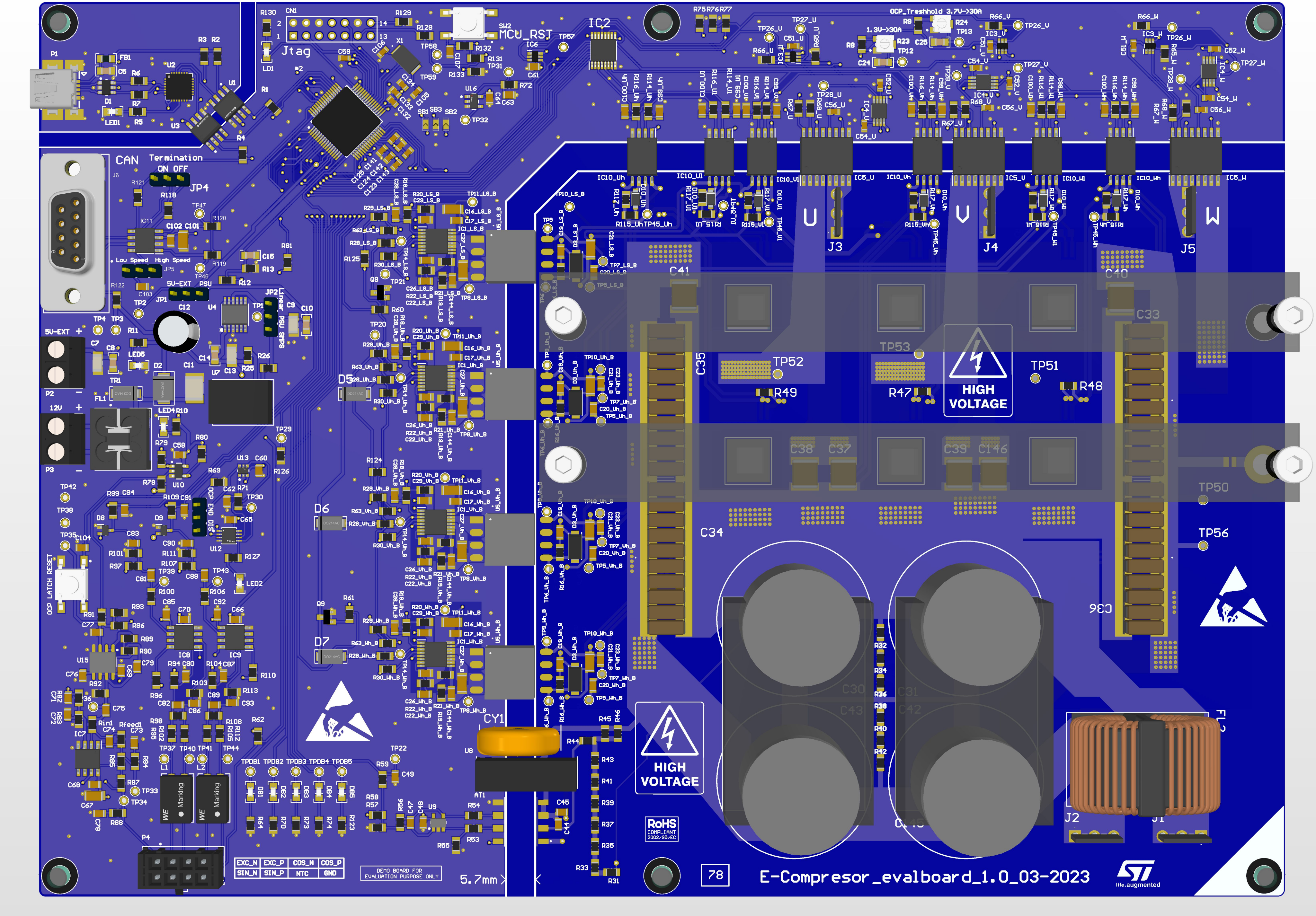

E-Compresor_evalboard_1.0_03-2023
78
HIGH VOLTAGE
HIGH VOLTAGE
CAN
Termination
ON OFF
Low Speed
High Speed
Jtag
MCU_RST
OCP LATCH RESET
U
V
W
J3
J4
J5
DEMO BOARD FOR EVALUATION PURPOSE ONLY
EXC_N
EXC_P
COS_N
COS_P
SIN_N
SIN_P
NTC
GND
RoHS
COMPLIANT
2002/95/EC
life.augmented
5.7mm

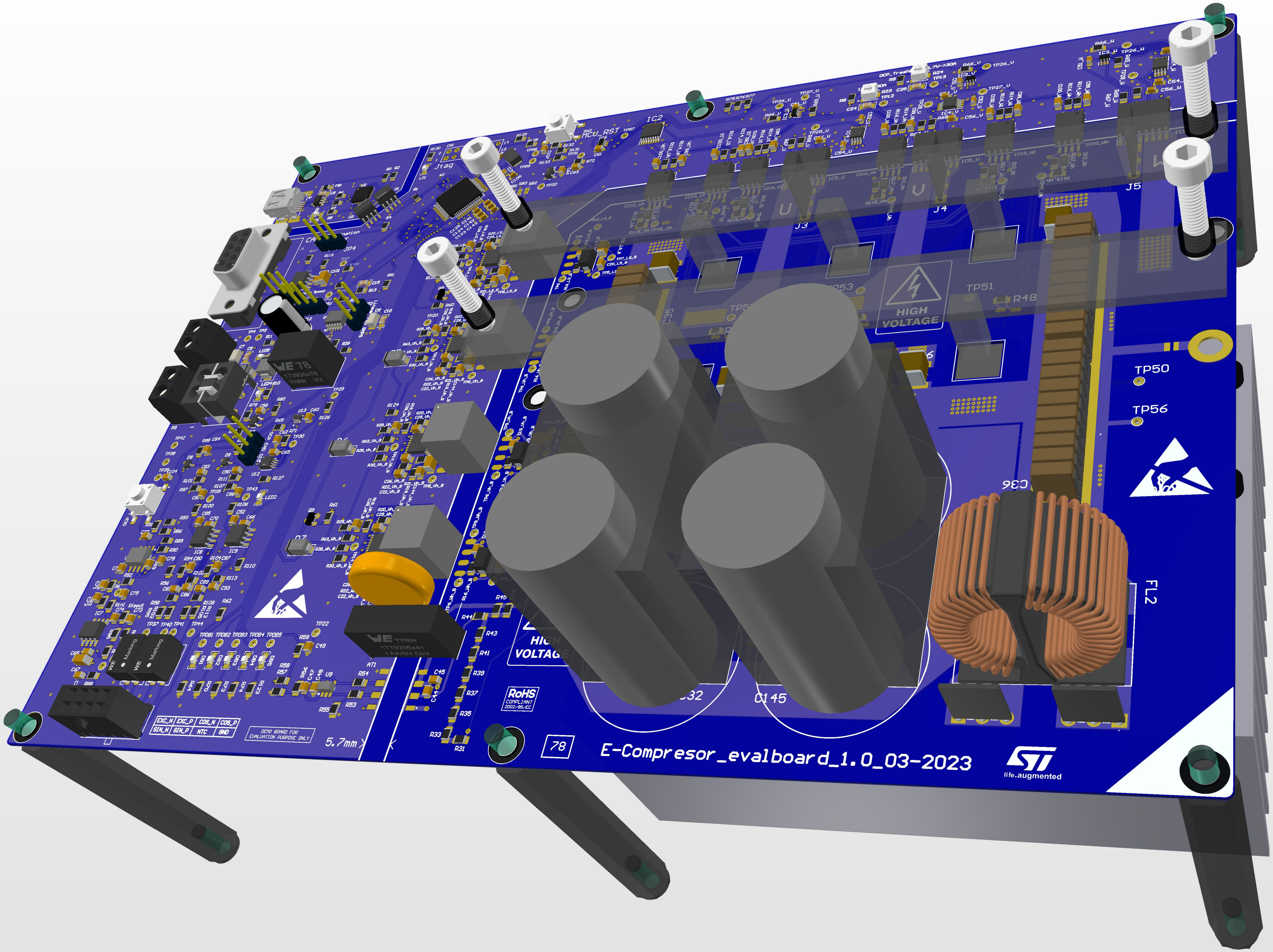

E-Compresor_evalboard_1.0_03-2023
life.augmented
HIGH VOLTAGE
TP50
TP56
TP51
R48
FL2
C145
J3
J4
J5
MCU_RST
Jtag
RoHS
78
5.7mm

Appendix C

Bibliography

1. PODHRÁZSKÝ, Adam. *Akumulátorová baterie pro elektrickou formuli. Bakalařská práce.* České vysoké učení v Praze: Fakulta elektrotechnická, 2016.
2. BUCHMANN, Isidor. *BU-204: How do Lithium Batteries Work* [online]. [visited on 2020-05-20]. Available from: `https://batteryuniversity.com/learn/article/lithium_based_batteries`.
3. HRABOVCOVÁ, Juha Pyrhönen Lappeenranta; Tapani Jokinen; Valéria. *Design of Rotating Electrical Machines, 2nd Edition.* Wiley, 2013. ISBN 978-1118581575.
4. *Power MOSFET Basics: Understanding the Turn-On Process. 1st rev.* VISHAY SILICONIX, 2015.
5. LEE, Paul. *Powering IGBT Gate Drives with DC-DC converters.* Technical Articles.: Murata Power Solutions, 2014.
6. NG, Liuping Wang; Shan Chai; Dae Yoo; Lu Gan; Ki. *PID and Predictive Control of Electrical Drives and Power Converters using MATLAB / Simulink.* Wiley, 2015. ISBN 9781118339442.
7. *SPRABQ8: Scalar (V/f) Control of 3-Phase Induction Motors. 1st rev.* Texas Instruments, 2013.
8. *Direct torque control* [online]. Wikimedia Foundation, 2001-2019 [visited on 2023-05-10]. Available from: `https://en.wikipedia.org/wiki/Direct_torque_control`.
9. *AN4642: Motor Control Application Tuning (MCAT) Tool for 3-Phase PMSM. 1st rev.* Freescale Semiconductor, 2013.
10. SORENSEN, Jens. *Sigma Delta Conversion Used for Motor Control. Analog Devices.* Technical Articles, 2015.
11. LEONHARD, Werner. *Control of Electrical Drives.* Springer-Verlag Berlin Heidelberg, 2001. ISBN 978-3-642-56649-3.
12. RÝZEK, Miroslav. *Řízení pohonu elektrického vozidla Formula Student.* České vysoké učení v Praze: Fakulta elektrotechnická, 2015.

13. TOMÁŠEK, Stanislav. *Design of an electric powertrain for the Formula Student-class vehicle Diplomová práce*. České vysoké učení v Praze: Fakulta elektrotechnická, 2019.

14. *RE-15-1-A15 datasheet* [online]. LTN SERVOTECHNIK GMBH [visited on 2021-05-10]. Available from: `https://www.ltn-servotechnik.com/fileadmin/imported/products/RE_15_EN_01.pdf`.

15. *FTF-AUT-F0234: An Overview of the Resolver Interface for Motor Control Applications. 1st rev.* Freescale, 2014.

16. *Introduction to the Controller Area Network (CAN)* [online]. Texas Instruments, Inc. [visited on 2020-05-20]. Available from: `http://www.ti.com/lit/an/sloa101b/sloa101b.pdf`.

17. LAWRENZ, Wolfhard. *CAN System Engineering: From Theory to Practical Applications*. London: Springer-Verlag, 2013. ISBN 978-1-4471-5612-3.

18. *NXJ1 Series: Isolated 1W Single Output SM DC/DC Converters*. Mansfield (Massachusetts): Murata Power Solutions, 2017.

19. VOBECKÝ, Jan a Vít ZÁHLAVA. *Elektronika*. Praha: GRADA, 2005. ISBN 978-80-247-1241-3.

20. ABBATELLI, Luigi; CATALISANO, Giuseppe. Investigation of 1200 V SiC MOSFETs Switching Performance in 4-pin Package. In: *PCIM Europe digital days 2021; International Exhibition and Conference for Power Electronics, Intelligent Motion, Renewable Energy and Energy Management*. 2021, pp. 1–5.

21. *AN5355, Mitigation technique of the SiC MOSFET gate voltage glitches with Miller clamp, Application note*. STMicroelectronics, 2019.

22. HUSÁK, Miroslav. *Mikrosenzory a mikroaktuátory*. Praha: Academia, 2008. ISBN 978-80-200-1478-8.

23. ZÁHLAVA, Vít. *Návrh a konstrukce desek plošných spojů: principy a pravidla praktického návrhu*. Praha: BEN - technická literatura, 2010. ISBN 978-80-7300-2.